PEOPLE'S DEMOCRATIC REPUBLIC OF ALGERIA

MINISTRY OF HIGHER EDUCATION AND SCIENTIFIC RESEARCH

University of Echahid Hamma Lakhdar El-Oued

Faculty of Technology

Department of Electrical Engineering

Dissertation

Submitted for obtaining the LMD doctorate degree on telecommunication

Specialty: Networks and Telecommunications

Presented by **Meriem Ad**

Theme

PHY Transceiver Design Based on NOMA Congnitive Radio

Jury Members: :

President	Hima Abdelkader	MCA	University of EL-Oued
Examiner	Hettiri Messaoud	Professor	University of EL-Oued
Examiner	Otmani Hamza	MCA	University of Ouargla
Examiner	Bensid Khaled	MCA	University of Ouargla
Supervisor	Khelil Abdellatif	Professor	University of EL-Oued

Academic Year : 2024/2025

Acknowledgements

I begin by expressing my profound gratitude to Allah for guiding me throughout the preparation of this thesis and for leading me from the darkness of ignorance to the light of knowledge. Al-hamdulillah.

I would also like to acknowledge my own perseverance, hard work, patience, and optimism, which have been essential throughout the years of study.

My heartfelt thanks go to my parents for their unwavering love, constant support, and unshakable confidence in me and my abilities. Their prayers have been a source of strength throughout this journey.

I am deeply grateful to my sisters, Asma and Sara, as well as the rest of my family, for their love and encouragement.

I would like to express my sincere appreciation to my supervisor, **Prof. Khelil Abdellaitf** for his exceptional guidance, support, and encouragement throughout my research. His extensive expertise, patience, and insightful feedback have been pivotal in shaping this thesis.

I would also like to extend my sincere gratitude to the members of my jury for their time, effort, and invaluable feedback.

I am equally deeply grateful to **Dr. Sultangali Arzykulov** for his remarkable humility and the time and effort he devoted to assisting me.

I would like to express my gratitude to the Ministry of Education and my country for their support and the opportunities they have provided me throughout my academic journey. I also wish to thank my university, the administrative staff, and all my professors for their contributions during my studies.

Finally, I would like to acknowledge my colleagues and friends for their continuous support, encouragement, and assistance throughout this process.

Dedication

I dedicate this thesis to my family, myself, and everyone who loves me. To all my friends or who sincerely prayed for me and helped me along the way.

A special dedication to someone who once told me in my baccalaureate exam defined my level. This thesis is my response to you 'this is my level'.

Thanks

Meriem Ad

Abstract

The exponential growth in wireless communication demands has intensified the need for efficient spectrum utilization. With spectrum resources becoming increasingly scarce, traditional access methods struggle to keep up with the ever-growing number of connected devices, especially in the context of Beyond 5G (B5G) and future 6G networks. This has led to a search for advanced technologies capable of improving spectrum efficiency, accommodating high-density user connections, and supporting diverse quality of service requirements. Cognitive Radio (CR) and Non-Orthogonal Multiple Access (NOMA) have emerged as promising technologies to address these challenges. CR allows dynamic access to underutilized spectrum by enabling secondary users to coexist with licensed primary users, while NOMA facilitates multiple users sharing the same frequency resources by assigning distinct power levels. When combined, CR and NOMA, forming CR-NOMA, leverage the strengths of both technologies, aiming to maximize spectrum efficiency and user access while minimizing interference. This thesis aims to conduct a comprehensive analysis of the CR-NOMA system's effectiveness in mitigating spectrum scarcity and enhancing system performance. By integrating Cooperative Communication with CR-NOMA, it seeks to further boost efficiency and expand coverage, addressing key challenges encountered in practical implementations. In real-world scenarios, system performance is often hindered by imperfections in Channel State Information (CSI) and Successive Interference Cancellation (SIC). This thesis thoroughly examines the extent to which these imperfections impact crucial performance metrics, such as bit error rate (BER), and outage probability (OP), across a range of operating conditions, offering insights into optimizing CR-NOMA under realistic constraints. First, we investigate a simple underlay CR assisted NOMA downlink transmission over the Rayleigh fading channel. Exact closed form expressions of the OP, achieved data rate and throughput of two CR-NOMA users are derived. The performance is demonstrated using both analytical and simulation results and also the influence of interference temperature constraint (I_{TC}) on the CR-NOMA system . Then, we investigate underlay CR-NOMA-based device-to-device (D2D) communications in the presence of Rayleigh fading channels. The study assumes a decode-and-forward (DF) mode, where nearby users act as helper users to assist distant users. We derived the closed-form expressions for OP and throughput at the end users in three scenarios: perfect SIC and CSI, imperfect CSI, and imperfect SIC. Thereafter, we examine the BER performance of underlay Cooperative CR based NOMA (CCR-NOMA) systems. We derive exact closed-form expressions for BER at distant users under perfect and imperfect CSI conditions.

These mathematical formulations are validated through Monte Carlo simulations.

The results can be summarized as follows: The simple system model shows superiority compared to the traditional multiple access scheme and the performance of user utilizing SIC technology is better than that of user who do not utilize SIC in CR-NOMA. Additionally, the near user outperforms the far user in CR-OMA. We also found the best result at I_{TC}=35 dB ,which is a key factor in the system performance. In CR-NOMA with D2D communication system , users employing SIC technology demonstrate superior performance compared to those who do not utilize SIC. Additionally, the OP performance of users employing CR-NOMA mode surpasses that of users using CR-OMA mode. The presence of imperfect CSI and imperfect SIC adversely affects the outage performance. Additionally, distant users utilizing the CCR-OMA protocol demonstrate better BER performance than those employing the CCR-NOMA protocol. The presence of imperfect CSI adversely affects BER performance. Moreover, the derived closed-form expressions for BER in the investigated system align well with Monte Carlo simulations. These findings provide valuable insights for optimizing the performance of CCR-NOMA systems in real-world scenarios.

Key words: *6G,NOMA,CR ,CR-NOMA,OP,D2D ,BER.*

Résumé

La croissance exponentielle de la demande en communications sans fil a intensifié le besoin d'une utilisation efficace du spectre. Avec des ressources spectrales de plus en plus limitées, les méthodes d'accès traditionnelles peinent à répondre à l'augmentation incessante du nombre d'appareils connectés, particulièrement dans le contexte des réseaux au-delà de la 5G (B5G) et des futurs réseaux 6G. Cela a conduit à la recherche de technologies avancées capables d'améliorer l'efficacité spectrale, d'accommoder un nombre élevé de connexions et de répondre aux diverses exigences de qualité de service. La Radio Cognitive (CR) et l'Accès Multiple Non Orthogonal (NOMA) se sont révélés être des technologies prometteuses pour relever ces défis. La CR permet un accès dynamique au spectre sous-utilisé en permettant aux utilisateurs secondaires de coexister avec des utilisateurs primaires sous licence, tandis que le NOMA permet à plusieurs utilisateurs de partager les mêmes ressources fréquentielles en attribuant des niveaux de puissance distincts. La combinaison de CR et NOMA, formant le CR-NOMA, exploite les forces des deux technologies, visant à maximiser l'efficacité spectrale et l'accès des utilisateurs tout en minimisant les interférences.

Cette thèse vise à réaliser une analyse exhaustive de l'efficacité du système CR-NOMA dans la résolution de la rareté spectrale et l'amélioration des performances du système. En intégrant la Communication Coopérative avec le CR-NOMA, l'étude vise à améliorer l'efficacité et à étendre la couverture, tout en traitant des défis cruciaux rencontrés lors des implémentations pratiques. Dans des scénarios réels, les performances des systèmes sont souvent compromises par des imperfections dans les informations d'état de canal (CSI) et dans l'annulation successive d'interférences (SIC). Cette thèse examine en détail l'impact de ces imperfections sur des indicateurs de performance cruciaux, tels que le taux d'erreur binaire (BER), la probabilité de panne (OP), dans diverses conditions d'exploitation, offrant des perspectives d'optimisation du CR-NOMA sous des contraintes réalistes.

Dans un premier temps, nous analysons une transmission en liaison descendante CR assistée par NOMA sous forme d'un simple modèle de recouvrement sous le canal à évanouissement Rayleigh. Des expressions exactes en forme fermée de l'OP, du débit de données atteint et du débit global pour deux utilisateurs CR-NOMA sont dérivées. Les performances sont démontrées à l'aide de résultats analytiques et de simulations, tout en étudiant également l'influence de la contrainte de température d'interférence (I_{TC}) sur le système CR-NOMA. Ensuite, nous explorons les communications de dispositif-à- dispositif (D2D) basées sur le CR-NOMA sous le recouvrement Rayleigh. L'étude suppose un mode de décodage-et-transmission (DF), où les utilisateurs proches servent d'assistants pour les utilisateurs éloignés. Nous avons dérivé des expressions en forme fermée pour l'OP et le débit global des utilisateurs finaux dans trois scénarios : CSI et SIC parfaits, CSI imparfait , et SIC imparfait . Ensuite, nous examinons les performances en BER des systèmes CCR-NOMA sous-jacents et coopératifs CR en conditions CSI parfaites et imparfaites. Ces formulations mathématiques sont validées par des simulations Monte Carlo.

Les résultats peuvent être résumés comme suit : Le modèle de système simple démontre une supériorité par rapport au schéma d'accès multiple traditionnel, et les performances des utilisateurs exploitant la technologie SIC sont meilleures que celles des utilisateurs qui ne l'exploitent pas dans le CR-NOMA. De plus, l'utilisateur proche surpasse l'utilisateur éloigné dans le CR-OMA.

Nous avons également trouvé le meilleur résultat à I_{TC}=35 dB, un facteur clé dans les performances du système. Dans le système de communication D2D CR-NOMA, les utilisateurs utilisant la technologie SIC démontrent des performances supérieures par rapport à ceux qui ne l'utilisent pas. De plus, la performance en OP des utilisateurs employant le mode CR-NOMA dépasse celle des utilisateurs utilisant le mode CR-OMA. La présence CSI imparfait et SIC imparfait affecte négativement la performance en termes de l'OP. De plus, les utilisateurs éloignés utilisant le protocole CCR-OMA montrent de meilleures performances en BER que ceux employant le protocole CCR-NOMA, et la présence CSI imparfait impacte négativement la performance en BER. En outre, les expressions en forme fermée dérivées pour le BER dans le système étudié sont en adéquation avec les simulations Monte Carlo. Ces résultats fournissent des perspectives précieuses pour l'optimisation des performances des systèmes CCR-NOMA dans des scénarios réels..
Mots clés : *6G,NOMA,CR ,CR-NOMA,OP ,D2D ,BER.*

ملخص

تزايد الطلب المتسارع على الاتصالات اللاسلكية أدى إلى تفاقم الحاجة إلى استخدام الطيف الترددي بكفاءة عالية. ومع ندرة موارد الطيف بشكل متزايد، تواجه أساليب الوصول التقليدية صعوبة في مواكبة العدد المتزايد من الأجهزة المتصلة، خصوصاً في سياق شبكات ما بعد الجيل الخامس (B5G) وشبكات الجيل السادس المستقبلية 6G. وقد أدى ذلك إلى البحث عن تقنيات متقدمة قادرة على تحسين كفاءة الطيف، واستيعاب الاتصالات ذات الكثافة العالية للمستخدمين، وتلبية متطلبات جودة الخدمة المتنوعة. برز الراديو المعرف (CR) والنفاذ المتعدد غير المتعامد (NOMA) كتقنيات واعدة للتصدي لهذه التحديات. يتيح CR الوصول الديناميكي إلى الطيف غير المستغل عن طريق تمكين المستخدمين الثانويين من التواجد مع المستخدمين الأساسيين المرخصين، بينما يسهل NOMA مشاركة العديد من المستخدمين لنفس الموارد الترددية من خلال تخصيص مستويات طاقة مختلفة. وعند دمج CR و NOMA في النظام المعروف بـ CR-NOMA، يتم الاستفادة من مزايا كلا التقنيتين بهدف تحقيق أقصى قدر من كفاءة الطيف والوصول إلى المستخدمين مع تقليل التداخل. تهدف هذه الأطروحة إلى إجراء تحليل شامل لفعالية نظام CR-NOMA في التخفيف من ندرة الطيف وتعزيز أداء النظام. من خلال دمج الاتصال التعاوني مع CR-NOMA، تسعى الأطروحة إلى تعزيز الكفاءة وتوسيع التغطية، ومعالجة التحديات الأساسية التي تواجه التطبيق العملي. في سيناريوهات العالم الحقيقي، غالباً ما تعيق أداء النظام العيوب في معلومات حالة القناة (CSI) وإلغاء التداخل التتابعي (SIC). وتدرس هذه الأطروحة مدى تأثير هذه العيوب على مؤشرات الأداء الأساسية، مثل معدل الخطأ في البتات (BER)، احتمالية الانقطاع (OP)، عبر مجموعة متنوعة من ظروف التشغيل، مقدماً رؤى لتحسين CR-NOMAفي ظل القيود الواقعية.

في البداية، نقوم بدراسة نظام CR-NOMA في حالة نقل البيانات عبر قناة رايلي المتلاشية. تم استنباط الصيغ لاحتمالية الانقطاع OP، معدل البيانات المحقق، والنفاذية للمستخدمين في CR-NOMA. يتم عرض الأداء باستخدام النتائج التحليلية والمحاكاة، كما تمت دراسة تأثير قيود درجة الحرارة التداخلية (I_{TC})على نظام CR-NOMA. بعد ذلك، قمنا بدراسة نظام اتصالات جهاز إلى جهاز (D2D) المعتمد على CR-NOMA في وجود قنوات رايلي المتلاشية. تعتمد الدراسة على نمط فك التشفير وإعادة الإرسال (DF)، حيث يعمل المستخدمون القريبون كمستخدمين مساعدين لدعم المستخدمين البعيدين. استنبطت الصيغ لاحتمالية الانقطاع والنفاذية في ثلاثة سيناريوهات: CSI و SIC المثالية، و CSI غير المثالية ، و SIC غير المثالية . بعد ذلك، ندرس أداء معدل الخطأ في البتات BER لنظام -CCR NOMA التعاوني(CCR-NOMA). تم استنباط صيغ دقيقة لـ BER للمستخدمين البعيدين في ظروف CSI المثالية وغير المثالية، وتمت المصادقة على هذه

الصيغ من خلال محاكاة مونت كارلو.

يمكن تلخيص النتائج على النحو التالي: يُظهر النموذج البسيط للنظام تفوقًا مقارنة بنظام النفاذ المتعدد التقليدي، كما أن أداء المستخدم الذي يستخدم تقنية إلغاء التداخل المتتابع (SIC) أفضل من أداء المستخدم الذي لا يستخدم هذه التقنية في CR-NOMA. بالإضافة إلى ذلك، فإن المستخدم القريب يتفوق على المستخدم البعيد في CR-OMA. وجدنا أيضاً أفضل نتيجة عند $I_{TC} = 35dB$ ، والذي يُعد عاملاً مهماً في أداء النظام. في نظام CR-NOMA مع الاتصالات من نوع D2D، يظهر المستخدمون الذين يعتمدون على تقنية SIC أداءً أفضل مقارنةً بالمستخدمين الذين لا يستخدمون SIC. بالإضافة إلى ذلك، فإن أداء OP للمستخدمين الذين يستخدمون وضع CR-NOMA يتفوق على أداء المستخدمين الذين يستخدمون وضع CR-OMA. يؤثر وجود CSI و SIC الغير مثالية سلباً على أداء الانقطاع. بالإضافة إلى ذلك، يظهر المستخدمون البعيدون الذين يعتمدون بروتوكول CCR-OMA أداءً أفضل في BERمقارنةً بأولئك الذين يستخدمون بروتوكول CCR-NOMA. يؤثر وجود CSI الغير مثالية سلباً على أداء BER. علاوة على ذلك، تتوافق الصيغ لـ BER المستنبطة مع محاكاة مونت كارلو. تقدم هذه النتائج رؤى قيمة لتحسين أداء أنظمة CCR-NOMA في السيناريوهات الواقعية. .

كلمات مفتاحية: *NOMA*، *NOMA*، *OP* ، *D2D* ، *BER*، الراديوا المعرفي.

Scientific Production

Paper- Published

- AD Meriem; KHELIL Abdellatif. Outage Performance of Underlay CR-NOMA-based D2D Communications under Imperfect CSI and SIC. International Journal of Sensors Wireless Communications and Control, 2024, 14.2: 104-112.DOI: 10.2174/012210327..
- Ad, Meriem, and Abdellatif Khelil. "BER Analysis of Underlay Cooperative Cognitive Radio-based NOMA System." International Journal of Sensors, Wireless Communications and Control (2024).DOI: 10.2174/0122103279275260240925050941

Conference Paper- Published - (Book Chapter)

- AD Meriem; KHELIL Abdellatif. Performance Investigation of CR-NOMA based Underlay Paradigm,Fifth International Conference on Electrical Engineering And Control Applications (ICEECA),2022. DOI: 10.1007/978-981-97-4776-4_38

Contents

List of Figures

List of Tables

List of Abbreviations

1G	Fisrt Generation
2G	Second Generation
3D	Three-dimensional
3G	Third Generation
3GPP	Third Generation Partnership Project
4G	Fourth Generation
5G	Fifth Generation
6G	Sixth Generation
ABER	Average Bit Error Rate
AI	Artificial Intelligence
AF	Amplify and Forward
ALOHA	Advocates of Linux Open-source Hawaii Association
AMPS	Advanced Mobile Phone System
APs	Access points
AR	Augmented reality
AoI	Age of Information
AWGN	Additive White Gaussian Noise
B5G	Beyond fifth generation
BCI	Brain-Computer Interaction
BPSK	Binary Phase Shift Keying
BER	Bit Error Rate
BDMA	Beam division multiple access
BS	Base Station
CA	Carrier aggregation
CC	Cooperative communications
CC-NOMA	Cooperative Communications NOMA

CCR-NOMA	Cooperative Cognitive Radio NOMA
CCR-OMA	Cooperative Cognitive Radio OMA
CDF	Cumulative distribution function
CDMA	Code division multiple access
C-NOMA-WDC	Cooperative NOMA without Diversity
CN	Cognitive Network
CNOMA-WDC	Cooperative NOMA without diversity combining
CoMP	Coordinated Multipoint
CONASENSE	Communication Navigation Sensing Services
CSI	Channel State Information
CR	Cognitive Radio
CR-FD-NOMA	Cooperative Relaying Full Duplex NOMA
CR-NOMA	Cognitive radio with non-orthogonal multiple access
CR-OMA	Cognitive radio with orthogonal multiple access
CRNs	CR Network
D2D	Device-to-device
DF	Decode and Forward
DL	Downlink
DPC	Dirty paper coding
DSA	Dynamic Spectrum Access
DSM	Dynamic Spectrum Management
E2E	End-to-End
EE	Energy efficiency
EDGE	Enhanced data rates for GSM evolution
ELPC	Extremely Low-Power Communications
ETSI	European Telecommunications Standards Institute
eMBB	enhanced Mobile Broadband
ERLLC/eURLLC	Enhanced Ultra-Reliable, Low-Latency Communication
F-NOMA	Fixed NOMA
FBMC	Filter bank multi-carrier
FCC	Federal Communications Commission
FDD	Frequency division duplex schemes
FeMBB	Further enhanced Mobile Broadband
FSO	Free-Space Optical

GNSS	Global Navigation Satellite Systems
GEO	Geostationary orbit
GPRS	General packet radio service
GSM	Global System for Mobile Communications
HAP	High altitude platforms
HBC	Human Bond Communication
HetNets	Heterogeneous networks
HSPA+	High Speed Packet Access+
HTS	High Throughput Satellite
IC	Interference Cancellation
IMT-2000	International Mobile Telecommunications 2000
IP	Internet Protocol
IoT	Internet of Things
ISTN	Integrated Space and Terrestrial Network
ITC	Interference Temperature Constraint
ITU	International Telecommunication Union
KPIs	Key performance indicators
LAP	Low altitude platforms
LDHMC	Long-Distance High-Mobility Communications
LEO	Low Earth Orbit
LOS	Line-of-Sight
LTE	Long Term Evolution
MA	Multiple access
MAC	Medium access control
MANET	Mobile Ad-hoc Networking
mBBMT	massive broad bandwidth machine type
MEC	Mobile Edge Computing
MGF	Moment Generating Function
MIMO	Multiple-input multiple-output
ML	Machine Learning
MLD	Maximum Likelihood Detection
mLLMT	massive Low-Latency Machine Type
mMTC	massive machine-type communications
MMSE	Minimum mean square error

MNO	Mobile network operators
MUD	Multiuser detection
MUI	Multiple user interference
MUST	Multi-User Superposed Transmission
mmWaves	millimeter Waves
NGSO	Non-geostationary orbit
NOMA	Non Orthogonal Multiple Access
NMT	Nordic Mobile Telephone
NR	New Radio
NS	Network slicing
OAM	Orbital angular momentum
OFDM	Orthogonal frequency division multiplexing
OMA	Orthogonal Multiple Access
OP	Outage Probability
O-RAN	Open Radio Access Network
OWC	Optical Wireless Communications
PA	Power allocation coefficient
PAN	Personal area network
PDF	Probability Density Function
PEP	Pairwise Error Probability
PN	Primary Network
PRs	Primary receivers
PUs	Primary users
QML	Quantum ML
QoE	Quality of experience
QoPE	Quality of Physical Experience
QoS	Quality of Service
QPSK	Quadrature Phase Shift Keying
QUIC	Quick UDP Internet Connections
RAN	Radio Access Network
RF	Radio frequency
RIS-IRS	Reconfigurable Intelligent Surfaces-Intelligent Reflecting Surfaces
RTIE	Real-Time Intelligent Edge
SBS	Secondary Base Station

SC	Superposed Coding
SDR	Software Defined Radio
SE	Spectrum efficiency
SIC	Successive Interference Cancellation
SINR	Signal-to-Interference-plus-Noise Ratio
SLA	Service level agreements
SON	Self-Organizing Networks
SOP	Secure outage probability
SMS	Short messaging systems
SNR	Signal-to-Noise Ratio
SRE	Smart Radio Environment
SSN	Self-Sustaining Networks
SUs	Secondary users
TACS	Total Access Communications System
TDMA	Time adivision duplex schemes
TDD	Time Division Duplex
THz	Tera-Herts
UAV	Unmanned aerial vehicle
UL	Uplink
umMTC	ultra-massive Machine-Type Communication
UMTS	Universal Mobile Telecommunications System
URLLC	Ultra-reliable low-latency communication
UV	Ultraviolet
UWB	Ultra-wideband
VR	Virtual reality
VLC	Visible Light Communications
V2X	Vehicle-to-Everything
WCDMA	Wideband CDMA
WSNs	Wireless Sensor Networks
XR	EXtended Reality
ZF	Zero-forcing

List of Symbols

PU	Primary User
PN	Primary Network
SN	Secondary Network
D_1	Unlicensed user 1
D_2	Unlicensed user 2
D_3	Unlicensed user 3
D_4	Unlicensed user 4
I	The interference from the PN affecting users in the SN
g_{SC}	Link from SN to user PU.
g_{D_q}	The Rayleigh fading channel coefficients of D_q user
S	The SC signal
m_1	Message of D_1
m_2	Message of D_2
b_1	PA coefficient of D_1
b_2	PA coefficient of D_2
E_{BS}	Transmit power constraints
I_{ITC}	The interference temperature constraint (ITC)
n	Additive White Gaussian Noise (AWGN)
$E\left[.\right]$	The expectation operator
h	The estimated channel coefficient
e	A complex Gaussian distributed random variable
α	The pathloss exponent

General introduction

Background

Fifth Generation (5G) and sixth Generation (6G) are the latest generations of cellular networks set to revolutionize communication, data access, and usage. 5G has already achieved significant success, with widespread implementation in countries such as China, the United States, Germany, Singapore and others. Technological and scientific evidence indicates that 5G networks are expected to deliver significantly faster speeds, ranging from 100 Mbps to 10 Gbps, compared to Fourth Generation (4G) Long Term Evolution (LTE) networks. It's important to note that the specific speed limits of 5G networks vary by country. As of now, the fastest recorded speed for 5G networks is approximately 360 Mbps. The exact speed that users experience on 5G depends on several factors, including their location, the available spectrum in that area, the number of users on the network, and vice versa [1]. Researchers in both industry and academia are currently invested on developing the vision, usage scenarios, and enabling technologies for future 6G wireless networks. 5G supports enhanced Mobile Broadband (eMBB) to achieve peak data rates up to 10 Gbps. In addition, Ultra-reliable low-latency communication (URLLC) decreases delays to lower than 1 ms, when massive machine-type communications (mMTC) support a huge density of devices, up to 1 million per square km. Moreover, the expected reliability and availability of 5G networks are projected to reach 99.99%. Nevertheless, 5G technology will just partially support the growing demands for intelligent wireless networks, which will have an important role in forging the highly digitized and data-driven society of the future. Therefore, 6G imposes more stringent needs on the network's key performance indicators, including data rate, reliability, uninterrupted coverage, latency, and more. 6G networks will demand, among other metrics, higher data rates reaching up to 1 Tbps peak values with extended coverage, a 10-fold improvement in energy and cost efficiency compared to 5G, centimeter-level positioning accuracy, and a density of device connections reaching $10^7/km^2$. To achieve these performance targets, 6G will utilize ultramassive Multiple-input multiple-output (MIMO) communications in the millimeter wave (mmWave) and terahertz (THz) bands. This approach can significantly enhance spectrum efficiency (SE) and energy efficiency (EE), especially when combined with adaptive modulation/coding, adaptive equalization, and power/rate control techniques [2].

Motivation

As wireless communication systems progress toward the 6G era, several critical challenges arise, including spectrum scarcity, massive connectivity, reduced transmission latency, and the demand for enhanced spectral efficiency. Non Orthogonal Multiple Access (NOMA) has emerged as a promising solution to address these challenges by enabling multiple users to share the same resource blocks simultaneously, unlike Orthogonal Multiple Access (OMA), which is limited by time or frequency constraints. NOMA can significantly enhance spectral efficiency, improve throughput at the cell edge, reduce latency, and support massive connectivity, all while maintaining user fairness. NOMA achieves this through Superposed Coding (SC) at the transmitter, coupled with Successive Interference Cancellation (SIC) at the receiver, allowing users to access shared resource elements across time, frequency, space, or code domains simultaneously. This capability makes NOMA a widely recognized solution for the future of wireless communication [3],[4]. Cognitive Radio (CR) technology, which enables intelligent spectrum detection and dynamic usage, further enhances spectral efficiency by allowing secondary users (SUs) to opportunistically access the spectrum. Underlay CR, a prominent approach within this framework, permits both primary and SUs to transmit concurrently on the same frequency band, minimizing interference to primary users. Unlike overlay CR, where specific spectrum bands are allocated to SUs, underlay CR allows both primary and secondary users to transmit concurrently on the same frequency band. This coexistence is facilitated through advanced interference management techniques such as power control, spectrum sensing, and dynamic spectrum access [5]. By combining NOMA's ability to serve multiple users simultaneously with CR's capability to optimize spectrum usage, the integration of these technologies in a CR-based NOMA network is expected to significantly improve spectral efficiency and serve more users while meeting their quality of service (QoS) requirements. In such a network, NOMA allows multiple SUs to operate on idle primary user (PU) channels. However, the dynamic nature of CR environments necessitates specialized communication strategies and protocols to adapt to challenges such as fluctuating PU channel availability, limited channel duration, and varying connection conditions. To efficiently manage these challenges, CR with NOMA (CR-NOMA) networks can organize

SUs into clusters, with each cluster using an available PU channel and employing NOMA techniques for simultaneous access. This approach is expected to enhance Beyond fifth generation (B5G) networks by supporting advanced services like eMBB, URLLC, and mMTC, providing greater flexibility and accommodating a wide range of applications [6], [7], [8] . This thesis intends to perform an in-depth analysis of the CR-NOMA system's ability to alleviate spectrum scarcity and improve overall system performance. By incorporating Cooperative Communication with CR-NOMA, it aims to increase efficiency and extend coverage while tackling significant challenges faced in real-world applications. This thesis thoroughly examines the effects of these imperfections on key performance metrics, including bit error rate (BER), outage probability (OP), achievable data rate, and throughput, under different operating conditions.

Contribution

The contributions of this thesis are summarized as follows: As previously discussed, NOMA is a promising radio access technology, and its combination with CR has been highlighted for its potential to enhance the performance of next-generation cellular communications. Similarly, cooperative communication is acclaimed for its capacity to significantly improve the overall performance of communication networks. The objective of this thesis is to undertake a comprehensive analysis of the CR-NOMA system, with particular emphasis on key performance metrics such as BER, OP, achievable data rate, and throughput, alongside the influence of imperfect Channel State Information (CSI) and imperfect SIC. The main contributions of this thesis are as follows:

- We analyze a simple underlay CR-NOMA system, examining the performance in terms of outage probability, data rate, and throughput under varying interference temperature constraint (I_{TC}) values. Finally, we compare these results with CR with OMA (CR-OMA) scheme.Theoretical outcomes are verified using Monte Carlo simulations.
- We explore an underlay CR-NOMA-based Device-to-device (D2D) system over Rayleigh channels in decode-and-forward (DF) mode, where near users serve as helper nodes for far users. We derive closed-form expressions for OP and throughput at the end users in three distinct scenarios: (1) Perfect SIC and perfect CSI , (2) Imperfect CSI, and (3) Imperfect SIC.Theoretical results are confirmed by employing Monte Carlo simulations.
- We assess the BER performance of underlay Cooperative Cognitive Radio (CCR-

NOMA) systems by deriving precise closed-form expressions for BER at distant users under both perfect and imperfect CSI conditions. These theoretical findings are validated through Monte Carlo simulations.

The Dissertation Organisation

The dissertation is divided into five chapters, summarized below:

- Chapter 1 outlines the theoretical foundations of 6G, exploring its potential characteristics, architecture, key technologies, performance metrics, and requirements.
- Chapter 2 presents the fundamental concepts of Cognitive Radio Networks (CRNs) and NOMA. We define these technologies and explain core concepts, including the various types and components of CRNs. We also discuss the general equations relevant to NOMA technology in both uplink and downlink scenarios.
- Chapter 3 investigates the performance of the CR-NOMA-based underlay paradigm in downlink (DL) scenarios. The OP and throughput have been derived, along with a comparison between CR-NOMA and CR-OMA.
- Chapter 4 studies the Outage performance of underlay CR-NOMA based D2D communication under imperfect CSI and imperfect SIC. The OP and throughput have been derived, along with a comparison between CR-NOMA and CR-OMA.
- Chapter 5 studies BER Analysis of Underlay Cooperative Cognitive Radio based NOMA System in perfect CSI and Imperfect CSI scenarios. The BER has been derived, along with a comparison between CR-NOMA and CR-OMA.
- In conclusion, we summarize the key findings and contributions of our research on CR-NOMA. Additionally, we highlight the importance of our work for the field of telecommunications and suggest potential avenues for future research based on our results.

Chapter 1

An Overview on 6G Technology

1.1 Introduction

Wireless communication has evolved significantly over the years, progressing from Fisrt Generation (1G) to 5G. Each generation has brought improvements in speed and performance. Now, we are preparing for the next major advancement: 6G. It is the next step after 5G, currently under development and expected to be ready by 2030. It will be significantly faster than 5G and will enable the connection of a wide range of devices to the internet. In this chapter, we will look at what 6G might be like, architecture, key technology, performance metric, and requirements ...etc.

1.2 Evolution of Mobile Communication

Communication has been an essential component of human life from the moment it began. The evolution of communication is a continuous process supported by advancing technologies. The transition from wired telephones to Artificial Intelligence (AI)-enhanced real-time communication has significantly contributed to creating a more connected and advancing society. The wireless communication sector is regarded as a "living" industry due to its continuous growth. The growth is directly proportional to societal demands. To date, we have experienced five generations of mobile communication and are now progressing toward future generations. Each decade sees the advent of a new generation in mobile communication, such as 1G, 2G, 3G, and 4G, each with new features and services tailored to meet user and network requirements. The key distinguishing factors among mobile generations include data traffic, latency, data rate, throughput, device density, coverage, security and reliability [9].

1.2.1 First Generation of Mobile Communication (1G)

1G was started in 1979, and it signified the first generation of cellular telephony. It operated using analogue technology and was specifically designed for voice calls. It employs narrow-band frequency channels for transmitting voice signals. During the 1G era, multiple regional standards emerged simultaneously, including the Nordic Mobile Telephone (NMT), Advanced Mobile Phone System (AMPS), and Total Access Communications System (TACS). 1G systems reached a maximum speed of 2.4 Kbps, characterized by limited battery life, reduced security features, and lower voice quality [9].

1.2.2 Second Generation (2G)

The second generation of mobile communication, introduced in the early 1990s, employs digital radio signals. The primary motivation for developing 2G was to insert the security and reliability of the communication channel. Regionally, there were numerous separate initiatives for the development of 2G standard systems. Figure . 1.1 depicts the initiatives undertaken by various countries. The European Telecommunications Standards Institute (ETSI) introduced Global System for Mobile Communications (GSM) in 1987. It executed time and frequency division duplex (TDMA/ FDD) schemes. Qualcomm introduced code division multiple access (CDMA) as an alternative. These multiplexing schemes enabled 2G systems to accommodate multiple users on one channel. Aside from voice calls, 2G systems provided data services, short messaging systems (SMS), and enhanced features such as call hold and conferencing, etc. 2G systems reached speeds of 50 Kbps with the general packet radio service (GPRS) and up to 1 Mbps with enhanced data rates for GSM evolution (EDGE)[9].

1.2.3 Third Generation (3G)

In 2001, 3G mobile systems emerged. The International Telecommunication Union (ITU) established the International Mobile Telecommunications 2000 (IMT-2000) framework for 3G cellular networks. 3G systems brought about revolutionary changes in mobile communications, introducing services such as email, web browsing, picture sharing, video downloading, and fast internet speeds of up to 200Kbps. It signified the transition from multimedia phones to smartphones. It provided a cost-effective boost in data rates alongside improved voice quality. The Universal Mobile Telecommunications System (UMTS) made its debut alongside 3G systems. Employing wideband CDMA (WCDMA), 3G achieved data rates of up to 2

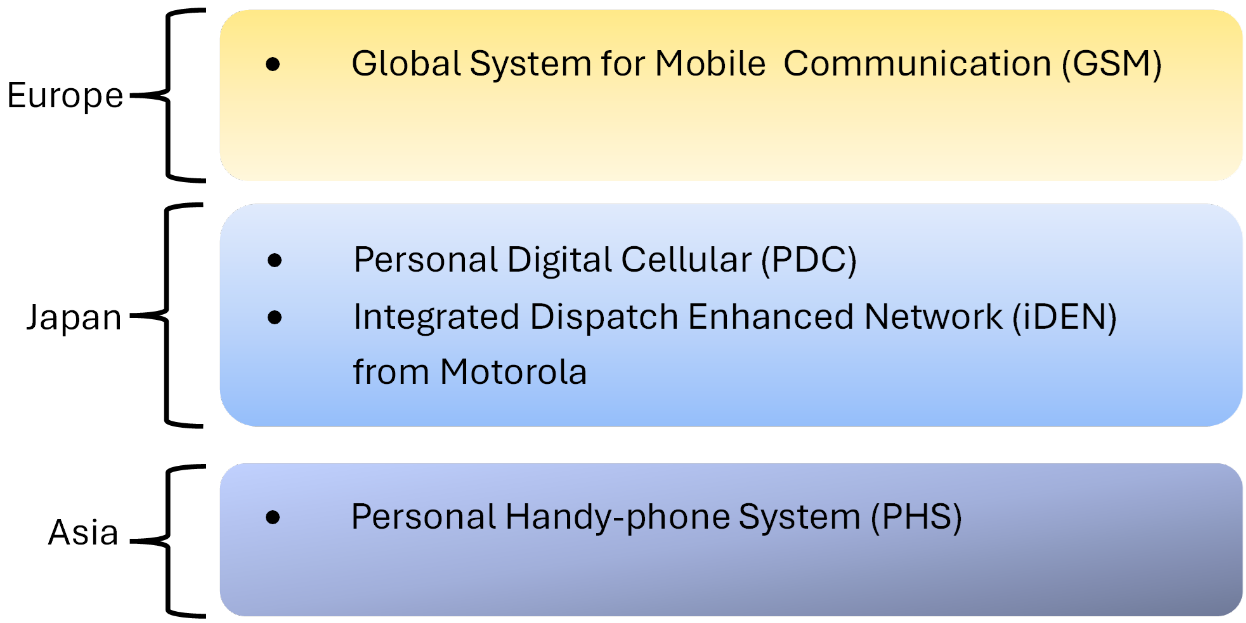

Figure 1.1: Global Initiatives for 2G Mobile Systems.

Mbps (stationary) and 384 kbps (mobility). The theoretical maximum data rate for High Speed Packet Access+ (HSPA+) reached 21.6 Mbps. High-speed internet transformed data streaming into one of 3G's standout applications[9].

1.2.4 Fourth Generation (4G)

4G mobile systems were built according to the IMT-Advanced demands. Their strategy aimed to provide users with high-speed, high-quality, and high-capacity services in a practical manner. It aimed to reach speeds of 100 Mbps (mobile) and 1 Gbps (stationary) while decreasing latency from 300ms to less than 100ms. 4G systems notably reduced network congestion, enhanced built-in security, and introduced multimedia and internet over Internet Protocol (IP) concepts. The primary technologies facilitating this are orthogonal frequency division multiplexing (OFDM) and MIMO. It also defined heterogeneous networks (HetNets), small cells and additional features like carrier aggregation (CA), Coordinated Multipoint (CoMP) and advanced MIMO transmissions[9].

1.2.5 Fifth Generation (5G)

5G systems are now in the commercial deployment phase, aiming to surpass their predecessor, 4G, with improved data rates, latency , connection density, and various other enhancements. These systems leveraged the 30 GHz to 300 GHz spectrum of mmWave to achieve a maximum of 35.46 Gbps. They utilized Small Cells technology to enhance coverage and minimize latency. 5G systems also leveraged advanced access technologies including beam division multiple access (BDMA), quasi-orthogonal sequences, NOMA, and filter bank multi-carrier (FBMC), and others. Scalable OFDM plays a dominant role in 5G networks, enabling ultra-low latency performance. It also integrated network slicing (NS) to offer customized services from mobile network operators (MNO) based on service level agreements (SLA). For users, the implementation of AI, Augmented reality /Virtual reality (AR/VR), and EXtended Reality (XR) introduced new use cases, applications, and services [9]. Fig. 1.2 highlights the differences between 1G,2G, 3G, 4G, 5G, and 6G [10].

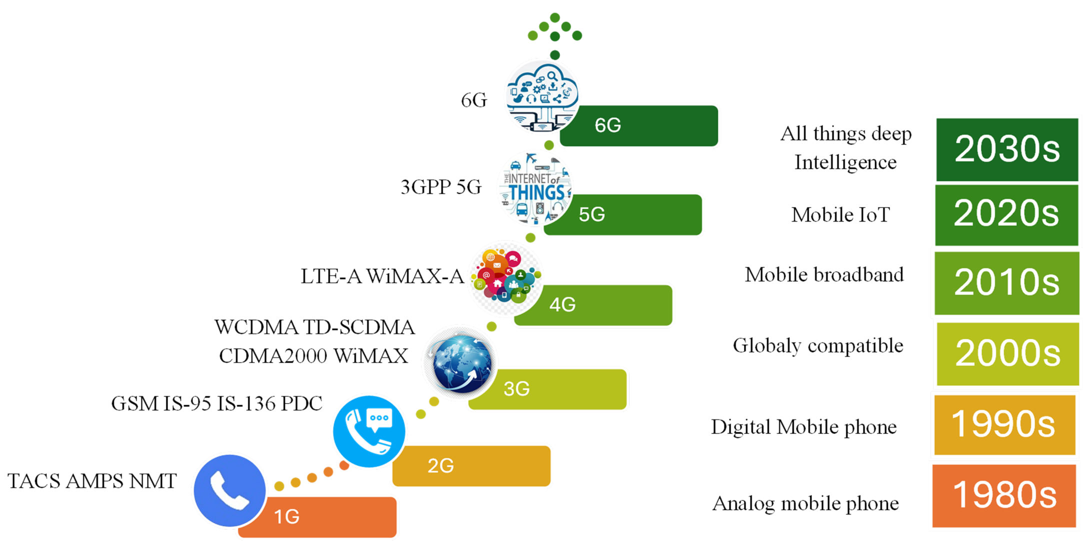

Figure 1.2: The Development of Mobile Communication.

1.3 The Gap from 5G to 6G

With increasing requirements for higher data rate, ubiquitous access, and seamless services anytime and anywhere, the 6G network faces enormous difficulties in accommodating different use cases and application scenarios that include novel ideas and visionary goals. As per the latest updates from ongoing discussions on IMT 2030 and beyond, there's a global desire for novel and revolutionary use cases and applications of 6G. These include ubiquitous intelligence, immersive multimedia, multi-sensory communications, E-health and well-being, digital twins and extended world, ubiquitous computing, smart industries and transportation, E-health and well-being, contiguous and ubiquitous connective, integrated sensing and communications, and sustainability. Despite the ongoing rapid expansion of 5G commercialization and coverage globally, there is a technological expectation that the capabilities of 5G may not fully support the envisioned use cases and applications of 6G. The transition from the 5G network to the envisioned future not only represents a significant gap in crucial yet conventional key performance indicators (KPIs) but also encompasses new multi-dimensional functionalities. Numerous research organizations and industrial companies have put forth their proposals for the KPIs necessary for 6G. These proposals are being systematically integrated and refined within the framework of IMT. The following KPIs have been specifically extracted from the IMT-2030 vision, although the exact targets are still under extensive negotiation [11].

1.3.1 Peak Data Rate

In communication networks, the peak data rate is undoubtedly the most crucial metric. For 5G networks, the peak data rate must achieve at least 20 Gbps for downlink transmissions and 10 Gbps for uplink (UP) transmissions per device under perfect conditions. In contrast, the peak data rate anticipated for 6G is expected to be at least 10 times greater than that of 5G. Although the goal has not been finished at IMT-2030, the ambitious peak data rate requirement for 6G could reach the Tbps level to support information services in applications like the Metaverse, digital twins, and XR, etc. Despite being extremely challenging, this goal has been widely recognized across research communities. The confidence in achieving this goal primarily arrive from potential new transmission technologies such as super-large scale antennas, THz communications, orbital angular momentum (OAM), and visible light communications. These innovations have the capability to greatly expand the dimensions and range of signaling space across frequency, spatial, and electromagnetic domains, and thus gain an ultra-high data rate[11].

1.3.2 User-Experienced Data Rate

User-experienced data rates is needed to reach 100 Mbit/s in urban or suburban areas and is predicted to achieve 1 Gbit/s in hotspot areas. However, these targets have not been consistently realized on average in practical 5G networks. Given the constraints of peak data rate and the number of users within the same coverage area, it's understandable that the achievable user-experienced data rate in 6G is expected to improve by a factor of ten compared to 5G. Therefore, achieving a minimum of 1 Gbit/s for user-experienced data in 6G is expected, with the success of this goal depending significantly on efficient interference management and ongoing reduction in cell size [11].

1.3.3 Spectrum Efficiency

The spectrum efficiency of 5G has been significantly enhanced, achieving levels of 30 bps/Hz for uplink and 15 bps/Hz for downlink transmissions. According to recent discussions in the research community, 6G is predicted to achieve approximately 1.5 to threefold greater spectrum efficiency when compared with 5G. It is important to mention that the increase in spectrum efficiency is not as significant as the increase in data peak rate. This is because the potential for improvement at the link-level has already been largely utilized, and present link-level transmission is approaching the Shannon limit. The primary approach to improving spectral efficiency could involve focusing on exploiting spatial-domain resources through the introduction of a super-large antenna array. At the same time, effective and thorough interference suppression over overlapping coverage areas is likewise crucial[11].

1.3.4 Area Traffic Capacity and Connection Density

Area traffic capacity is defined as the total throughput provided within a unit of geographic area. According to the 5G vision specified by IMT-2020, the area traffic capacity requirement is $10Mbit/s/m^2$, while the 6G network will achieve a 100-times bump. The area traffic capacity can vary between $100Mbit/s/m^2$ and 1000 $Mbit/s/m^2$, depending on various application scenarios. This KPI signifies a revolutionary increase in the capability of mobile networks to provide continuous coverage. Connection density indicates the number of accessible devices per unit area. According to the 6G vision, the average estimated density is tenfold greater than that of 5G, and some more aggressive estimates propose a 100-fold improvement. This indicates that the connection density might potentially reach 10^7 to 10^8 devices $/km^2$, which is equivalent to 10 to 100 devices per m^2. The explosive increase in connection density aims to connect devices used by humans and machine-type nodes, creating a fully-connected smart cyber-physical system/network[11].

1.3.5 Mobility

Extending coverage is one of the core missions of the 6G network. In addition to satellite coverage, services provided by terrestrial access points and stations need to be extended to commercial airplanes and high-speed trains. In these cases, the moving speed can reach 1000 km/hour with specific Quality of Service (QoS) demands, which is twice as much as the the greatest mobility considered in 5G. The maximum Doppler frequency spread could exceed 15 kHz at a carrier frequency of 2 GHz, and this effect worsens with higher carrier frequencies. OFDM-like modulation approaches face even more stringent challenges in these scenarios, requiring the new ceiling-breaking techniques for the traditional physical layer in extremely high-mobility regimes[11].

1.3.6 Latency and Reliability

The IMT-2020 vision aims to limit air-interface latency to within 1 millisecond and achieve 99.999 reliability in 5G systems. This enables URLLC, supporting applications such as industrial automation and self-driving cars. However, due to the random-access procedures required for handling bursty traffic, collisions between different users' requests are inevitable, making it extremely challenging to achieve 1-millisecond latency in 6G networks. Although delays caused by collisions are often classified as access delays rather than air-interface latency, the accumulated latency like a whole, which is generally attributed to access delay, queuing delay, and air-interface latency (encompassing both transmission and processing delays)—can significantly impact users' Quality of Experience (QoE). In this scenario, reducing air-interface latency remains a significant factor in improving the QoE, as it decides how quickly each packet can traverse the link bottleneck over the air. Accordingly, extensive discussions are advocating for reducing air-interface latency as much as possible, aiming for the challenging target of 0.1 milliseconds[11].

1.3.7 Positioning and Sensing Capabilities

Positioning is a new KPI formally introduced for 6G, setting it apart from the visions established for 5G. Both research communities and industries aim to achieve accurate positioning function by capturing and extracting propagation features. This advancement would undoubtedly be beneficial for resource allocation, security monitoring, and other applications. Positioning functions can be further categorized into vertical positioning and horizontal positioning, each presenting its own set of challenges. The well-recognized accuracy for positioning requires to be around the centimeter level to enable practical use cases. The sensing function represents a more general yet powerful capability for 6G networks. Sensing functions encompass ranging, velocity and angle estimation, object detection, localization, imaging, and mapping. All the information may be tailored, fused, and distributed, simplify diverse applications, and eventually be crucial to creating the digital-twin system in a wide sense[11].

1.3.8 AI Capability

AI capabilities are envisioned to be integrated into the IMT-2030 vision, aiming to provide intelligent functionalities across IMT systems. These functionalities are specifically designed to support AI-enabled user applications. These applications include data collection, AI training, inference, computing, and more. However, specific applications or modes have not yet been well formulated or demonstrated. It's unsurprising that AI capabilities have introduced new tasks for mobile communications networks. Consequently, research on integrating essential communication functions with AI-supported abilities will continue to attract significant research attention[11].

1.3.9 Security, Privacy, and Trustworthiness

From a commercial standpoint, security protection for mobile communications networks has performed adequately through the evolution to 5G. However, with 6G, there are much more aggressive and ambitious requirements for security. Firstly, security needs to be guaranteed throughout the entire lifecycle of IMT-2030. Secondly, safeguarding user privacy becomes increasingly critical, encompassing not just user data or information, but also extending to the user's actions and intentions. Thirdly, two extremely challenging targets widely recognized as essential features for securing 6G networks are the zero-trust principle and one-time pad secure transmissions. Lastly, ensuring the security and continuous operation of the network has now been elevated to an ultra-critical role. Maintaining a substantial portion of the network operational and functioning normally during extreme weather events, faults, and natural disasters is crucial[11].

1.3.10 Sustainability

One controversial issue with 5G networks is the high energy consumption required to maintain their large-scale infrastructure. Continuously improving energy efficiency and reducing energy consumption is undoubtedly a central mission of 6G, aligning with global initiatives for carbon neutrality. Achieving a continual reduction in environmental impact is a high priority for 6G, aiming to contribute to sustainable and harmonious living conditions globally. In this time, sustainability demands are also imposed on certain network services itself. Particularly, extremely massive machine-type devices are key for implementing a fully connected cyber-physical network with sensing capabilities. As a result, extending the lifetime of not only the battery but also the devices' hardware has become a more serious concern than ever before. Additionally, software extensibility will be crucial in prolonging the devices' lifetime. Overall, the vision for 6G is becoming clearer, which is rather exciting yet also faced with an enormous gap with currently 5G systems, motivating a decade of ongoing research from standardization organizations, academic researchers, and also industrial bodies in related areas [11].

1.4 6G Architecture

The journey towards 6G has begun, and research into the 6G architecture is already underway. With most requirements worldwide, a financially sustainable and rapid 5G rollout has already begun. The development of the 5G architecture is still in progress and is likely to continue for another eight or more cycles. In addition, real-time dispatching and synchronization among natural, digital, and physical individuals are utilized to portray the future as spontaneous occurrences that generate artificially changed mortality experiences. From the network's perspective, tangible elements could be intricately linked with intercept and system-on-chip architectures. The digital aspect would represent next-generation software architecture and binary-digital representation. The natural component would involve collaboration with biosensors and novel mortal-machine integrations. To meet the stringent requirements for rigidity, implicit, belief, protection, efficiency, and automation necessary for robots to achieve various operational goals, they may need to be closely interconnected in tandem. The Het-Pall system, which includes extensive Pall computational resources, serves as the foundation for the 6G network. Simplicity can be achieved by utilizing concurrent RAN-CORE imposed microservices, innovative cell-liberated architectures, and trap architectures. A new information and data framework will be an essential element of 6G, given the crucial role of information and AI/Machine Learning (ML) optimization in the construction and maintenance of the 6G network. The networks can be changed for specific requirements, like sub-networks but additionally optimized slices, thanks to the 6G armature's stiffness. Robotization and connectivity, supported by an orchestrating framework and clear purpose, would be essential components for many industries. The secure armature, specific protocol options, charging and policy enforcement mechanisms, as well as network visibility are additional elements not covered in this discussion but are crucial topics for future studies to fully describe all the 6G armature. This section delineates the architectural changes necessary for 6G based on three components, as depicted in Fig. 1.3[12].

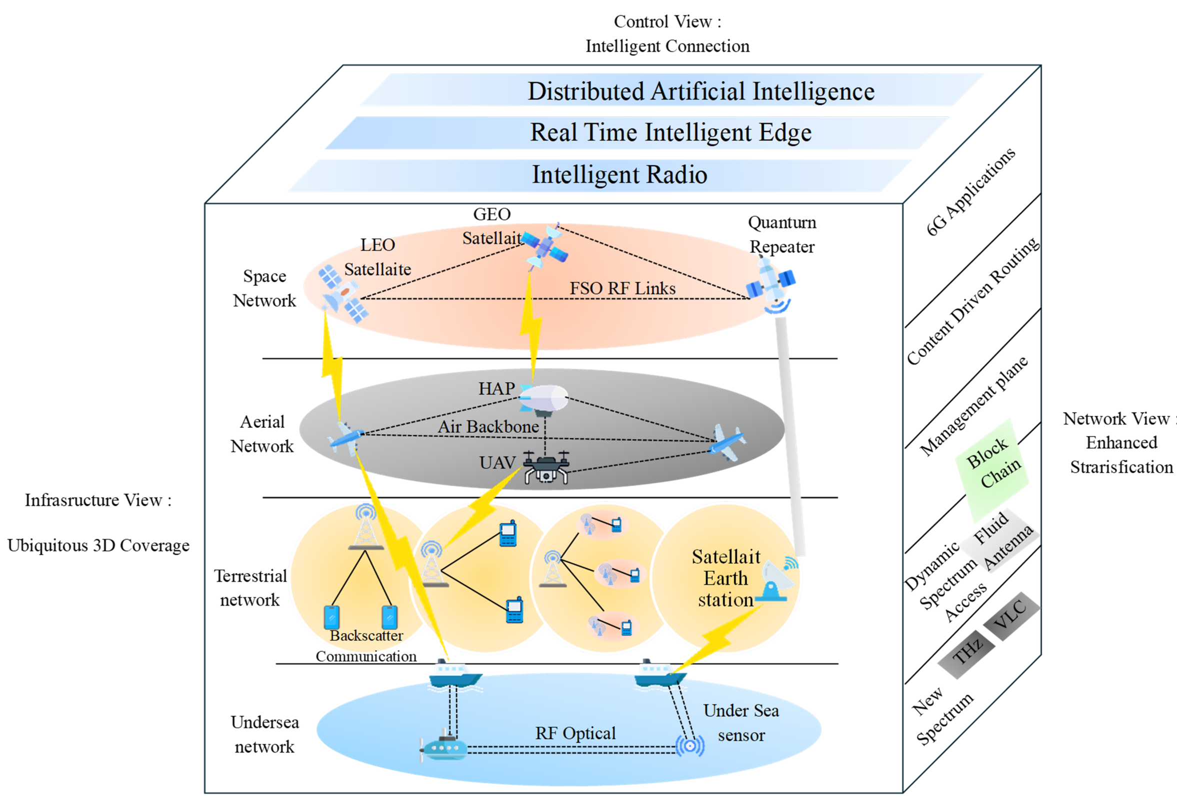

Figure 1.3: 6G Architecture.

1.4.1 From Terrestrial to Ubiquitous Three-dimensional (3D) Coverage

Enhancing the comprehensiveness of communication coverage is a goal in the design of next-generation networks. The current network design is constructed on ageing terrestrial cellular infrastructures. Non-terrestrial networks will be integrated into 6G to provide comprehensive wireless connectivity[12].

1.4.1.1 Space-Network

High Throughput Satellite (HTS) devices are recognized for providing broadband Internet solutions with pricing and capacity identical to terrestrial offerings. In the geostationary orbit (GEO), where most communications satellites reside, they orbit at an altitude of 35,786 km. This distance introduces considerable latency and makes connectivity with terrestrial mobile networks impossible. A proposed non-geostationary orbit (NGSO) satellite system and multiple satellite constellations aiming to capitalize on offering extremely high-internet connectivity with low latency, potentially generating significant revenue. Compared to a network of terrestrial optical fibers. a Low Earth Orbit (LEO) satellite system using co-routing radio-frequency and laser technologies may offer reduced latency connectivity [12].

1.4.1.2 Aerial-Network

High altitude platforms (HAP) operate in the stratosphere, whereas low altitude platforms (LAP), which are usually at a height little and over a few kilometers. These platforms can be broadly classified as two types of aerial networks. HAP networks can offer greater coverage and can last longer compared to LAP networks. Unmanned aerial vehicle (UAV)-based LAP networks, on the other hand, can be deployed more quickly, easily modified to meet communication system requirements, and function perfect narrow communication. In disaster emergency situations, where facilities are severely damaged or entirely absent, UAV networks provide mobile communication solutions. The proposed new trajectory optimization and path guidance techniques significantly aid in conserving energy[12].

1.4.1.3 Undersea-Network

The three primary categories of underwater wireless networks are radio frequency, acoustical, and optical communications. Due to the unpredictable and complex underwater setting, which leads to challenging network coverage, severe signal attenuation, and mechanical damage to equipment, there are many difficulties that need to be fixed[12].

1.4.2 Direction to Smart Network Connectivity

In recent times, there has been a significant emphasis from businesses and researchers on ML, which is a particular category of artificial intelligence. Furthermore, the integration of edge computing and artificial intelligence collaboratively reduces costs while enhancing consumer satisfaction. The creation of the 6G framework should thoroughly consider the possible uses of AI within networks and embrace an AI-driven approach, making intelligence a fundamental component of the 6G architecture. According to the baseline knowledge, a small and remote network object can intelligently modify the design based on several preset options in a distinctive yet predictable manner. The ultimate expectation for smart networks is their autonomous development, where they evolve and adapt independently[12].

1.4.2.1 Real-Time Intelligent Edge (RTIE)

Delivering compelling intelligent applications will be essential for the next-generation network, especially for services like autonomous cars, which are highly sensitive to response delays and hence take real-time, intelligent interactions with their environment. These services cannot rely solely on centralized cloud AI using static data, instead, they require RTIE capabilities that can make predictions, inferences, and decisions based on real-time information, is urgently required[12].

1.4.2.2 Intelligent-Radio (IR)

IR represents a comprehensive and expansive concept that encompasses both computational techniques and hardware. It operates as a single-entity approach for estimating hardware resources, where transceiver methods can dynamically configure based on hardware data. From this perspective, IR can effectively utilize the available spectrum through the physical layer. It enables adjustments to transmission methods and signal strength as needed[12].

1.4.2.3 Distributed-AI

The future of networking will likely be characterized by a sizable, decentralized framework, where intelligent decisions are made at numerous bitwise steps. Distributed AI utilizes shared resources within the system through a parallel process, which requires appropriately partitioning information and models to accelerate learning and enhance inference consistency[12].

1.4.3 Novel Infrastructure

TCP/IP has indeed served as the cornerstone of current network protocol design, proving highly successful. Recent shortcomings in the internet infrastructure pose challenges to reliably delivering future-oriented applications, primarily due to various emerging issues. Certain TCP/IP-based protocols, involving QUIC (Quick UDP Internet Connections), are somewhat reduced such difficulties. Regrettably, these patch-like protocols just contribute to the complexity of the internet and do little to resolve its base limitations. The current mode used by network layer packets, known as header-payload mode, is static and independent from the requirements of higher-level applications. Metadata and instructions set by app designers could play a crucial role in future IP protocols, enabling a wide range of potential developments and offering customized internet connectivity options. Similarly, the transport layer also needs further enhancements to meet future communication requirements [12].

1.5 Performance Metrics

6G targets to offer high QoS, QoE, and Quality of Physical Experience (QoPE). QoS related to the performance of the network, whereas QoE pertains to the performance as perceived by the users. QoPE is a newly-introduced metric that considers human perception too. Rapid adoption is occurring for promising applications such as XR, holographic telepresence, autonomous driving, eHealth, and under-water communication. In order to optimize the customer experience, network operators are putting greater emphasis on end-to-end service quality. Therefore, when transitioning to 6G networks, it is crucial that the architectural developments maintain these requirements for quality. Therefore, a 6G cellular network is anticipated to provide high levels of QoS, QoE, and QoPE, while also ensuring reliability and security. The move from Self-Organizing Networks (SON) to Self-Sustaining Networks (SSN) is expected to enable 6G networks to achieve high levels of automation, allowing them to independently maintain QoS, QoE, and QoPE. While measuring performance metrics remains subjective at this early stage due to 6G's infancy, this section underscores its foundational importance. Advancements in QoS, QoE, QoPE, and SSN, are expected to be useful for future 6G communications[13].

1.5.1 Improving Quality of Service (QoS)

Applications such as XR, holographic telepresence, autonomous driving, e-Health, and others are becoming increasingly relevant and are not just distant future concepts. These applications pose significant challenges to meet stringent QoS requirements, such as achieving a massive data rate of 1 Tbps, less than 1 ms end-to-end round-trip latency, 99.99999% reliability, ground to aerial coverage, and high spectral and energy efficiency. Therefore, the key attributes of QoS include network availability, performance reliability, uninterrupted coverage, security and privacy, and system integrity. The abundance of THz spectrum and the implementation of super-massive MIMO are expected to alleviate resource constraints while ensuring higher QoS. AI and ML will also play a crucial role in efficiently utilizing user information, thereby enhancing the QoS. Nevertheless, the upcoming 6G applications present novel QoS concerns that cannot be sufficiently addressed by traditional QoS models and metrics. Thus, the exploring novel QoS metrics and models, and their interdependencies in wireless links in different constraints are required for enhancing 6G mobile wireless networks[13].

1.5.2 Refining Quality of Experience (QoE)

QoE is deemed a critical performance metric for the 6G era, particularly due to the sensitivity of applications like telepresence and telesurgery to factors such as data rate, reliability, and latency. The concept of QoE is challenging to measure due to its subjective nature. The QoS metrics used in 5G, which primarily include packet loss rate, end-to-end latency, and round-trip times, are now seen as less effective for the emerging applications of 6G wireless networks. QoE focuses on the user's perceived satisfaction, aesthetic experience, comprehension, and manageability of applications. Therefore, in addition to QoS, user experience outcomes are also crucial parameters to ensure QoE, as illustrated in Fig. 1.4 To further enhance QoE, network and service management must undergo significant transformation through advanced research in automation, cognitive operations, AI, and ML[13].

1.5.3 Quality of Physical Experience (QoPE)

The future 6G expects an increase in human-centric services that are tightly connected with human users. The innovative concept of wireless Brain-Computer Interaction (BCI) presents a novel emotion-driven application that necessitates 6G connectivity. Leveraging wireless BCI technology, users can interact not only with their surroundings and other people but also with the embedded devices in their environment. Utilizing such technology could enable individuals to control and monitor their environment through gestures and communicate via haptic messages. The performance metrics required to support wireless BCI services will differ from those of 5G technology. In addition to the rate-latency-reliability requirements, BCI involves the physical perception and actions of humans, leading to the development of a new set of QoPE metrics. These metrics will integrate human physiological factors with QoS and QoE metrics, as illustrated in Fig. 1.4[13].

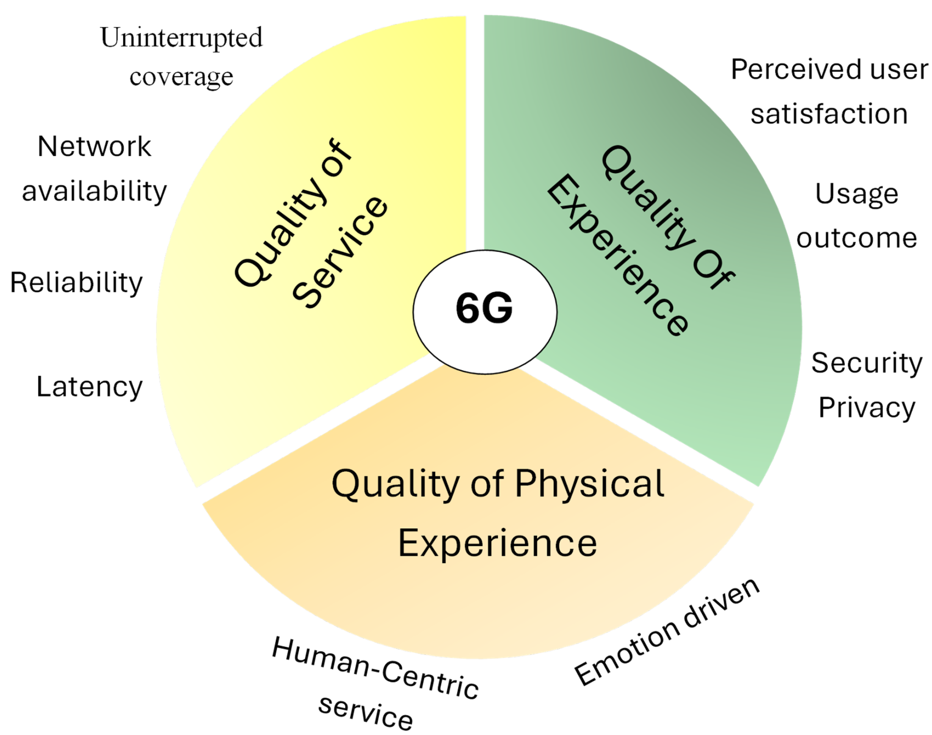

Figure 1.4: The relation between QoS, QoE, and QoPE.

1.5.4 Self-Sustaining Networks

5G technology pioneered the concept of an intelligent communication network by incorporating AI and ML-based operations. User experience and network automation are expected to improve by reducing human intervention and automating functionalities such as wireless network configuration, optimization, and healing. 6G will necessitate a move from traditional self-organizing networks to an AI-based intelligent, cognitive, and self-sustaining network. This transition has the potential to sustain long-term KPIs even amidst highly dynamic and complex scenarios stemming from 6G applications. AI and ML will empower 6G to enable operations such as self-aggregation, self-learning, self-optimization, and self-adaptiveness autonomously, without requiring human intervention, as depicted in Fig. 1.5 [13].

Figure 1.5: The concept of SSN

1.6 Standardization

The success of mobile communications from 1G to 5G is largely due to proprietary technologies that have been standardized over time. Each generation has required substantial investment in research and development to transform innovations into standards, hardware, software, and services. This standardization process has provided a foundation for technology vendors to develop products and services. The process has been stable, involving a defined community of technology vendors, mobile network operators, system integrators, academia, and regulators. With 5G, the ecosystem expanded to include enterprises and industries, introducing numerous use cases and new stakeholders. Unlike previous generations, 5G standardization follows a single coordinated approach to meet IMT-2020 requirements. This contrasts with the multiple standards paths seen in 3G and 4G. The 5G service-based architecture, convergence of communication, IT, data, and user-centricity challenge the traditional Third Generation Partnership Project (3GPP) process. Recent geopolitical and societal changes, including issues related to data sovereignty, AI, and digital infrastructure, have influenced discussions on national roles in standardization. The ongoing competition in technology, particularly in semiconductors and digital sovereignty, is exemplified by initiatives like the US "Clean Network Initiative," addressing data privacy and security. These developments raise concerns about potential fragmentation in 6G standardization [14].

1.7 6G Requirements

To enable new applications, 6G networks must offer enhanced capabilities that surpass those of 5G networks. Fig. 1.6 illustrates the essential requirements that 6G networks must meet to support future applications. Based on various studies, 6G networking requirements can be categorized as follows:

- Further enhanced Mobile Broadband (FeMBB): The mobile broadband speed must exceed the limits of 5G, achieving peak data rates at the Terabits per second (Tbps) level. Additionally, the user-experienced data rate should be enhanced to reach Gigabits per second (Gbps) levels.

- Ultra-massive Machine-Type Communication (umMTC): Connection density is going to raise in 6G due to the increasing number of Internet of Things (IoT) devices and the new concept of IoE. These devices are connected to each other and provide cooperative services in autonomously.

- Enhanced Ultra-Reliable, Low-Latency Communication (ERLLC/eURLLC): The end-to-end (E2E) latency in 6G should be reduced to microsecond (μs) levels to support new high-end real-time applications.

- Extremely Low-Power Communications (ELPC): The network energy efficiency of 6G will be improved by 10 times compared to 5G and 100 times compared to 4G. This enhancement will enable extremely low-power communication channels for resource-constrained IoT devices.

- Long-Distance High-Mobility Communications (LDHMC): With the support of fully integrated satellite technologies, 6G will facilitate communication in extreme locations such as space and the deep sea. Furthermore, AI-based automated mobility management systems and proactive migration systems will support seamless mobility at speeds exceeding 1000 kmph.

- High-Spectrum Efficiency: The spectrum efficiency in 6G will be further improved, achieving up to 5 times the efficiency of 4G and nearly double that of 5G networks.

- High-Area Traffic Capacity: The exponential growth of IoT will require improving the area traffic capacity by 100 times compared to 5G networks, achieving up to 1 Gbps traffic per square meter in 6G networks.

- Massive Low-Latency Machine Type (mLLMT): In 6G, URLLC and mMTC services must be connected and new unified solutions are required to meet the challenge of providing effective and quick massive connectivity.

- Mobile broad bandwidth and low-latency (MBBLL), massive broad bandwidth machine type (mBBMT), massive, low-latency machine type (mLLMT) [15] .

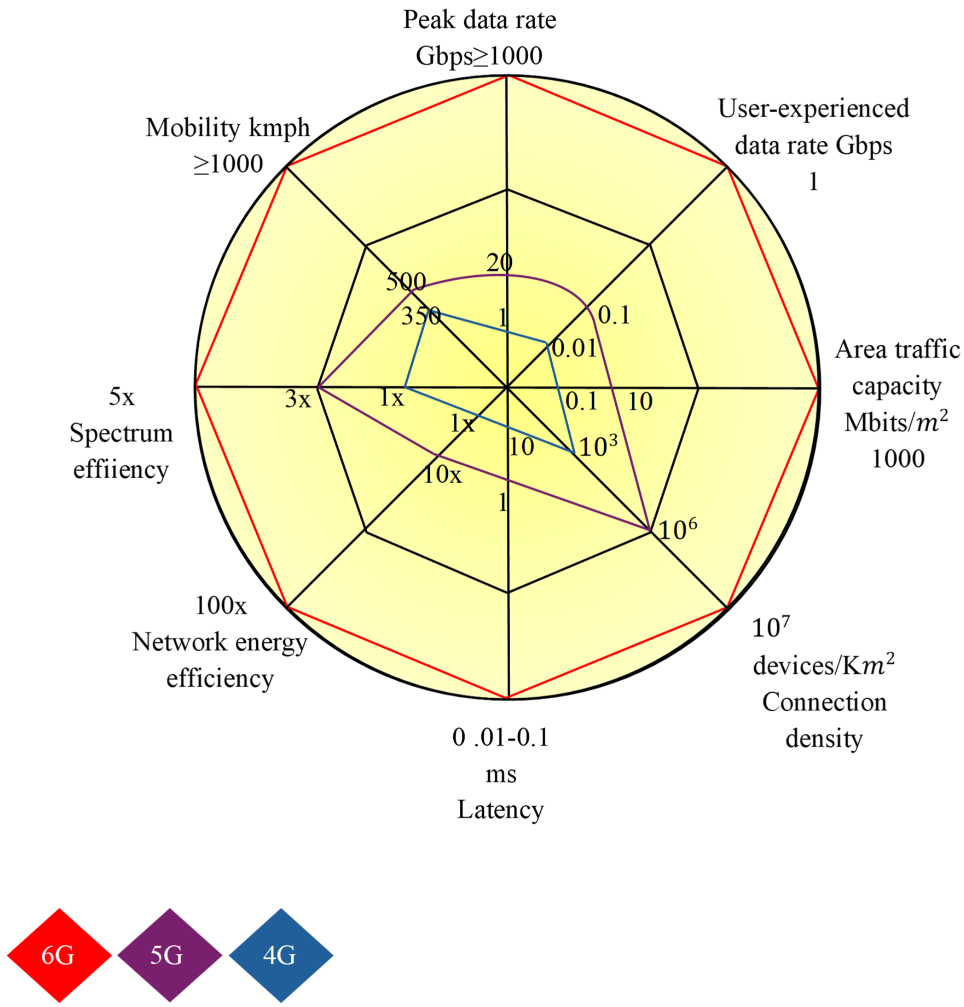

Figure 1.6: 6G Visions.

1.8 Key Technologies

To meet the demanding performance needs of disruptive applications and use cases, disruptive technologies in radio transmission and networking will be developed and implemented to create the 6G system. So far, the wireless community has shared insights into potential technologies through academic publications, white papers, and research project topics. This section offers readers a comprehensive view of potential 6G technological enablers, which can be divided into several categories:

- New Spectrum: including mmWave, THz communications, and optical wireless communications (OWC)

- New Air Interface: consisting of massive MIMO, intelligent reflecting surface, and next-generation multiple access.
- New Networking: encompassing open Radio Access Network (RAN) and non-terrestrial networks
- New Paradigm:, driven by the convergence of communication, computing, and sensing, as well as the integration with AI technology[16].

1.8.1 Millimeter Wave

mmWave technology, introduced in 5G, will remain crucial in 6G networks, expanding bandwidth with carrier frequencies up to 300 GHz. This technology enhances channel capacity, device portability, integration, and supports larger antenna arrays with narrower beams, beneficial for applications like detection radars and physical layer security. Different frequencies within the mmWave band exhibit variable atmospheric and molecular absorption, allowing for diverse use cases. Specific bands (35, 94, 140, and 220 GHz) enable long-distance transmission, while others (60, 120, and 180 GHz) are suited for short-range, covert networks. However, mmWave technology faces challenges such as significant non-linear signal distortions, restricted effective transmission range, and reliance on Line-of-Sight (LOS) paths. High propagation loss, poor diffraction, and increased channel sensitivity to mobility exacerbate these issues, especially in dense environments with obstacles[16].

1.8.2 Terahertz Communications

Despite current spectral redundancy, mmWave technology may not meet future bandwidth demands. Therefore, higher frequency wireless technologies, such as THz and optical bands, are expected to be crucial in 6G networks, offering substantial bandwidths. Like mmWave, THz waves struggle with high path loss, relying on directive antennas and LOS channels, resulting in small coverage. However, THz frequencies provide larger bandwidths, enabling ultra-high performance in throughput, latency, and reliability. THz systems are less sensitive to atmospheric effects compared to mmWave and optical systems, simplifying beamforming and tracking. This makes THz communication a valuable supplementary solution for indoor communications, wireless backhaul, and cyber-physical applications with stringent QoS requirements. The higher frequency also allows for the integration of over 1000 antennas in a single THz Base Station (BS), supporting extreme traffic capacity and massive connectivity, essential for ultra-massive machine-type communications like the IoE. Despite its advantages, THz technology faces significant technical challenges, particularly in developing essential hardware circuits like antennas, amplifiers, and modulators. Efficiently modulating baseband signals onto high-frequency carriers using integrated circuits remains a critical challenge for practical deployment . Fig. 1.7 illustrates the millimeter and terahertz wave band [17],[16].

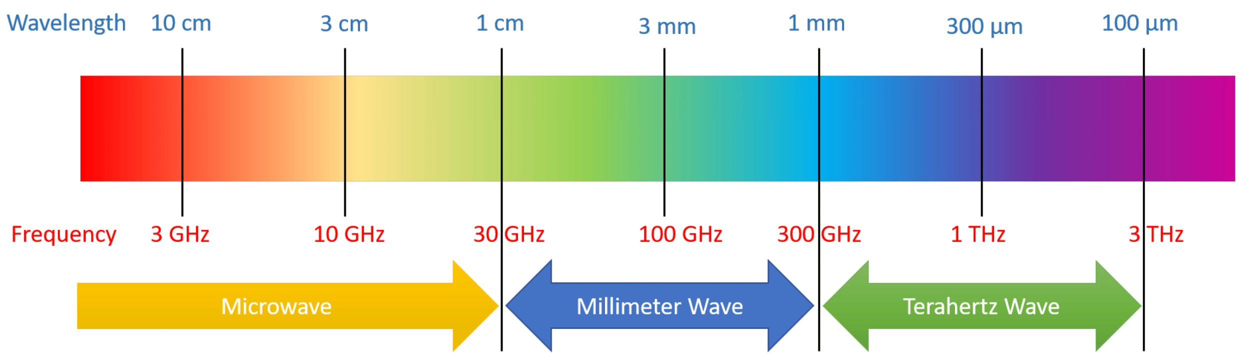

Figure 1.7: Millimeter and Terahertz wave band

1.8.3 Optical Wireless Communications (OWC)

OWC leverage Infrared, visible light, or Ultraviolet (UV) frequency bands, offering substantial bandwidth without requiring spectrum regulation. This technology provides high-speed, low-cost access due to the availability of optical emitters and detectors, and mitigates security risks and radio radiation concerns, making it ideal for environments sensitive to electromagnetic interference like intelligent transportation systems, aircraft, and medical settings, it is present in Fig. 1.8 . OWC, especially in the visible light spectrum (Visible Light Communications or VLC), has gained attention for its efficiency and minimal power consumption. Operating between 400-800 THz, VLC uses LEDs and image sensors or photodiode arrays for transceivers, offering long lifespans, low costs, and unlicensed spectrum access. VLC is particularly suitable for battery-sensitive applications like IoT and Wireless Sensor Networks (WSNs) and performs well in non-terrestrial environments such as aerospace and underwater settings, potentially becoming a key component of the 6G ecosystem. Terrestrial point-to-point OWC, known as Free-Space Optical (FSO) communications, utilizes the near Infrared band to deliver high data rates over long distances using focused laser beams, providing a cost-effective solution for terrestrial backhaul bottlenecks, crosslinks among space, air, and ground platforms, and high-capacity inter-satellite links for LEO satellites. Additionally, advancements in solid-state optical transmitters and detectors are enhancing UV communication, offering non-LOS capabilities with broad coverage and high security benefits [18], [16].

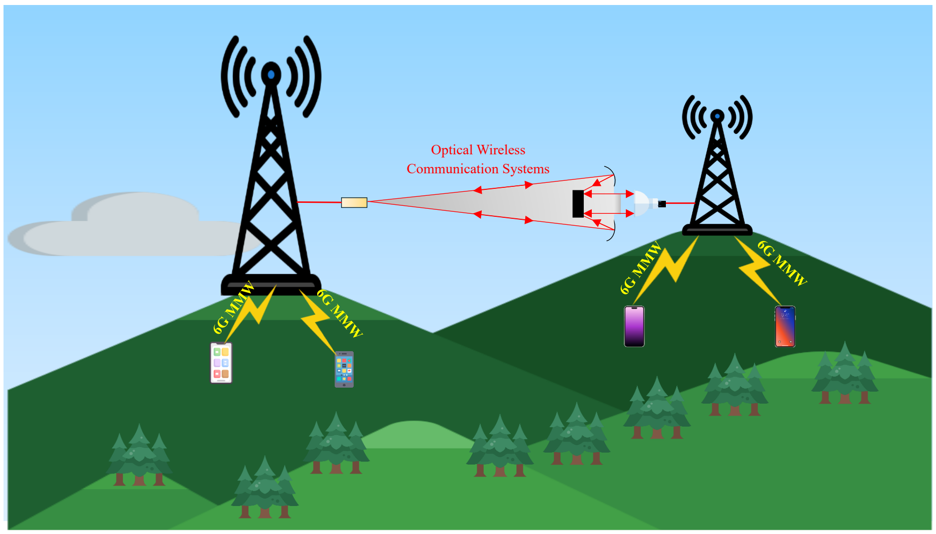

Figure 1.8: The integration of 6G signals with OWC systems

1.8.4 Massive MIMO

Massive MIMO is a key technology in 5G New Radio (NR), utilizing many antennas to concentrate transmission energy precisely on small areas . Fig. 1.9 presents this technology . This enhances both spectral and energy efficiency and is cost-efficient due to the use of low-cost, low-precision RF components. In 5G, up to 64 antennas are used at lower frequencies (around 700 MHz) and up to 256 antennas at higher frequencies (around 4 GHz). Massive MIMO operates in Time Division Duplex (TDD) mode to exploit channel reciprocity, and analog beamforming is preferred at even higher frequencies (mmWave). Massive MIMO is expected to be crucial for 6G, especially in deploying higher mmWave and THz bands, with an even greater number of antenna elements. This will impose technical challenges on precoding schemes, RF implementation, hardware impairments, detection algorithms, and interference management. The aim for 6G is to develop more spectral-efficient, energy-efficient, and cost-efficient Massive MIMO schemes. Cell-free Massive MIMO, a distributed scheme with no traditional cells or cell boundaries, is gaining attention. In this scheme, numerous distributed access points (APs) serve users simultaneously on the same time-frequency resource, providing uniform QoS and eliminating the under-served problem at the cell edge. This makes cell-free Massive MIMO a promising solution for private networks in industrial applications. The synergy between cell-free and cellular networks is expected to advance next-generation mobile networks[16],[17].

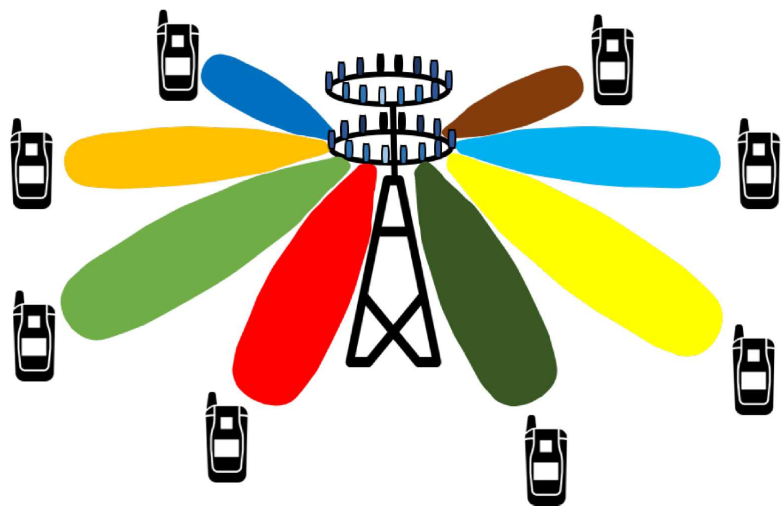

Figure 1.9: Massive MIMO.

1.8.5 Intelligent Reflecting Surfaces

Utilizing high-frequency bands over 6 GHz in 6G networks introduces challenges like higher propagation loss, lower diffraction, and severe blockage. Massive MIMO has been effective in compensating for these issues with active beamforming in the mmWave range, but it may not suffice for future 6G requirements. Intelligent Reflecting Surfaces (IRS), also known as Reconfigurable Intelligent Surfaces (RIS), are emerging as a promising solution. Fig. 1.10 present the architecture of the RIS technologies . IRS consists of programmable material sheets that can modify their radio reflecting properties. When placed on surfaces like walls and ceilings, IRS creates a Smart Radio Environment (SRE) by enabling passive beamforming. This enhances channel gain at a low cost and with low power consumption compared to active massive MIMO arrays. IRS can cover large surfaces, facilitating accurate beamforming with ultra-narrow beams and works universally across all RF and optical frequencies, making it cost-effective for 6G. However, IRS technology still faces challenges in channel and surface modeling and estimation, particularly in the near-field range. Additionally, commercial deployment depends on external evaluations, such as building assessments not owned by mobile operators. Therefore, standardizing frameworks, virtual interfaces, agreements, and signaling protocols is necessary to enable 6G operators to effectively access and utilize IRS-equipped objects in both public and private domains [16],[19],[20] ,[21]

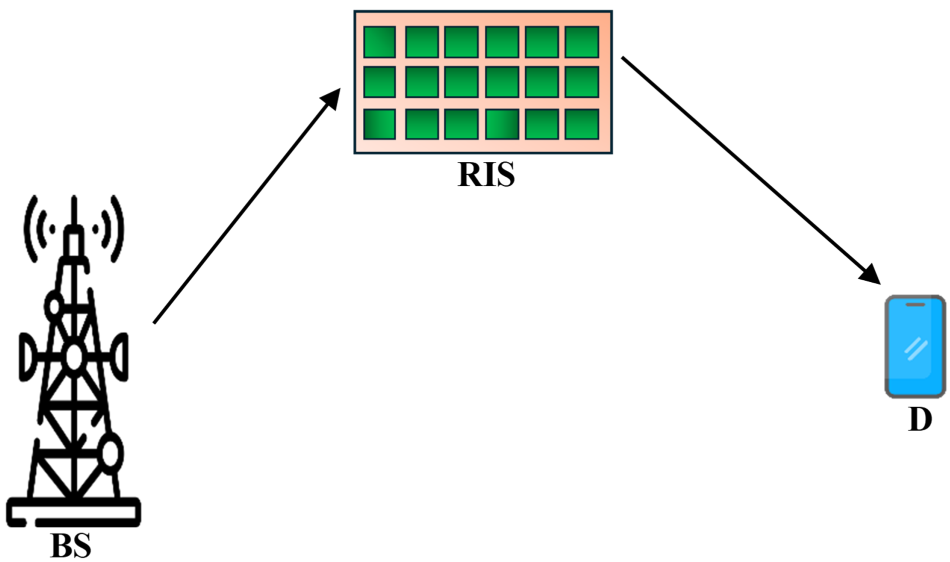

Figure 1.10: Architecture of IRS

1.8.6 Next-Generation Multiple Access (NGMA)

LTE and NR use OFDMA as their orthogonal multiple-access technology, which, unlike CDMA used in 3G, is effective against multi-path fading and pairs well with MIMO to enhance spectral efficiency. However, the full potential of MIMO-OFDM requires precise MIMO precoding and resource mapping, which becomes increasingly complex with the rise of massive and ultra-massive MIMO systems. To address these complexities, AI-driven MIMO-OFDM transceivers have been proposed for 6G systems to optimize real-time adaptation. In contrast to OFDMA, NOMA allows multiple users to share the same radio resource unit, enhancing system throughput and connection density. NOMA has evolved from downlink-focused

Multi-User Superposed Transmission (MUST) in LTE Release 13 to uplink grant-free transmission in Release 16, reducing control signaling, latency, and power consumption. NOMA is seen as crucial for 6G networks, supporting massive connectivity and new spectra, including mmWave, THz, and optical frequencies. When combined with Coordinated CoMP, NOMA outperforms traditional OMA in power and spectral efficiency. However, NOMA's reliance on successive interference cancellation increases receiver complexity, especially in cooperative decoding scenarios requiring specific D2D interfaces and careful handling of security concerns[16].

1.8.7 Open Radio Access Network (O-RAN)

To support disruptive use cases, 6G network infrastructure must be flexible, smart, and open to multi-vendor equipment and multi-tenancy. This will be achieved through softwarization, cloudification, virtualization, and network slicing. A key development in this context is the O-RAN, which aims to create a resource-efficient, cost-effective, software-driven, virtualized, slicing-aware, centralized, open-source, open hardware, and intelligent radio network. O-RAN, driven by the O-RAN Alliance, enables a standardized, open, multi-vendor, and AI-powered hierarchical structure, allowing third parties and mobile operators to deploy innovative applications and services. Based on the NFV Management and Orchestration (NFV-MANO) reference architecture by ETSI, O-RAN uses commercial off-the-shelf hardware, virtualization, and software, reducing CAPEX, OPEX, and energy consumption. However, O-RAN faces challenges, including the integration of multi-vendor technologies, harmonizing management and orchestration frameworks, and addressing performance validation and troubleshooting. Ongoing research from both industry and academia is crucial to advance O-RAN and realize its potential in future 6G networks[16].

1.8.8 Non-Terrestrial Networks

Legacy cellular systems focused on terrestrial infrastructure, limiting wide-area coverage. In remote areas like oceans, mountains, and sparsely populated regions, terrestrial networks are impractical or cost-ineffective, and they are also vulnerable to natural disasters. To address these issues, the 6G network aims to integrate non-terrestrial infrastructures, creating an Integrated Space and Terrestrial Network (ISTN). An ISTN includes:

1. Ground layer: terrestrial base stations
2. Airborne layer: High Altitude Platforms (HAPs) and UAVs

3. Spaceborne layer: satellite constellations

Fig. 1.3 presents the basic architecture of ISTN. Terrestrial networks only cover limited areas, so satellites have been the traditional solution for extensive coverage. However, GEO satellites have high costs, low data rates, and high latency. In contrast, LEO satellites offer lower latency and propagation loss, making them more suitable for direct connectivity with mobile and IoT devices. The Iridium constellation, with 66 LEO satellites, has been a technological milestone despite its initial commercial struggles. SpaceX's advancements in reusable rockets have reduced space launch costs, enabling larger space infrastructures. For 6G, integrating satellite networks is recommended to achieve global ubiquitous coverage, ensuring connectivity anywhere and anytime [16],[22].

1.8.9 Artificial Intelligence

AI is emerging as a key enabler for 6G networks, addressing the complexity and heterogeneity of mobile networks with advanced ML techniques. ML, including supervised, unsupervised, and reinforcement learning, is valuable for optimizing various aspects of radio and network management, from the physical layer to network operations. Deep learning, a subset of ML, offers significant benefits such as improving adaptive transmission parameters in massive MIMO systems, enhancing fading channel estimation, optimizing RF designs, and advancing network management and orchestration for Mobile Edge Computing (MEC) and network slicing. Cutting-edge techniques like federated learning and transfer learning are also gaining traction. Federated learning processes data locally to protect privacy and collaboratively refines models without exposing sensitive information. Transfer learning allows for quick adaptation of pre-trained models to new environments with minimal data, facilitating faster and more efficient model deployment. Additionally, the AI-as-a-Service paradigm leverages edge computing resources to provide AI capabilities to end-user devices like robots, smart cars, and drones, which require significant computational power but have limited on-device resources. This approach supports AI tasks such as computer vision, speech recognition, and motion control, enhancing the capabilities of next-generation terminals[16].

1.8.10 Communication-Computing-Sensing Convergence

Mobile edge networks enhance computing and caching capabilities at the network edge, facilitating low-latency, high-bandwidth, and location-aware services. As IoT and the Tactile Internet expand, an increasing number of sensors and actuators connect to mobile networks, envisioning the next-generation system as a comprehensive platform for ubiquitous communication, computation, storage, sensing, and control. In control systems, wireless connectivity is preferred for its integration and mobility advantages over wired connections, giving rise to URLLC. Traditionally, control and communication systems are designed separately—control components are developed first, followed by a wireless system to meet the performance criteria. For URLLC, key performance indicators include 99.999% reliability and 10 ms latency. Recent studies suggest the need for in-loop co-design of communication and control systems, where the Age of Information (AoI) affects closed-loop reliability. The AoI, which measures the freshness of information in feedback channels, is influenced by sensor sampling rates and decision rates. Thus, communication system performance is intertwined with control system design. Similarly, in cloud computing, managing task aging and congestion is crucial. Long-running tasks can block other tasks, leading to inefficiencies. To mitigate this, preempting tasks and optimizing scheduling to reduce AoI is necessary. Effective preemption and scheduling require coordination among terminal devices, network controllers, and cloud servers, rather than relying on individual systems alone [16].

1.9 Challenges

Developing 6G involves several challenges, including standardizing spectrum allocation for interoperability and advancing high-frequency (THz) spectrum hardware. Integrating THz antennas and ensuring power efficiency in OWC are critical issues. Enhancing design and signal processing techniques, such as spatial mode multiplexing, can improve FSO capacity. Channel modeling is vital for designing radio systems, requiring a balance between deterministic and statistical approaches. Addressing hardware aspects in channel modeling and using AI/ML techniques for IRS are necessary. Device-free localization presents challenges, necessitating regular environment measurements. Developing new devices for future applications requires optimizing design across network levels, generalizing solutions to simplify customized optimization [11].

1.10 Role of Patents and Licensing

For the past fifty years, mobile communications companies have relied on patent licensing to generate value. ETSI has managed the evolution and control of standards, ensuring fair and non-discriminatory licensing. This model has facilitated global technology co-development and adoption. The 5G era expanded the ecosystem to include more stakeholders, requiring advancements in radio access networks (RAN) and new licensing rules for 6G. Companies may need to cooperate vertically while competing horizontally, necessitating precise FRAND licensing rules due to the complex landscape. The convergence of ecosystems will introduce new roles in system integration and management. 6G systems will likely focus on core capabilities for lower layers, with open interfaces allowing for modular and programmable functions. This openness fosters competition and innovation. Balancing intellectual property protection with wide diffusion is crucial. A significant debate revolves around who should pay for SEP licenses. Establishing fair licensing rules is essential to avoid disputes and promote innovation, ensuring 6G functions as a general-purpose technology [14].

1.11 CONASENSE and the Future Wireless Communications

To comprehend the intricates of future use cases, which 6G can support, an instance and starting point must be addressed and discussed. For this purpose, CONASENSE is explained in this section. CONASENSE is an abbreviation for four key research fields of combining Communication, Navigation, Sensing, and Services. The concept of CONASENSE was envisioned by society's researchers around 2012, and since then, several articles and books have been published about it. The CONASENSE concept focuses on integrating and enabling the main areas into a future society that will live and experience the convergence of cyber and physical spaces. This theory concentrates on systems interconnectivity to enable the coexistence of five dimensions: the traditional three physical dimensions, plus time, and the cyber world. This integrated approach aims to create a new reality that can offer innovative services for humanity. Every aspect of this idea influences the way researchers perceive and develop new communication networks and their interconnected services. Presented below is an overview of the CONASENSE architecture:

1.11.1 Communication

This research area concentrates on a CRN designed to optimize data transmission, provides energy efficiency through nanogenerators, and advanced data compression and protocols for a decentralized, complex, and heterogeneous network[23].

1.11.2 Navigation

The future sensors' capacity to offer every network node a precise location in time and space down to centimeter-level is important in various future wireless applications. It will be helpful for autonomous vehicles to drones and nanotechnologies utilized in the medical field. Thus, the combination of Global Navigation Satellite Systems (GNSS) with other external sensors will provide 99.999% reliability and safety for these services[23].

1.11.3 Sensing

Sensing plays a crucial role in providing context awareness for the data exchanged between network nodes. It also ensures guaranteed data transmission and supports geolocation-based services. From this perspective, quantum communications and semantic algorithms emerge as strong candidates to provide technical solutions[23].

1.11.4 Services

There are numerous services poised to benefit from CONASENSE, including flying cars, drones, and space exploration, among others. Evaluating the CONASENSE architecture indicates that 6G will play a pivotal role in merging the virtual and physical worlds[23].

1.12 Knowledge Home in the 6G Era

Knowledge Home, short for Knowledge Human Bond Communication Beyond 2050, embodies the concept of integrating human five senses to interact with the environment and surroundings using technology. The five human senses—optic (vision), auditory (hearing), olfactory (smell), gustatory (taste), and tactile (touch)—form the sensory organs that enable human sensorial cells to receive and transmit information. Thus, Knowledge Home concept will bring all these sensorial stimuli to communicate with a wireless network that may establish a near to real-time interaction with everyone in a personal area network (PAN). With this concept in mind, environments such as homes, offices, smart transport systems, spaceships, or even stadiums can provide human responses based on the analysis of the five senses. They can interact and propose appropriate responses according to the sensory information captured within the PAN area. The responses provided by sensors analyzing human senses can vary widely, from adjusting temperatures based on people's reactions in the environment to contacting authorities to assist individuals in distress situations locally. For all these ideas to become reality, Human Bond Communication (HBC) requires a robust and intelligent network that prioritizes high QoS for data traffic. Therefore, to handle the significant amount of real-time data traffic generated by sensors and human interactions, an intelligent network must be carefully planned and implemented [23].

1.13 Conclusion

In this chapter, we discuss the main concepts related to 6G networks. We begin with the evolution of mobile communications from 1G to 5G. Subsequently, we analyze the different KPIs, highlighting the Peak Data Rate as the most important metric among others. We present the proposed architecture for the next generation of networks, emphasizing the critical role of artificial intelligence in building the new infrastructure. Alongside existing performance metrics, a new metric called QoPE emerges, reflecting the anticipated increase in human-centric services that are closely connected with users. We also examine the roles of standardization and patents in the creation of existing and future generations of mobile networks. Key technologies are categorized into essential new components: spectrum, air interface, networking, and paradigm. Finally, we explore key use cases encompassing communication, navigation, sensing, and services. In the next chapter, we will explore CR and NOMA technologies, and the main concepts related to it.

Chapter 2

Theoretical Background about CR and NOMA

2.1 Introduction

The use of the Internet today is witnessing great demand from people. Day after day, the number of users increases and thus the number of devices increases, to the point that there are expectations that the number of devices connected to the Internet will exceed the number of people on Earth. This great demand for purchasing the latest electronic devices is offset by the fact that the spectrum is fixed as our need for more and more applications increases in the future. Hence the problem of spectrum scarcity emerged, and one of the most important solutions proposed to solve it is to use a technology called CR, which can be further enhanced by integrating it with NOMA technology.

In this chapter, we will explore the definitions of these technologies and discuss fundamental concepts such as the types and network components of CRNs. Additionally, we will cover the general equations relevant to NOMA technology in both uplink and downlink scenarios.

2.2 Basic Concepts of Cognitive Radio (CR)

2.2.1 Definitions

From a tautological perspective, a CR can be defined by “A radio that is cognitive,” or paraphrasing Descartes, “Cogitat, ergo est CR. ” It means “It thinks, therefore it’s a cognitive radio”. In the 1999 Joseph Mitola III paper that first coined the term “cognitive radio” and give the first definition in [24], after that Haykin give another definition but it was better and more specific in [25]. Until the Federal Communications Commission (FCC), has defined a CR as : "A radio that can change its transmitter parameters based on interaction with the environment in which it operates" , it is the best definition and summery this technology in few words [24], In addition to all these definitions, there are other definitions. so that every individual, organization, or institution formulates a definition of this technology in a way that suits its specialization. For brevity, we have not mentioned the rest of the definitions for more details in references [24],[26].

2.2.2 The Characteristics

According to the FCC, CR can be characterized by two primary features:

- Cognitive capability: The identification of unused areas of the spectrum at a certain time or location can be achieved by real-time interaction with the radio environment. As depicted in Figure . 2.1, the utilization of CR allows for the utilization of temporally or frequency unutilized spectrum, commonly known as a spectrum hole. As a result, the optimal spectrum can be chosen, shared among other users, and utilized without causing disruption to the licensed user.
- Reconfigurability: A CR's hardware design allows it to be configured to operate on a range of frequencies for both transmission and reception, as well as different access technologies. This capability enables the selection and reconfiguration of the optimal spectrum band and the most suitable operational settings. To enable these functionalities, CR necessitates the implementation of a new radio frequency (RF) transceiver architecture. The specifics of this transceiver will be detailed in in the next section [27].

2.2.3 Software Defined Radio (SDR)

The CR is built using a SDR network [28]. This type of radio has software defining its carrier frequency, signal bandwidth, modulation, and network access. Recent SDR systems integrate essential cryptographic techniques, forward error correction coding, and source coding for voice, video, or data inside their software structure [29].

2.2.4 Spectrum Holes

"A spectrum hole is a band of frequencies assigned to a primary user but at a particular time and specific geographic location, the band is not being utilized by that user". Spectrum holes can be divided into two distinct types: temporal and spatial spectrum holes, as seen in Fig. 2.1. The appearance of a temporal spectrum hole is characterized by the absence of primary transmission within a certain frequency band of interest for a given time period. The geographic location that is distant from primary receivers (PRs) presents the presence of a spatial spectrum hole. The development of many antennas results to the creation of additional dimensions of spectrum holes, such as the code and angle dimension [30].

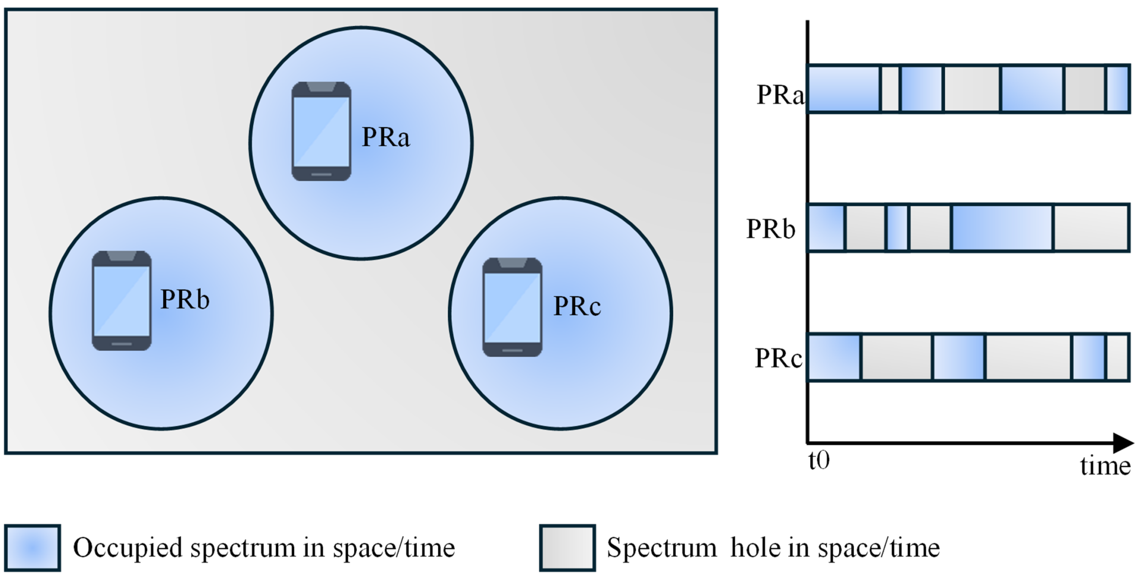

Figure 2.1: Temporal and spatial spectrum holes .

2.2.5 Cognitive Cycle

The cognitive cycle illustrated in Fig. 2.2 includes a summary of the primary stages involved in the CR process. The cognitive cycle enhances the process of intelligent adaptations by facilitating the learning and sharing of information among the many entities inside the network. The CR cycle consists of six primary sections:

- Environment: This involves networks as well as the environmental conditions that surround it, like physical channels, other devices, users, networks, and other things that have the potential to impact network conditions, such as obstacles, weather conditions, trading rules, and economic indicators.

- Sense: The various CR entities contain the ability to sensing and monitoring the environment, like the spectrum bands, levels of interference, parameters of the physical propagation channel, and the positions of PUs and SUs.
- Plan: SUs formulate strategies and evaluate them just before taking decisions.
- Decide: Decisions depend on knowledge and learning, and the process of making decisions results in the best use of the system's resources.
- Act: SU will behavior on the environment based on the decisions that were made. This can happen in a series of behaviors, such as routing of packets, access the media, allocating resources, and changing of transmission schemes.
- Learn: Learning is the most important part of the CR cycle. Each node has a knowledge base and a learning tool that helps it keep track of all the information required about the network and its conditions. This lets the system learn from actions happening currently and in the past, guess what actions will happen in the future, and use that information smartly when planning and making decisions [31].

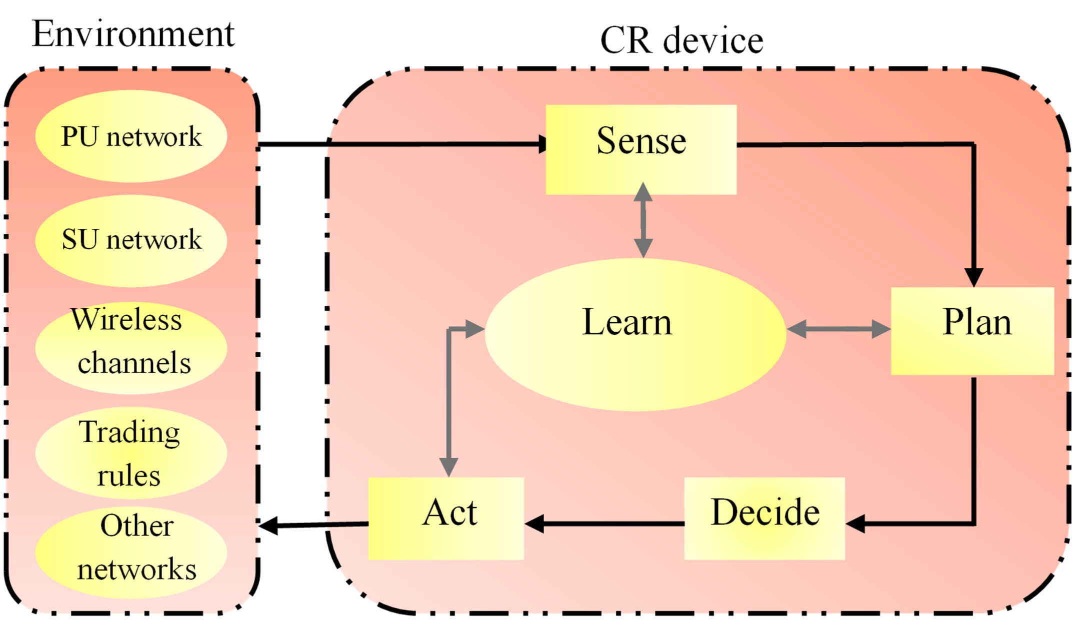

Figure 2.2: The CR cycle elements.

2.2.6 Physical Architecture of the CR (CR Transceiver)

SDR is equipped with a unique transceiver that presents the capability of reconfiguration, in contrast to the traditional transceiver (refer to Fig. 2.3). The control bus is responsible for achieving the reconfiguration and standard operational efficiency of CR. It establishes processing parameters to satisfy the required standard of CR. Therefore, the system is referred to as parameter controlled SDR. An SDR terminal consists mainly of base-band processing, front-end radio, and data processing modules. The procedure entails the first conversion of the analog RF signal into its digital complex baseband representation, followed by the application of band-pass filtering, and amplification occurs next. Another radio frequency (RF) is created locally. A two-way splitter adapted to combine the radio frequency and the signal. The entire mode of modulation operates on quadrature modulation. Low-pass filtering, and analog-to-digital conversion are applied to the main elements I and Q. During the analog-to-digital conversion process, the sampling rate is changed to match with the standard of the signals. This happens to ensure the signal processor functions at a minimal rate. In sampling, the rate of digitization must be uniform for every signal to be processed. This is according to Shannon's sampling theory. Before adapting of sampling rate to that of signal standard, an additional important factor was figured out. In the signal processing, signal mixer, filter, and analog-to-digital converter cause impairments in both branch signal processing owing their inherent mechanism. To avoid this issue, corrections are implemented before adapting sampling rate to the signal standard. The minimum rate of digitization depends on the chip rate. In general, sampling rate remains as four times the chip rate, so it is enough for the subsequent processing. When it's precisely synchronized, there happens a diminution by a ratio of four [32].

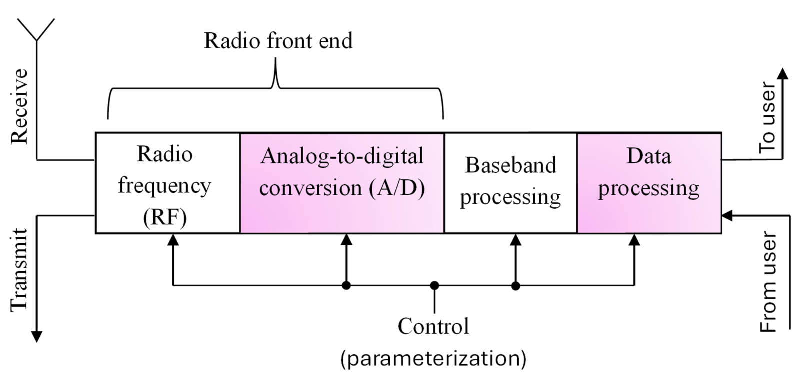

Figure 2.3: The CR Transceiver .

2.2.7 Cognitive Radio Networks (CRNs) Architecture

Usually cross-layer design has been employed to enhance various protocols by enabling nodes to utilize pertinent information in their decision-making process, with the aim of enhancing the networks performance. Nevertheless, this method is constrained by its inability to optimize numerous objectives and learn information from the environment around it. Consequently, there is a requirement for a recently advanced and smart technique that allows learning and planning. The concept of cognition has been defined as the process of learning via perception, reasoning, and knowledge. CRNs can be described as a self-aware, self-organizing, and adaptive networks that apply intelligent adaptations. These adaptations happen when the nodes within the network perform observations pertaining to the network state, while the nodes share information among each other that is outside the borders of the layered architecture, and since nodes learn and reason prior to creating and carrying out enhanced decisions. Cognition is growing in significance in research areas as it allows higher intelligence and enhanced networks[27].

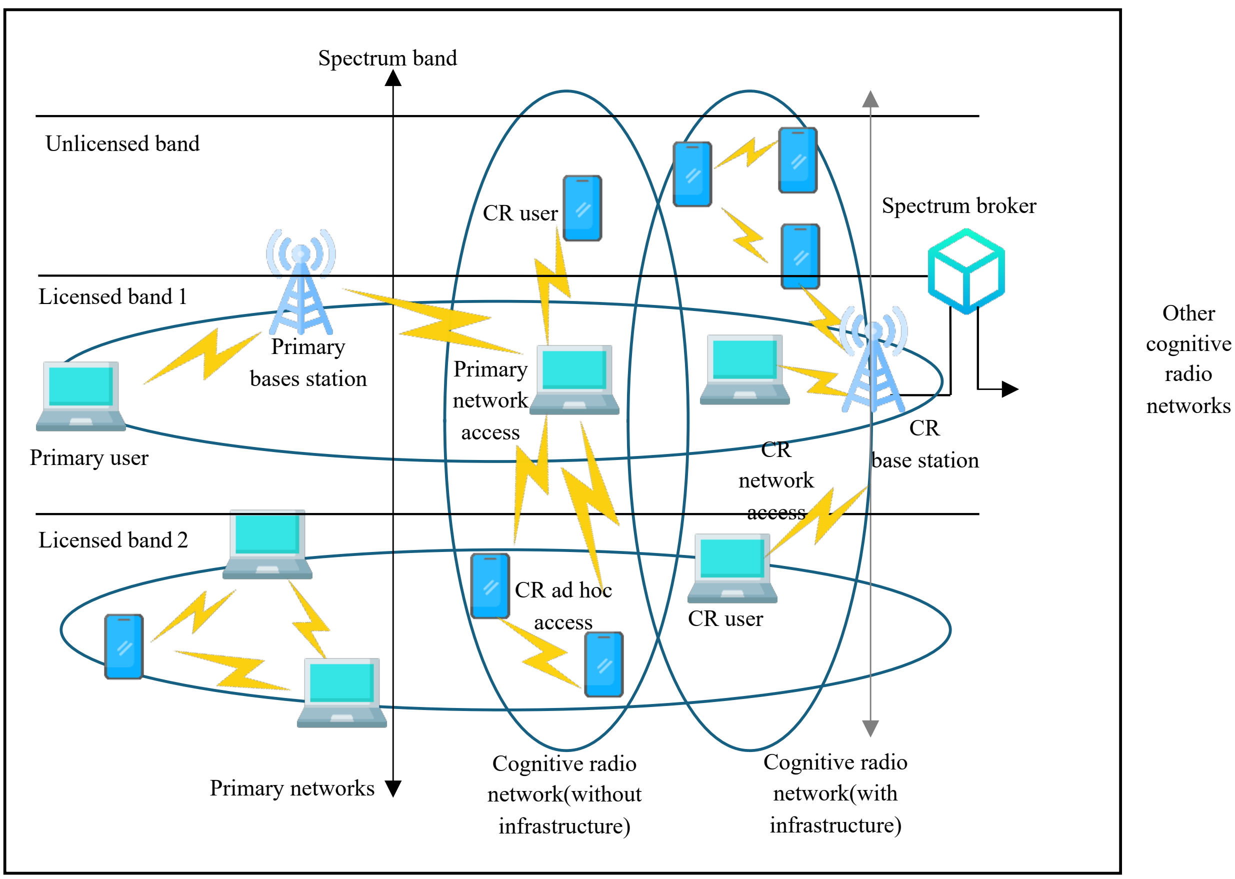

Figure 2.4: CRN architecture

2.2.7.1 The Components of a Network

The CR network architecture, as depicted in Fig. 2.4, comprises two different groupings of components: the primary network (PN) and the CRN. The term "primary network" denotes an already existing network in which the primary users already have a license to operate within a specific spectrum band. PU activities are regulated by primary base stations (PBS) when PNs include an infrastructure. The operations of primary users should remain unaffected by unlicensed users because their priority in spectrum access. The CR network cannot obtain a license for use in the wanted band. Thus, more functionality is needed for CR users to utilize the licensed spectrum band. CR networks referred to could be supported by CR base stations that offer single-hop connection to CR users. Finally, CR networks might involve spectrum brokers that play a function in spreading the spectrum resources between various CR networks[27].

2.2.7.2 Spectrum Heterogeneity

CR Users possess the ability to utilize both the licensed sections of the spectrum utilized by primary users and the unlicensed sections of the spectrum via wideband access technology. As a result, the operational modes for cognitive radio networks can be categorized into unlicensed and licensed band operation:

- Licensed band operation: The primary network predominantly operates within the licensed band, prompting cognitive radio networks to prioritize the detection of primary users within this scenario. Channel capacity is influenced by interference from adjacent primary users. Moreover, when primary users have access in the spectrum band that is already being used by CR users, these users should quickly leave that spectrum band and transition to the available spectrum.

- Unlicensed band operation: When primary users are not present, CR users possess equal entitlement to utilize the spectrum. Therefore, advanced techniques for spectrum sharing are necessary to enable CR users to vie for access to the unlicensed frequency band[27].

2.2.7.3 Heterogeneity of the Network

As illustrated in Figure. 2.4, CR users can execute in three distinct types of access:

- CR network access: CR users have the ability to connect to their designated CR base station, utilizing both unlicensed and licensed spectrum bands. Due to all interactions happening in the CR network, their spectrum sharing policy can be unaffected by the policy of the primary network.

- CR ad hoc access: CR users have the capability to communicate with other CR users via an ad hoc connection across both unlicensed and licensed spectrum bands.
- Primary network access: CR users can additionally access the primary base station via the licensed band. Unlike other access methods, CR users necessitate an adaptive medium access control (MAC) protocol, facilitating roaming across various primary networks employing diverse access technologies. As depicted in Figure . 2.4 of the CRNs architecture, several functionalities are necessary to support spectrum management within CRNs. The subsequent section offers an outline of the spectrum management framework and its constituent components [27].

2.2.8 Framework for Spectrum Management

The diagram in Fig. 2.5 depicts the spectrum management framework utilized for CR network communication [27]. The numerous interactions highlight the necessity for a cross-layer design approach in spectrum management functions. Subsequent sections will explain the discussion of the four basic spectrum management functions [33].

2.2.8.1 Spectrum Sensing

An essential necessity in CRNs involves scanning the complete frequency range to detect primary users. This function is referred to as spectrum sensing, it is executed either individually by a cognitive user or cooperatively by a cluster of cognitive users. Spectrum sensing methods hold significant importance in CRNs as they facilitate awareness of the network's environment. Cognitive users adaptively employ idle spectrum bands by implementing spectrum sensing to monitor primary and secondary user activities. Techniques such as cyclostationary feature detection, matched filter detection, energy detection, and matched filter detection are utilized for detecting both primary and cognitive user activities. Nonetheless, there exists a trade-off between accuracy and complexity when choosing the spectrum sensing technique for CRNs. Moreover, the suitability of available frequency bands for communication is assessed through analysis. Various characteristics like interference, signal-to-noise ratio (SNR), link error rate, holding time, and delays are considered to identify the most suitable frequency band. Following the selection of a frequency band, the cognitive user transmits within that chosen band. When a cognitive user or network identifies a transmission by a primary user,

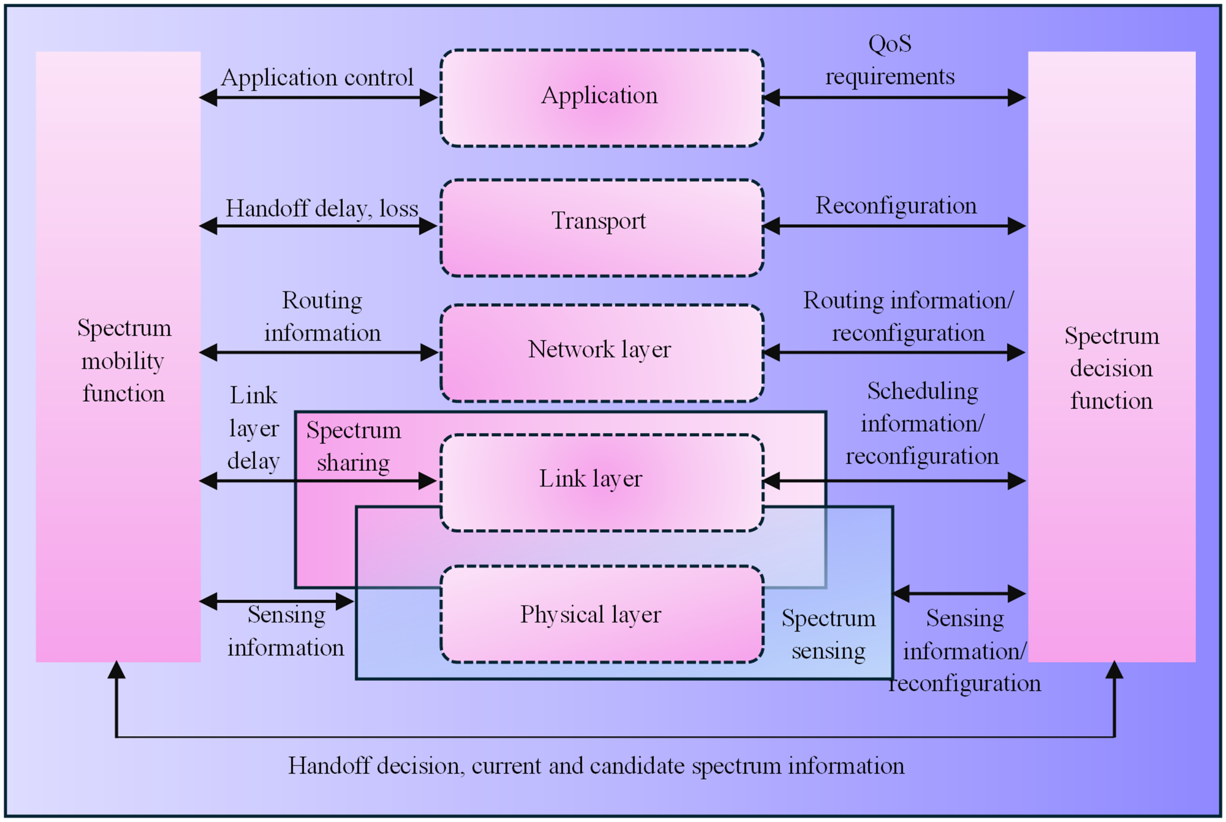

Figure 2.5: Framework for Spectrum management in CRNs .

it is required to leave the respective frequency band and seek an available one, a procedure termed spectrum handoff. The time taken for spectrum handoff introduces vulnerability in cognitive radio networks, leaving them susceptible to attacks. A cognitive radio transceiver identifies a vacant spectrum, often called a spectrum hole, and devises a strategy to utilize it without disrupting primary user transmissions. Spectrum sensing can take the form of either centralized or distributed approaches. Centralized spectrum sensing involves a sensing controller (such as an access point or base station) detecting the target frequency band, and then disseminating this information to other nodes within the system. This approach can minimize the complexity of user terminals, as all sensing functions are handled by the sensing controller. However, centralized spectrum sensing may face challenges related to location diversity. For instance, the sensing controller might struggle to detect an unlicensed user situated at the edge of the cell. In distributed spectrum sensing, unlicensed users separately conduct spectrum sensing, and the outcomes of this sensing can be utilized individually by cognitive radios (known as non-cooperative sensing) or exchanged with other users (referred to as cooperative sensing). While cooperative sensing involves additional communication and processing burdens, it yields superior spectrum sensing accuracy compared to non-cooperative sensing[34].

2.2.8.2 Spectrum Analysis

The information acquired through spectrum sensing guides the scheduling and plan of spectrum access for unlicensed users. In this scenario, the communication needs of unlicensed users are considered for optimizing transmission parameters. The primary elements of spectrum management include spectrum analysis and optimization of spectrum access. Spectrum analysis involves analyzing of information obtained via spectrum sensing in order to get information on spectrum holes, such as the estimation of interference, the duration of availability, and the probability of collision with a licensed user resulting from sensing error. The spectrum is accessed by making a decision that optimizes system performance, considering factors such as frequency, bandwidth, modulation mode, transmit power, location, and duration, in line with the desired objective such as maximizing unlicensed user throughput while adhering to constraints like keeping interference below a set threshold for licensed users[34].

2.2.8.3 Spectrum Sharing

Once a spectrum access decision is made following spectrum analysis, unlicensed users access spectrum holes. This access is facilitated through a cognitive MAC protocol, specifically designed to prevent collisions with licensed and other unlicensed users. Additionally, the cognitive radio transmitter must negotiate with the cognitive radio receiver for transmission synchronization to guarantee proper data reception. A cognitive MAC protocol may utilize either a predetermined allocation MAC (such as FDMA, TDMA, CDMA, NOMA) or a random-access MAC (like ALOHA, CSMA/CA). The Dynamic Spectrum Access (DSA) approach notably increases frequency band utilization and improves communication system performance. An essential element of DSA within cognitive radio technology is spectrum sharing, enabling effective and equitable spectrum allocation or scheduling solutions among licensed and cognitive users. In this model, the radio spectrum can be utilized simultaneously by both primary and cognitive user network. Furthermore, cognitive users can access the radio spectrum opportunistically when it is underutilized by primary users. Access by an unlicensed user is permitted if it keeps interference at the primary receiver below a specified acceptable threshold, ensuring no disruption to the primary user's ongoing communication. This sharing happens without the primary user being aware of the cognitive user, given that the cognitive user's transmission has minimal influence on the conditions for which primary user devices are designed. This model of spectrum sharing is an interesting alternative because it boosts access to and utilization of spectrum while guaranteeing coexistence with established legacy systems[34].

2.2.8.4 Spectrum Mobility

Spectrum mobility refers to the capability of a cognitive radio user to shift between different operating frequency bands. If a licensed user begins using a radio channel currently occupied by an unlicensed user, the unlicensed user can switch to an unused spectrum band. During the process of spectrum handoff, adjustments need to be made to the protocol parameters across various layers of the protocol stacks to align with the new operating frequency. The spectrum handoff needs to guarantee uninterrupted data transmission for the unlicensed user in the new spectrum band. Spectrum mobility enables cognitive radio users to transition to unused frequency bands if the primary user becomes active during ongoing CR communication. Though, the mobility of both primary and secondary users insert complexity to the spectrum design of CRNs. The existence or not of a licensed channel for a stationary or pedestrian cognitive user in a specific location will be ambiguous when the licensed user moves very fast. Furthermore, the sensing decision of the specific channel in the situation cannot be accurate for the quick-moving cognitive user, due to the channel availability status at the present location of the cognitive user could have changed. Therefore, repeated spectrum sensing is advisable for rapid cognitive users to reduce false alarms and enhance the probability of detecting a licensed channel. Furthermore, it is important to create effective spectrum handoff techniques for cognitive users to smoothly transition between spectrums, allowing them to predict and prepare for channel occupancy by the primary user when their transmission begins on that channel. A Markov process has been employed to forecast how primary users will act by analyzing their previous actions. This enables the cognitive user to leave the channel before the primary user return transmission, thereby preventing the cognitive user's transmission from being abruptly terminated. The approach of leaving the licensed channel is known as proactive handoff. Conversely, in reactive spectrum handoff, the spectrum is promptly relinquished without the cognitive user being informed beforehand. Cognitive users must keep certain of the inactive channels to reduce the disruption to their ongoing communication. The redistribution of the spectrum band to cognitive users can be accomplished through either the control channel or the central coordinator within the distributed MAC protocol. This study proposes approaches for inter-cell and intra-cell spectrum handoff in the context of cognitive users. The authors present a methodology that utilizes the Poisson distribution to inherent a spectrum mobility characteristic [34].

2.2.9 Spectrum Access Techniques

In a shared-use model, the spectrum can be utilized by cognitive users through three distinct modes: spectrum underlay, spectrum interweave, and spectrum overlay. Each mode will be explained below [34]. There are other types of spectrum access techniques but in this thesis focus on the main types for more details in [33].

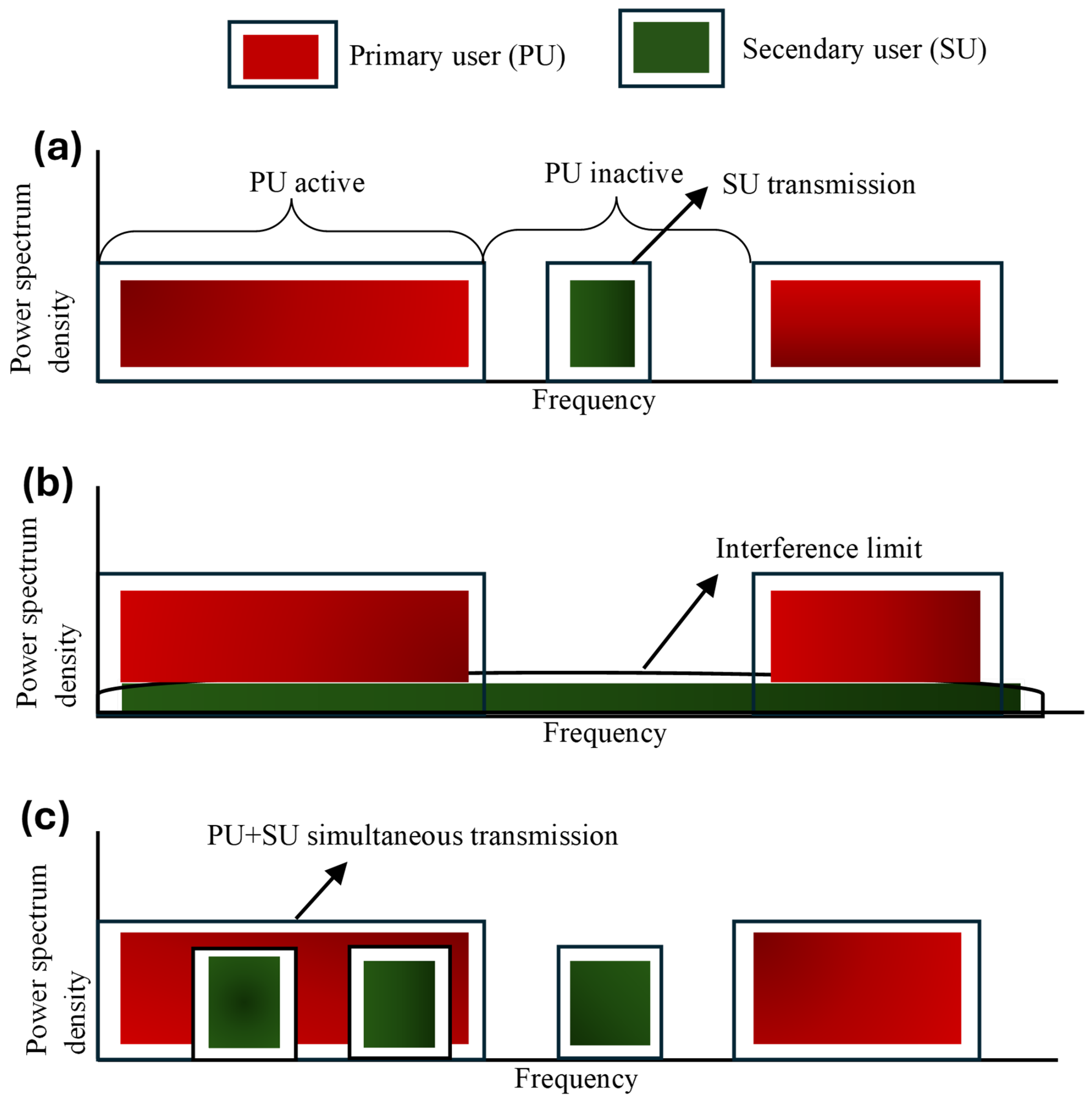

Figure 2.6: Spectrum Access Techniques (a)Interweave (b) Underlay, and (c) Overlay.

2.2.9.1 Spectrum Interweave

When the primary user does not utilize the spectrum at a specific time, frequency, or space, cognitive users can opportunistically access it using the spectrum interweave access method, as illustrated in Fig. 2.6. (a). Hence, a cognitive user aiming to use the spectrum interweave method to access a frequency band must conduct spectrum sensing to identify any activity by a primary user in that spectrum range. When a cognitive user detects an inactive primary user's spectrum white space, they can access that unused spectrum. After the primary user resumes transmission, the cognitive user needs to leave the spectrum. The spectrum interweave method is applicable for cognitive radio in FDMA, TDMA, or OFDM wireless systems[34].

2.2.9.2 Spectrum Underlay

In the spectrum underlay access method, the cognitive user can transmit simultaneously with a primary user, as depicted in Fig. 2.6(b). Nevertheless, the cognitive user's transmitting power must be restricted to ensure that the interference it generates for the primary user stays below the interference temperature. It is defined as the threshold of interference established at the primary user's receiver, beyond which it can tolerate interference without affecting its functionality. The spectrum underlay method is applicable to cognitive radio systems employing CDMA or ultra-wideband (UWB) technology. Unlike the spectrum interweave technique, the spectrum underlay technique does not require spectrum sensing to identify spectrum gaps for cognitive user transmission. However, the cognitive user must ensure that its transmission remains below the interference threshold to avoid causing interference[34].

2.2.9.3 Spectrum Overlay

In the spectrum overlay mode, simultaneous transmission by primary and cognitive users is permitted, as illustrated in Fig. 2.6 (c). Nevertheless, interference at both the cognitive and primary receivers is managed through advanced coding and interference cancellation methods. While spectrum overlay shows potential as a spectrum sharing approach, it demands substantial cooperation with the primary user and a thorough understanding of the primary user's message signal. Additionally, the cognitive user assists in relaying the primary user's information by allocating some of its power for this purpose while utilizing the rest of its power for transmitting its own data. Consequently, the rise in the primary user's SNR is balanced by a reduction in SNR caused by the interference from the secondary user, leading to no overall change in SNR at the primary receiver. As a result, the primary user remains unaware of the cognitive user's existence. Furthermore, the cognitive transmitter employs dirty paper coding to minimize interference at the cognitive receiver [34].

2.2.10 Comparison between different CR Techniques

Table. 2.1 outlines the distinctions between the underlay, overlay, and interweave CR strategies. While underlay and overlay methods allow for concurrent cognitive and non-cognitive communication, the primary aim of the interweave technique is to prevent simultaneous transmissions with non-cognitive or existed users. It's worth noting that cognitive radio approaches necessitate varying quantities of side information: underlay systems require understanding the interference levels generated by the cognitive transmitter to the non-cognitive receiver(s), interweave systems demand considerable side information regarding the activity of non-cognitive or established users (this information can be acquired through robust primary user sensing),and overlay systems necessitate a significant amount of side information as noncausal knowledge of the non-cognitive user's codebook and potentially its message. In addition to device-level power constraints, the transmit power of the cognitive user in the underlay and interweave methods is determined by the interference constraint and the scope of sensing, respectively. Although underlay, overlay, and interweave are three separate cognitive radio approaches, hybrid strategies can also be developed to blend the benefits of various approaches [35].

Underlay	• Channel side information: the cognitive transmitter recognizes the channel strengths to primary receiver(s). • Cognitive users may transmit simultaneously with the primary user while keeping interference under a permissible threshold. • Cognitive users' transmit power is constrained by the interference threshold.
Interweave	• Activity side information: the cognitive user identifies spectral holes in space, time, or frequency where the primary user is not active. • Cognitive users may transmit simultaneously with a primary user in case of false spectral hole detection. • Cognitive user's transmit power is constrained by the range of its spectral hole sensing.
Overlay	• Codebook side information: cognitive nodes recognize channel gains, codebooks, and the messages of the primary users. • Cognitive users may transmit simultaneously with the primary user; interference can be offset by using a portion of cognitive user power to relay the primary user's message. • Cognitive users may transmit at any power level, as interference to primary users can be offset by relaying their messages.

Table 2.1: Comparison between CR Techniques

2.2.11 Dynamic Spectrum Management (DSM)

Generally, spectrum management entails arranging the utilization and allocation of the spectrum and determining its users. The primary objective of spectrum management is to increase the societal gains derived from the radio spectrum by accommodating a maximum number of efficient users, while also ensuring manageable interference between different users. Emerging dynamic spectrum management regimes are approaching as we transition from static methods, with cognitive radio playing an enabling role. Cognitive radio facilitates diverse spectrum utilization activities to achieve "additional spectrum usage." The primary spectral tasks are outlined as follows:

- Dynamic Spectrum Sensing: Utilizing its sensing capabilities, cognitive radio can detect accessible spectral resources. Spectrum sensing techniques employed by cognitive radio may involve energy detection, matched filter detection, interference-specific detection, and cyclostationary feature detection.

- Dynamic Spectrum Access: Simply sensing an available band is insufficient unless the detected spectrum is accessed and utilized effectively. CR can dynamically choose accessible spectrum and intelligently adjust its necessary parameters to operate efficiently on it. Spectrum sharing or access can be achieved through distributed, centralized, cooperative, and non-cooperative schemes. When multiple spectrum holes are present, CR can intelligently select the most suitable ones for current transmission requirements.

- Dynamic Spectrum Management: Dynamic spectrum sensing and access both of them demand cognitive coordination, , management, planning, and characterization of available spectrum for intelligent decision making. This decision process may be dynamic in utilizing the spectrum opportunity before it becomes vacant again[36].
  The major spectrum management tasks performed by CR can incorporate the following:

- Rules: Identifying policy, etiquette, and additional rules suitable to the identified spectrum and intelligently handling these rules.

- Duration and release: Estimating the duration of unoccupied spectrum. Multiple users sharing a RF interface may have various usage durations. Spectrum release can perfectly occur in stages as every service finishes its communications task.

- Prioritize: The accessed spectrum that's available can be required after by multiple nodes at the same time. CR can intelligently prioritize their spectrum access.

- Coordination and synchronization: Cognitive spectrum management can consider the estimated receiving capabilities of the destination(s) and establish a dependable method for coordinating between the source-destination and spectrum-usage synchronization.

- Interference: Identifying present active interference-tolerant and intolerant services who need the vacant spectrum.

- Performance metric: Spectrum management may involve cognitive decision making to determine if transmission over the new available spectrum would enhance communication. This can be achieved by employing metric measurement and assessment of cognitive wireless communication performance.

In summary, DSM can provide consumers, military, government, and civil groups with an enhanced method of information conveyance, cognitive abilities, and knowledge about the locations, path distances, trajectories, available radio resources, and desired QoS. Consequently, each scenario can achieve an optimal solution. Spectrum sensing, detection, and management functions can also be collaboratively performed across multiple nodes. In contrast, research and implementation employing collaboration require further study. As a result of spectrum optimization, CR can facilitate transitioning to a new spectrum with reduced interference and improved SNR quality. CR's capability to function across various spectrums can offer ubiquitous connectivity, greater spectral and user capacity, and greater data rates. Communication could potentially be established at any moment and in any location across various dimensions (time, frequency, space, etc.) as long as the spectrum is accessible. As a result, cognitive radio might eliminate wireless communication failures caused by spectrum scarcity [36].

2.3 Basic Principles of NOMA

2.3.1 Non-Orthogonal Multiple Access (NOMA)

Cellular communication systems are fundamentally based on multiple access. It denotes a technique that enables multiple users to utilize a common communication channel. NOMA enables multiple users to simultaneously utilize the same resource elements, such as time, frequency, space, or code. The original concept of NOMA is based on CDMA, which is an OMA technique according to most recent studies. However, there are some papers that classify it as a NOMA technique [37].

2.3.2 Dominant NOMA Solutions

NOMA schemes can be classified into two categories: power-domain NOMA and code-domain NOMA [38].Most papers and books provide a definition of the concept NOMA within the power domain. In this thesis, we are also interested in this aspect.

- NOMA via Code Domain Multiplexing: NOMA via code domain multiplexing shares a fundamental concept with CDMA, in which unique codes are assigned to individual users.The transmission for multiple users is subsequently carried out using the identical time-frequency resources. The code domain NOMA contains various schemes such as

LDS-OFDM, SCMA, SAMA, LDS-CDMA, and MUSA [39]. While it can be further categorized, we will not delve into those details in this thesis.

- NOMA via Power Domain Multiplexing: In NOMA, all users operate within the same frequency band and simultaneously, with their power levels serving as the distinguishing factor. NOMA employs SC during transmission, enabling the SIC receiver to differentiate between users in both the uplink and downlink channels [40].

2.3.3 Multiuser Detection Techniques (MUD)

Even when employing orthogonal multiplexing techniques like CDMA or OFDMA, interference resulting from channel distortion and out-of-cell interference cannot be completely eliminated in wireless systems. MUD focuses on the demodulation of mutually interfering digital streams of information in wireless communications. It is also studied for demodulation in low-power inter-chip and intra-chip communications.Multiple user detection includes both receiver technologies that work together to find all the interference signals or to single-user receivers that are made to repair only one user but are strong enough to handle interference from other users as well as background noise.Multiuser detection is a powerful technique that utilizes the structure of interfering signals to minimize multiple user interference (MUI). It offers several benefits including enhanced spectral efficiency, improved receiver sensitivity, and increased capacity to support more users in the system [41]. The approaches used for multi-user multiple-input multiple-output (MU-MIMO) in a multi-user detection (MUD) system may be categorized into linear and non-linear schemes. The performance of linear MUD approaches, such as low complexity zero-forcing (ZF) and minimum mean square error (MMSE), is constrained. Conversely, non-linear MUD techniques like ML, SIC, PIC, MPA, PDA could realize optimal performance but at the expense of significant computational complexity, which grows exponentially with the number of consumers [42],[43].

2.3.3.1 Interference Cancellation (IC)

Multi-user IC techniques can be broadly classified into two primary categories: pre-interference cancellation (pre-IC) and post-interference cancellation (post-IC). Pre-IC techniques are utilized on the transmitter side to mitigate interference by precoding methods, such as the well-known dirty paper coding (DPC), which employs the transmitter's awareness of the CSI. In contrast, post-IC techniques are commonly employed on the receiver side to mitigate interference. There are two distinct groups within the post-IC approach, namely parallel and successive. PIC surpasses SIC when accurate power control is implemented to assure similarity of all signals received. In contrast, SIC performs more effectively when the received powers differ, as it can detect the signal of the strongest user first. The remodulated bit is identified, and its interference is subtracted from the received signal. By performing this procedure in a consecutive manner, we are able to obtain the signal with the lowest strength [44],[45].

2.3.3.2 Superposition Coding (SC)

The concept of SC was initially introduced by Cower in 1972, with the aim of optimally utilizing the ordering of channels. Theoretical evidence from 1973 to 1974 demonstrated that SC offers the potential to achieve the capacities of Gaussian broadcast channel capacity as proposed by Bergmans, as well as the general degraded broadcast channel capacity as proposed by Gallager. In NOMA downlink networks, the BS utilizes SC signals to transmit the combined information of all downlink NOMA users. In order to execute SC, the signals of different users are allocated various power levels, while according to constraints on the total transmit power. These signals are then combined and superimposed. In contrast to the water-filling power allocation policy observed in OMA, NOMA systems tend to allocate higher power to users with poor channel gains and lower power to users with favorable channel gains. This policy ensures a fair chance for all users[46].

2.3.3.2 Successive Interference Cancellation (SIC)

SIC is a technique employed by receivers in NOMA networks to eliminate co-channel interference. Efficient interference management is important in NOMA networks to improve network capacity, and SIC is considered the most effective method for achieving interference cancellation. The primary concept behind SIC is the successive decoding of superimposed signals. In order to apply SIC, users are initially classified based on the quality of their channels. Users with high channel quality are classified as strong users, whereas users with low channel quality are classified as weak users. According to the SIC strategy, a NOMA receiver will always decode the strongest signal's superposition while classifying the other weak signals as interference until it is able to decode its own signal. For instance, let's consider a NOMA downlink network consisting of K users, with the first user being lowest powerful and the kth user being the most powerful. The k-th user must initially decode all signals that are more powerful than its own signal (i.e., from the signals of the first user to the signals of the K-1st user) and after that eliminate them in a sequence. Nevertheless, signals that are weaker than the decoding signal at that moment are just considered as interference. According to the SIC policy, the strongest user can perform interference-free decoding by eliminating the signals of other users. Meanwhile, the weakest user decodes its own signal by considering all other users' signals as interference. It is noteworthy to mention that SIC has the potential to be achieved. The limitations of Shannon capacity in both the broadcast channel and multiple access networks are determined by the region boundaries. Several SIC versions have been used in numerous IEEE 802.154-enabled practical systems as well as certain commercial systems because of the minimal hardware design complexity required. Examples of applications include wireless sensor networks, smart home automation, industrial automation, health monitoring, and smart agriculture [46].

2.3.4 NOMA Network for both DL and UP Scenarios:

2.3.4.1 The Downlink NOMA Network

In the downlink NOMA network, the BS broadcasts a combined signal to all mobile users. This signal is a superposition of the supposed signals from numerous users with varied allocated power factors. This transmission occurs at the transmitter side, as depicted in Fig. 2.7.The SIC process is expected to be executed successively at the receiver of each user until the user's signal is recovered. The allocation of power factors between users is determined based on their channel conditions, following an inverse proportional relationship. The user suffering a poor channel condition gets more of transmission power compared to the user having a good channel condition. Hence, as the user having the biggest transmission power considers the signals of other users as interference, it simply recovers its own signal without allowing in any SIC operation[47].

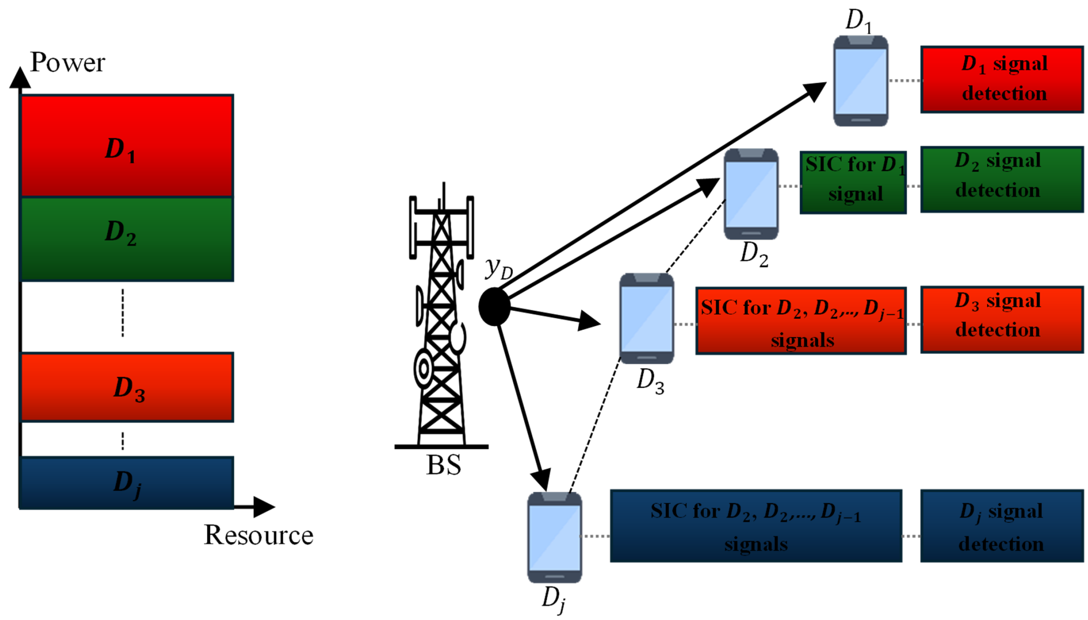

Figure 2.7: The scenario of the DL NOMA network.

However, it is necessary for other users to execute SIC processes. When using SIC, each user's receiver first determines signals that are higher than its own that it desires to receive. Subsequently, the previous signals are deducted from the received signal, and this repetitive procedure occurs until the corresponding user's signal is identified. In the final step, individual users decode their particular signals by considering other users with lower power coefficients as interfering noise. The signal to be sent at the BS can be expressed as:

$$S = \sum_{k=1}^{J} \sqrt{b_k E_{BS}} m_k \tag{2.1}$$

Where m_k is the information of user k (U_k). E_{BS} is the transmission power at the BS and b_k is the power allocation (PA) coefficient for user k subjected to $\sum_{k=1}^{J} b_k = 1$ and $b_1 \geq b_2 \geq \ldots \geq b_J$ since without loss of generality the channel gains are supposed to be ordered as $|g_{D_1}|^2 \leq |g_{D_2}|^2 \ldots \leq |g_{D_J}|^2$, where g_{D_j} is the channel coefficient of j^{th} user. The received signal at j^{th} user can be presented such as:

$$y_{D_{m,d}} = g_{D_j} S + n_j \tag{2.2}$$

Where n_j is zero mean complex additive Gaussian noise with a variance of σ^2; It can be expressed as $n_j \sim CN(0, \sigma^2)$. By using equation (2), the instantaneous Signal-to-Interference-plus-Noise Ratio (SINR) of the j^{th} user to detect the q^{th} user, $q \leq j$, with $q \neq J$ can be expressed as:

$$\gamma_{q \to j} = \frac{b_q \rho_S |g_{D_j|^2}}{\rho_S |g_{D_j|^2} \sum_{k=q+1}^{J} b_k + 1} \tag{2.3}$$

Where $\rho_S = \frac{E_{BS}}{\sigma^2}$ presents the SNR. For obtaining the needed information of the j^{th} user, SIC process will be applied for the signal of user $q \leq j$. Therefore, the SINR of the j^{th} user can be expressed as

$$\gamma_j = \frac{b_j \rho_S \left| g_{D_j} \right|^2}{\rho_S \left| g_{D_j} \right|^2 \sum_{k=j+1}^{J} b_k \ + 1} \tag{2.4}$$

The SINR of the J^{th} user is shown as

$$\gamma_J = b_J \rho_S |g_{D_J}|^2 \tag{2.5}$$

When the SINR expression of downlink NOMA is determined, the sum rate analysis can be carried out easily. The achievable data rate in downlink NOMA for the j^{th} user can be mathematically represented as[47]:

$$R_{j,d} = \log_2 (1 + \gamma_j) = \log_2 \left(1 + \frac{b_j \rho_S |g_{D_j}|^2}{\rho_S |g_{D_j}|^2 \sum_{k=j+1}^{J} b_j + 1} \right) \tag{2.6}$$

2.3.4.2 The Uplink NOMA Network

The uplink NOMA network scenario is illustrated in Fig. 2.8, every mobile user sends its signal to the base station (BS). SIC iterations are performed at the BS to determine the signals of mobile users.

With the assumption that the downlink and uplink channels are reciprocal, and that the BS sends PA coefficients to mobile users, we can write the received signal at the BS for synchronous uplink NOMA as:

$$y_{D_{j,u}} = \sum_{k=1}^{J} g_{D_k} \sqrt{b_k E_{BS}} m_k + n_j \tag{2.7}$$

Where g_{D_k} and E_{BS} denotes the channel coefficient of the k^{th} user and the maximum transmission power supposed to be equal for all users. n_j presents the zero mean complex additive Gaussian noise and the variance of σ^2; It can be expressed as $n_j \sim CN(0, \sigma^2)$. The BS decodes the signals of users in an ordered manner based on the PA coefficients of users. Subsequently, the SINR for the j^{th} user $j \neq 1$ can be determined by [48],[47]:

$$\gamma_j = \frac{b_j \rho_S |g_{D_j}|^2}{\rho_S \sum_{k=1}^{j-1} b_j |g_{D_j}|^2 + 1} \tag{2.8}$$

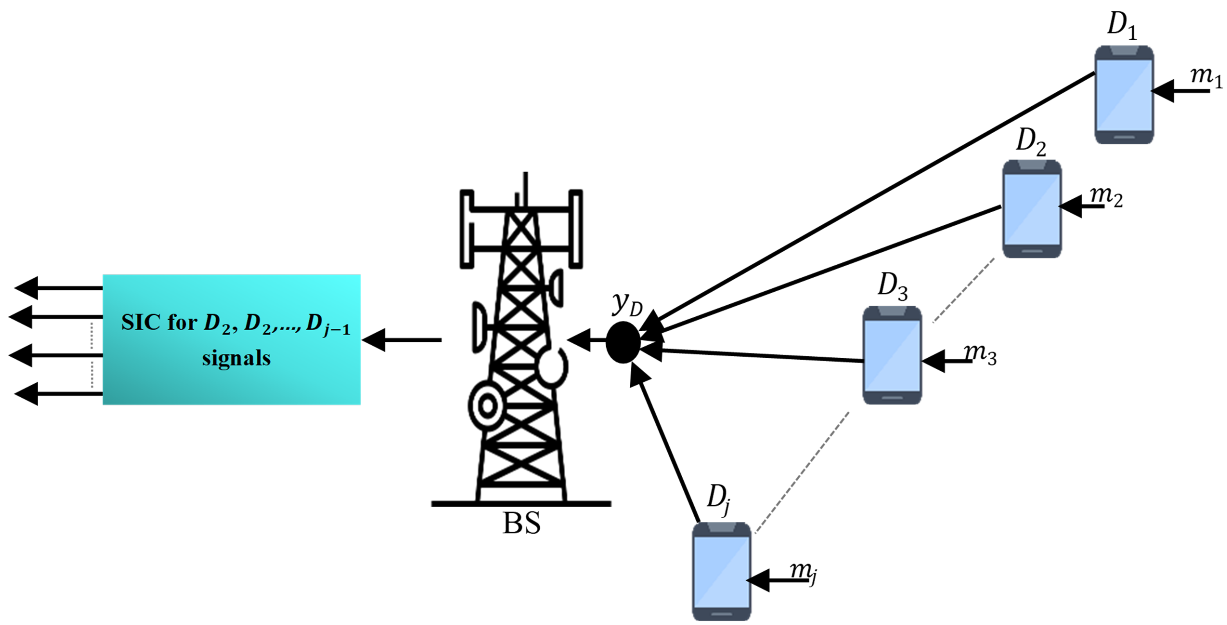

Figure 2.8: The scenario of the UP NOMA network.

Where $\rho_S = \frac{E_{BS}}{\sigma^2}$.

2.4 Conclusion

In this chapter, we learned about the most important concepts, starting with the definition of cognitive radio, its network components, in addition to the cognitive radio transceiver that explains how this technology works, the other types of spectrums sharing, and a comparison between them. Cognitive radio provides the ideal solution to the problem of spectrum scarcity. Enhance the efficiency of cognitive radio technology, numerous studies have proposed integrating it with NOMA technology. Additionally, we provided an overview of the NOMA technique, discussing its definition and key methods such as SIC and SC. Alongside, the main equations are presented for both uplink and downlink scenarios. In the next chapter, we will study the simulation of the combination of CR and NOMA.

Chapter 3

Performance Investigation of CR-NOMA based Underlay Paradigm

3.1 Introduction

Cisco predicted that the mobile user's number will increase 13.1 billion by 2023, with the number of Internet-enabled devices increasing from 18.4 billion in 2018 to 29.3 billion. This increase in consumption will be inundated the 4G and 5G wireless networks' connectivity capabilities. Furthermore, this upward development shows no signs of lessening in the coming decade, ignoring the fact that just about 70% of the world's population is accounting for this demand. As a result, one of the most significant goals for the 6G, will provide huge access [47].With the explosive growth of smart devices, the present spectral limitations are insufficient to support a new requirement. The underlying CR technology has emerged as an effective solution for opportunistically accessing idle spectra in licensed bands and improving spectrum usage in cognitive systems, hence reducing spectrum constraint [49],[27]. Haykin defined cognitive radio as an intelligent wireless system that is aware of its surroundings and uses the understanding-by-building methodology to learn from the environment and adapt its internal states to statistical variations in incoming RF stimuli by making real-time changes in certain operating parameters [50]. The underlay CRNs defined as, it allows cognitive users to operate if the interference caused by non-cognitive users is less than a certain threshold [35]. Users can share the same resource elements in the time, frequency, space, or code domains using NOMA. Each user in NOMA works in the same band and at the same time, with their power levels separating them. NOMA employs SC at the transmitter in order for the SIC receiver to distinguish between users in both the uplink and downlink channels [51],[52],[53],[54]. A combined investigation of the CR and NOMA technologies could theoretically improve spectrum utilization performance much more as in [55].

3.1.1 Related Works

The authors of [56] investigated the impact of user pairing on the efficiency of two NOMA systems, fixed power allocation with NOMA (F-NOMA) and CR-NOMA. Authors derived the OP expressions for NOMA and CR-NOMA. The application of NOMA to large-scale underlay cognitive radio networks with randomly deployed users discussed in [57]. Closed-form expressions of the OP are derived using stochastic geometry to characterize the performance of the network. NOMA outperform traditional multiple access scheme (OMA) in underlay CRNs by carefully designing target data rates and user power allocation coefficients. The authors of [58] proposed transmission schemes for CR-NOMA with and without D2D in which the far NOMA user cooperates with the relay through two links. The performance analysis provided in terms of the outage probability and throughput. The results indicated that CR-NOMA work good with D2D transmission capability. In [59] the authors investigated the impact of PA on spectrum efficiency and fairness performance of CR-NOMA. The parameters that cause the channel outage have been investigated, and outage probability conditions have been derived. The performance of the secure outage probability (SOP) in the case of a fixed PA scheme investigated in [60] to determine the security of CR-NOMA systems. In CR-NOMA, a transmit power limitation at the secondary results in changing secure performance. The main factors affecting system performance is the threshold data rates and the influence of interference from the primary network.

3.1.2 Motivation and Contributions

Motivated by the aforementioned references and existing literature, most studies focus on enhancing the OP by incorporating additional technologies. However, to the best of our knowledge, the exact closed-form expressions for the OP performance of a simple underlay CR-NOMA system have not been extensively explored. In this chapter, we derive mathematical expressions for the OP, data rate, and throughput of both near and far users. The key contributions of this study are summarized as follows:

- Derivation of the closed-form expression characterizing the OP for near and far users in a simple underlay CR-NOMA system.
- Investigation of the impact of varying the ITC on system performance.

- Comparative analysis of the CR-NOMA with the conventional CR-OMA protocol.

The remainder of this chapter is structured as follows: Section 2 explains the system model, Section 3 presents the results, Section 4 provides a discussion, and Section 5 concludes the chapter.

3.2 System Model

As depicted in Fig. 3.1, this chapter considers a downlink underlay CR-NOMA system. The model examines the performance of the secondary network (SN), which consists of a BS and two NOMA users, D_1 and D_2. User D_1 is located farther from the BS, while user D_2 is closer to the BS. The secondary network operates alongside a primary network (PN) that includes a PU, whose presence affects the performance of the SN. We assume that the channel coefficients follow the Rayleigh fading model, with $n_1 = n_2 = n_0$, and the power allocation factors satisfy $b_1 > b_2$ and $b_1 + b_2 = 1$. The signal transmitted by the BS is [55]:

$$S = \sqrt{E_{BS}}\left(\sqrt{b_1}m_1 + \sqrt{b_2}m_2\right)$$

Where, $E_{BS} = \min\left(\frac{I_{ITC}}{|g_{SC}|^2}, E_{BS}\right)$. The received signal at user D_j, where $j = \{1, 2\}$, is expressed as [61]:

$$y_{D_j} = g_j S + n_j \tag{3.1}$$

3.3 Performance Analysis

3.3.1 Calcuation of SNR

The signal to SNR for D_1 can be given by [62]:

$$\gamma_{D_1} = \frac{|g_{D_1}|^2 \rho_S b_1}{|g_{D_1}|^2 \rho_S b_2 + 1} \tag{3.2}$$

Where $\rho_S = \frac{\mathrm{E_{BS}}}{\sigma^2}$ is the transmission SNR at the BS. $\sigma^2 = \sigma_I^2 = \sigma_S^2$, SNR D_2 for decoding D_1 (before SIC) is:

$$\gamma_{D_{1,2}} = \frac{|g_{D_2}|^2 \rho_S b_1}{|g_{D_2}|^2 \rho_S b_2 + 1} \tag{3.3}$$

After cancellation of D_1 signal using SIC, the signal to noise ratio at D_2 for decoding its own signal is,

$$\gamma_{D_2} = |g_{D_2}|^2 \rho_S b_2 \tag{3.4}$$

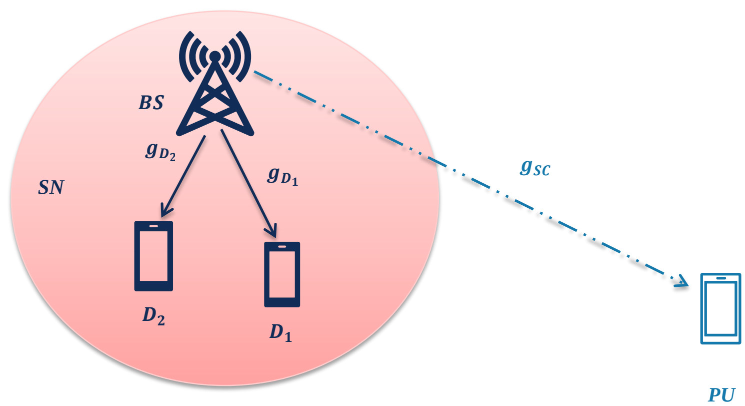

Figure 3.1: System model of simple underlay CR-NOMA.

3.3.2 Calculation Achievable Data Rate:

The achievable data rate for D_1 is,

$$\begin{aligned} R_{D_1} &= \log_2\left(1+\gamma_{D_1}\right) \\ &= \log_2\left(1+\frac{\left|g_{D_1}\right|^2\rho_S b_1}{\left|g_{D_1}\right|^2\rho_S b_2+1}\right) \end{aligned} \tag{3.5}$$

The corresponding achievable data rate at D_2 for decoding the D_1 signal (before SIC) is,

$$\begin{aligned} R_{D_{1,2}} &= \log_2\left(1+\gamma_{D_{1,2}}\right) \\ &= \log_2\left(1+\frac{\left|g_{D_2}\right|^2\rho_S b_1}{\left|g_{D_2}\right|^2\rho_S b_2+1}\right) \end{aligned} \tag{3.6}$$

After cancellation of D_1 signal using SIC, the corresponding achievable data rate at the D_2 for decoding its own signal is,

$$\begin{aligned} R_{D_2} &= \log_2\left(1+\gamma_{D_2}\right) \\ &= \log_2\left(1+\left|g_{D_2}\right|^2\rho_S b_2\right) \end{aligned} \tag{3.7}$$

3.3.3 Calculation Outage Probability (OP)

In this section, we discuss the OP. The message is an outage if the achievable SNR of that message is under a predefined targeted SNR. It is calculated using the probability density function and cumulative distribution function of channel g_{D_j}, it can be written by [61]:

$$f_{|g_{D_j}|^2}(y) = \frac{1}{\lambda_j} e^{-\frac{y}{\lambda_j}} \tag{3.8}$$

$$F_{|g_{D_j}|^2(y)} = 1 - e^{-\frac{y}{\lambda_j}} \tag{3.9}$$

Where the channel gain as $\lambda_j = d_j^{-\alpha}$,$\alpha$: is the path-loss exponent. $\rho_I = \frac{\mathrm{I_{ITC}}}{\sigma_I{}^2}$ $\gamma_{1,th} = 2^{R_1} - 1$,R_1: the target rate for user D_1 and Pr(.): the probability function, the outage probability of D_1 can be shown by [61]:

$$OP_{D_1} = 1 - \Pr\left\{\gamma_{D_1} > \gamma_{1,th}\right\} \tag{3.10}$$

$$\begin{aligned} OP_{D_1} = 1 - \Bigg[&\Pr\left\{ |g_{D_1}|^2 > \frac{\gamma_{1,\mathrm{th}}}{\rho_S\left(b_1 - \gamma_{1,\mathrm{th}} b_2\right)}, \; |g_{SC}|^2 < \frac{\rho_I}{\rho_S} \right\} \\ &+ \Pr\left\{ |g_{D_1}|^2 > \frac{\gamma_{1,\mathrm{th}}\,|g_{SC}|^2}{\rho_I\left(b_1 - b_2\gamma_{1,\mathrm{th}}\right)}, \; |g_{SC}|^2 > \frac{\rho_I}{\rho_S} \right\} \Bigg] \end{aligned} \tag{3.11}$$

$$OP_{D_1} = \left[1 - \left(\int_0^{\frac{\rho_I}{\rho_{CU}}} f_{|g_{sd}|^2}(x) \int_{\frac{k}{\rho_{CU}}}^{\infty} f_{|g_1|^2}(y), dy, dx + \int_{\frac{\rho_I}{\rho_{CU}}}^{\infty} f_{|g_{sd}|^2}(x) \int_{\frac{kx}{\rho_I}}^{\infty} f_{|g_1|^2}(y), dy, dx\right)\right]$$

$$OP_{D_1} = 1 - \left[\left(\left(1 - e^{-\psi}\right) \times e^{-\frac{k}{\rho_S \lambda_1}}\right) + \epsilon_1 e^{-\phi}\right] \tag{3.12}$$

Where $k = \frac{\gamma_{1,th}}{\left(b_1 - \gamma_{1,th} b_2\right)}$, and $\epsilon_1 = \frac{\lambda_1 \rho_I}{\lambda_{SC} k + \lambda_1 \rho_I}$, $\phi = \frac{\lambda_1 \rho_I + \lambda_{SC} k}{\rho_S \lambda_1 \lambda_{SC}}$, $\psi = \frac{\rho_I}{\rho_S \lambda_{SC}}$.

The outage probability of D_2 can be written by :

$$OP_{D_2} = 1 - \Pr\left\{\gamma_{D_{1,2}} > \gamma_{1,th}, \gamma_{D_2} > \gamma_{2,th}\right\} \tag{3.13}$$

The same steps to solving expression acquired from Equation (10), it can be obtained the outage for D_2 in the following:

$$OP_{D_2} = 1 - \left[\left(\left(1 - e^{-\psi}\right) \times e^{-\frac{\theta}{\rho_S \lambda_2}}\right) + \epsilon_2 e^{-\nu}\right] \tag{3.14}$$

Where $\gamma_{2,th} = 2^{R_2} - 1$ and $\theta = \max\left(\frac{\gamma_{2,th}}{b_2}, \frac{\gamma_{1,th}}{b_1 - \gamma_{1,th} b_2}\right)$. $\epsilon_2 = \frac{\lambda_2 \rho_I}{\lambda_{SC}\theta + \lambda_2 I}$, $\nu = \frac{\lambda_2 \rho_I + \lambda_{SC}\theta}{\rho \lambda_2 \lambda_{SC}}$.

3.3.4 Throughput

The throughput can obtained by using each user's outage behavior [54],[63]:

$$T_1 = R_1 \left(1 - OP_{D_1}\right) \tag{3.15}$$

$$T_2 = R_2 \left(1 - OP_{D_2}\right) \tag{3.16}$$

3.4 Results and Discussions

This section contains the analytical results for our system. The use of the CR-NOMA system with two users has been considered. Simulations are used to calculate outage probability, achievable capacity and throughput. The simulation model is established in Fig. 3.1. We assume that two CR-NOMA users have fixed PA factors: b_1= 0.8. In the simulations, we consider I_{ITC}= 20 dB, α=3.5.The terms "th." and "sim." refer to analytical results and simulated curves, respectively.

Fig. 3.2 illustrates the achievable data rate comparison between CR-NOMA and CR-OMA for users D_1 and D_2 as a function of SNR. The data rate for D_2 is consistently higher than that of D_1. As the transmit SNR increases, the achievable data rate rises until it reaches a saturation point, observed between 22 dB and 50 dB. This saturation highlights the impact of the ITC within the system. It is evident that the performance of CR-NOMA exceeds that of CR-OMA, primarily due to the use of SIC and SC techniques, which effectively manage interference. In contrast, with CR-OMA, the user located closer to the base station exhibits better performance, while distant users experience reduced data rates.

Fig. 3.3 depicts the outage probability (OP) results for D_1 and D_2, derived from equations (11) and (13), respectively. The results show that in the CR-NOMA system, D_2 consistently achieves lower outage probability compared to D_1 across all SNR values. Similarly, in the CR-OMA system, D_2 demonstrates superior performance over D_1. A comparative analysis of CR-OMA and CR-NOMA indicates that CR-NOMA exhibits better overall outage probability performance. Moreover, the simulation results confirm the accuracy of the analytical OP findings for both OP_{D_1} and OP_{D_2}.

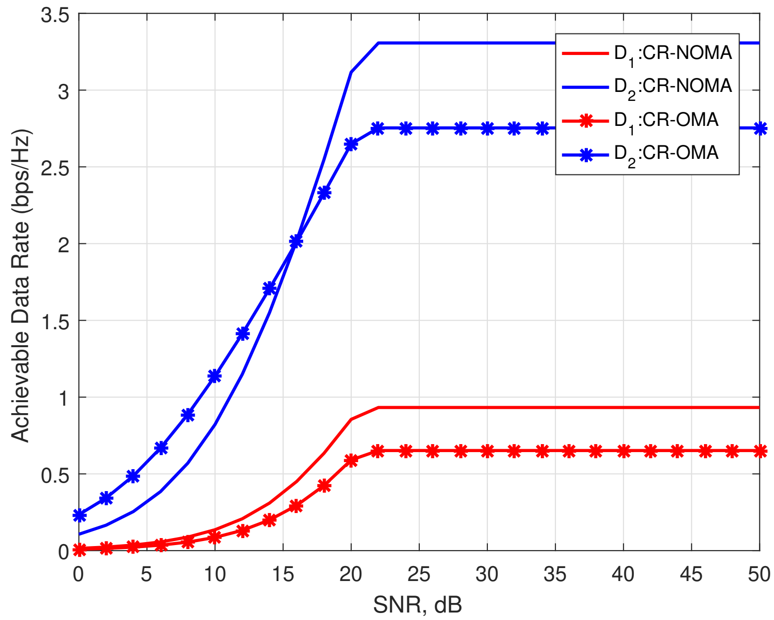

Figure 3.2: Achievable data rate comparison between CR with NOMA/OMA of D_1 and D_2 versus SNR

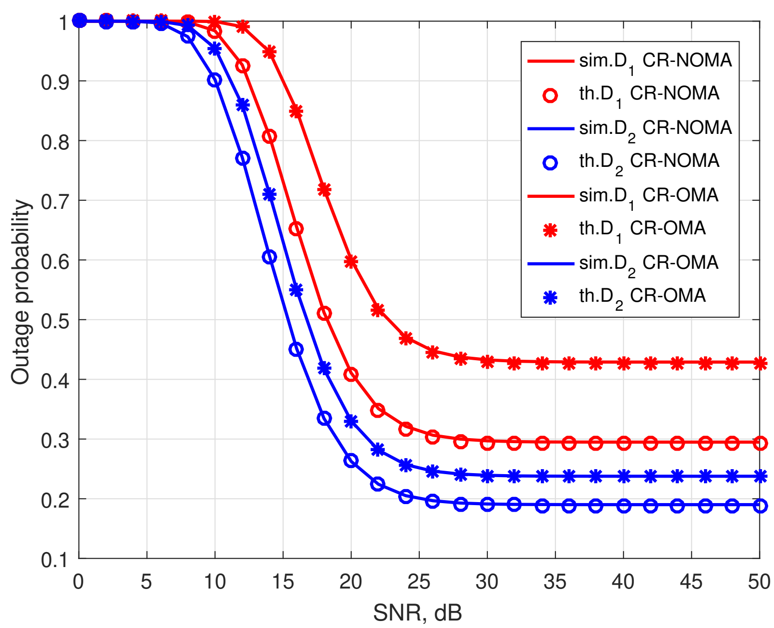

Figure 3.3: Outage probability comparison between CR with NOMA/OMA of D_1 and D_2 versus SNR.

Fig 3.4 presents a throughput comparison between CR-NOMA and CR-OMA for D_1 and D_2 as a function of SNR. It can be observed that D_2 consistently achieves higher throughput compared to D_1. As the transmit SNR increases, the throughput exhibits a saturation trend, particularly noticeable when the SNR ranges from 22 dB to 50 dB.

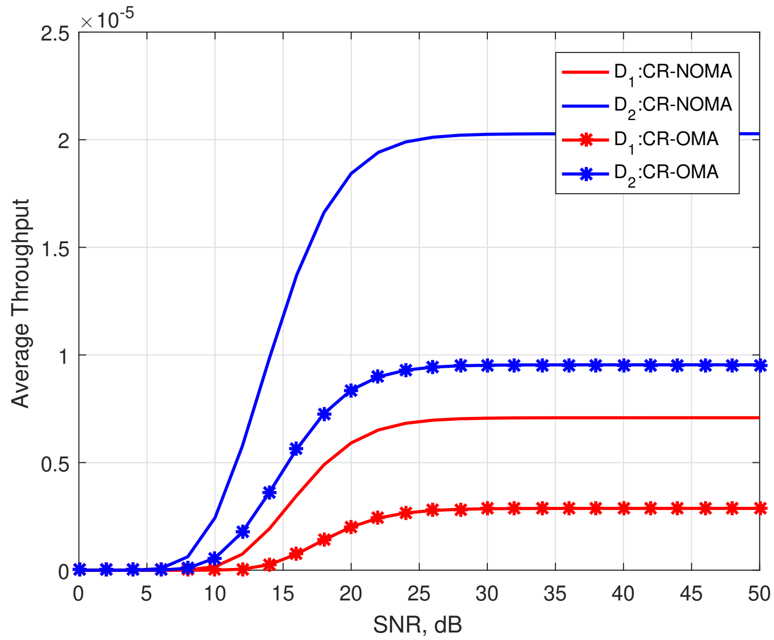

Figure 3.4: Throughput comparison between CR with NOMA/OMA of D_1 and D_2 versus SNR

The impact of interference, denoted as $I_{ITC} = 10, 20, 35$ dB, on the achievable data rate and outage probability for two users is illustrated in Fig. 3.5 and Fig. 3.6, respectively. As observed, lower levels of interference result in improved system performance, with the highest performance achieved at $I_{ITC} = 35$ dB.

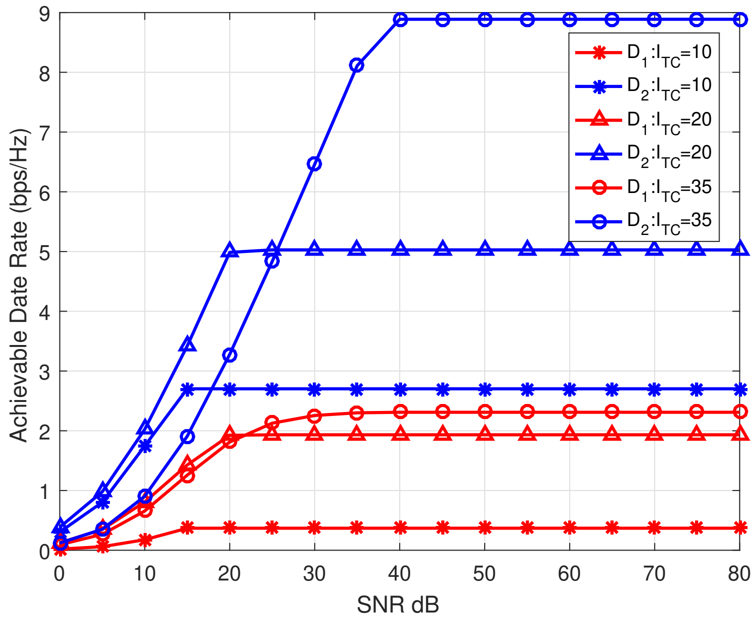

Figure 3.5: Achievable data rate comparison between CR with NOMA/OMA of D_1 and D_2 versus SNR as varying I_{ITC}

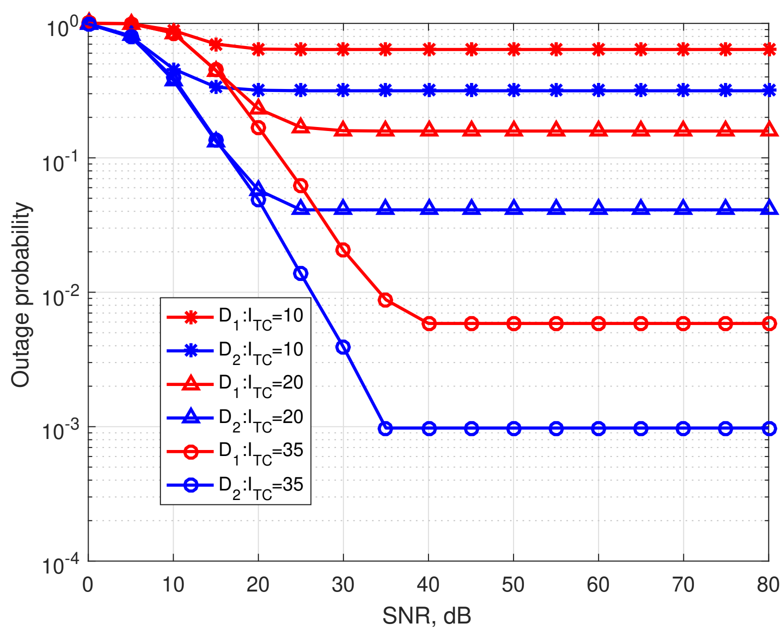

Figure 3.6: Outage probability comparison between CR with NOMA/OMA of D_1 and D_2 versus SNR with different choices of I_{ITC}

3.5 Conclusion

In this chapter, the performance of simple underlay CR-NOMA system is presented and investigated. We derived the closed-form expressions for the outage probability, achievable data rates and throughput o. The results confirm that the system has shown user D_2 has a better performance compared to the user D_1. The impact of ITC from the primary network is the basic factor affecting CR-NOMA system performance, the best results were obtained at I_{ITC} =35 dB. The system CR-NOMA had a better performance than CR-OMA for two users.

Chapter 4

Outage Performance of Underlay CR-NOMA based D2D Communications under Imperfect CSI and SIC.

4.1 Introduction

The evolution of wireless communication has witnessed remarkable advancements from the 1G to the upcoming 6G. Each generation has brought significant improvements in terms of data rates, capacity, and network capabilities. With 1G, we witnessed the birth of analog cellular networks, enabling voice communication on a limited scale. The subsequent generations, namely 2G, 3G, 4G, and 5G, introduced digital technologies, higher data speeds, and enhanced multimedia capabilities. However, the future of wireless communication lies in the development of 6G, which aims to revolutionize connectivity and enable unprecedented applications and services. Building upon the foundation laid by 5G, 6G will leverage advanced technologies such as millimeter waves, massive MIMO, and terahertz frequencies to achieve unparalleled data rates and ultra-low latency. Moreover, 6G will integrate innovative communication techniques to further enhance the efficiency and reliability of wireless networks [60],[61],[62]. One such technique is NOMA, which allows multiple users to share the same time-frequency resources simultaneously. NOMA improves spectral efficiency and supports a massive number of connections, making it ideal for the anticipated explosion of IoT devices and applications [64]. In addition to NOMA, the future of wireless communication will see the integration of cognitive radio and D2D communication. Cognitive radio technology enables intelligent spectrum sensing and utilization, enabling dynamic spectrum access and efficient spectrum sharing. Underlay cognitive radio is a prominent approach within the cognitive radio paradigm that focuses on enabling secondary users to opportunistically access the spectrum while ensuring minimal interference to the primary users. Unlike overlay cognitive radio, which involves the allocation of dedicated spectrum bands for secondary users, underlay cognitive radio allows simultaneous transmission of primary and secondary users in the same frequency band. This coexistence is achieved through sophisticated interference management techniques, such as power control, spectrum sensing, and dynamic spectrum access [65]. D2D communication facilitates direct communication between user devices, bypassing the base station, which can enhance network capacity, reduce latency, and enable new proximity-based services. The combination of NOMA, cognitive radio, and D2D communication in 6G will pave the way for future communication systems that are highly efficient, flexible, and capable of supporting diverse applications ranging from AR and VR to smart cities and autonomous systems. The seamless integration of these technologies will revolutionize wireless communication, enabling a hyper-connected world where devices intelligently cooperate, networks adapt dynamically, and communication experiences reach unprecedented levels of sophistication and efficiency [66].

4.1.1 Related Works

The authors of the reference [67] investigated the use of NOMA-assisted mobile ad-hoc networking (MANET) for long-term radio access. The downlink scenario investigates the performance of the considered NOMA-based system on a Nakagami-m fading channel. The authors derived the closed-form expression of BER at the end users supported by ad-hoc networks cooperating through the near NOMA user as well as the far NOMA user. The downlink cooperative NOMA without diversity combining (CNOMA-WDC) is studied in the reference [68]. The near user assists the far user by acting as a helper user in DF mode. The analytical closed-form BER expression for the near user using Rayleigh fading is derived. In [69], the authors investigated the combination of downlink cooperative NOMA (C-NOMA) with a D2D network in Amplify-and-Forward (AF) and DF schemes is explored to achieve a remarkable tradeoff between outage performances and transmit power at BS. By transmitting the effect of the power division coefficient, the results showed that the OP transmits the SNR and transmits the power of the preferred scheme. The authors in the reference [70] proposed and investigated a dual-hop cooperative relaying scheme based on NOMA, in which two sources communicate with their corresponding destinations in parallel via a common relay over the same frequency band. The demonstration of the proposed protocol was carried out in terms of ergodic sum capacity using simulations and mathematical analysis, considering both perfect and imperfect SIC. C-NOMA networks with relaying user selection have been investigated in the reference [71], where a two-stage user selection scheme is used to optimize the weak user's received SNR. The analytical expressions for C-NOMA users' OP under two types of channel estimation errors are calculated by derivation. In the reference [72], the authors investigated a DF cooperative underlay CR-NOMA network. In the presence of imperfect CSI, exact closed-form expressions for OP of two NOMA secondary destination users are derived. The outage behavior and throughput performance of the complex model of EH-assisted CR-NOMA is investigated as awareness of imperfect SIC at the receiver in the reference [58].

4.1.2 Motivation and Contributions

Motivated by these works, in the reference [67] the derivations of BER were investigated when the system consists of four users (nearby users act as helper users to help far users) in the presence of Nakagami fading channels. In the reference [68] the derivations of BER were investigated. The system contains two users (near users act as helper users to help far users) in the presence of Rayleigh fading channels. In the reference [69] the derivations of OP were investigated. The system contains two users (near users act as helper users to help far users) in the presence of Rayleigh fading channels. The above works investigated with perfect CSI and SIC assumptions, and it is not a practical and realistic scenario. The NOMA mode was used in the previous works. According to the author's knowledge, underlay CR- NOMA-based D2D communication under imperfect CSI and SIC has not received much attention and investigation. In this chapter, the underlay CR-NOMA-based D2D system over the Rayleigh channel in DF mode, where near users (D1, D2) act as helper users to help far users (D3, D4). The derivation of the closed-form expressions for OP and throughput at the end users were investigated in three scenarios: (1) Perfect SIC and perfect CSI. (2) Imperfect CSI. (3) Imperfect SIC. The contributions of this chapter are summarized as follows:

- We derived the closed form expressions of the far users (D3 and D4), in terms of OP and throughput.
- We analyzed the performance of our considered system under imperfect SIC and CSI.
- We used CR-OMA as benchmark for comparison.

- We discussed the optimal PA value.

The remainder of the chapter is organized as follows: Section 2 describes the system model; and Section 3 presents the discussion of the results. Finally, section 4 depicts the chapter's conclusion.

4.2 System Model

We investigate in this chapter the performance of the underlay CR NOMA based D2D system over Rayleigh fading channel for the downlink scenario. Fig. 4.1 depicts the system model, which includes a PN and an underly SN. There are five users and BS in this model. The user in the PN is a PU,and there are two NOMA users (far-user (D_1) and near-user (D_2)) cooperated with the two weak users (D_3 and D_4) at the cell edge.

The SN receives interference from PU. Four users' power in the SN is influenced by the PU in the PN. Four users in SN also impact the PU in the PN, and g_{sc}, g_{1c}, g_{2c}, g_{3c} , g_{4c} indicate link from BS,D_1,D_2, D_3 and D_4 to PU, respectively. Due to the existence of the PN, the SN meets interference from the primary base station (PBS), $I_j \sim \mathcal{CN}(0, \eta_j N_0), j \in \{1, 2, 3, 4\}$: are the interference channels from PBS affecting users in SN. The Rayleigh fading channel coefficients g_{D_j}, where $j = 1, 2, 3, 4$ are used for link $BS - D_1$, BS-D_2,$D_1 - D_3$ and $D_2 - D_4$, respectively. The BS sends S as a SC signal involving m_1 message of D_1 and m_1 message of D_2 :

$$S = \sqrt{E_{BS}} \left(\sqrt{b_1} m_1 + \sqrt{b_2} m_2 \right) \tag{4.1}$$

The secondary network transmission is limited by transmit power constraints as follows: $E_{BS} < \min\left(\frac{ITC}{|g_{SC}|^2}, \bar{E}_{BS}\right)$. Where I_{ITC} and $\bar{E}_{BS}$ denote the ITC at D_j , $j = 1, 2, 3, 4$ and the maximum average transmit power at BS, respectively. b_1 and b_2 are the power allocation coefficients for user D_1 and D_2 , respectively.

4.3 Performance Analysis

4.3.1 Perfect SIC and CSI

In the first time slot, the received signal from the user D_j,j=1,2 is expressed as [68],[67], [72] , [54], [73]:

$$y_{D_j} = S_{g_i} I_j + n_{D_i}(2) \tag{4.2}$$

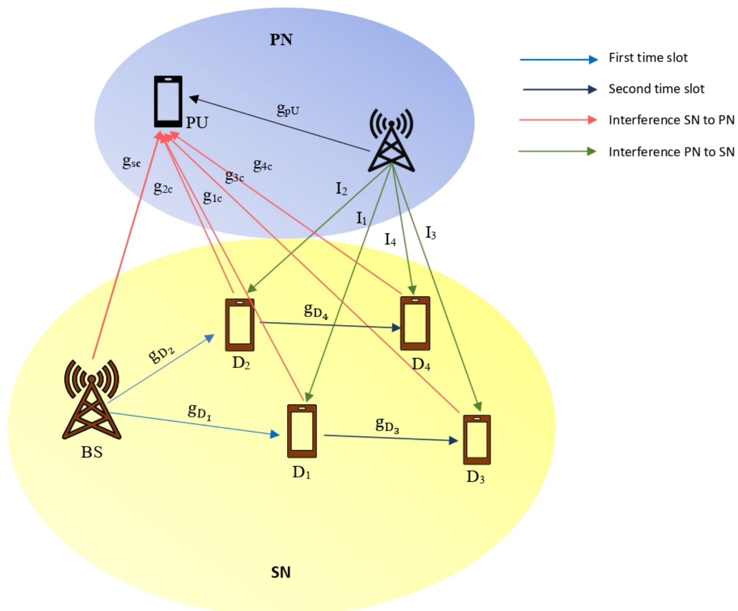

Figure 4.1: The system model of the underlay CR-NOMA-based D2D.

Regarding detection, the SINR after detecting m_1 message of user D_1 can be calculated as:

$$\gamma_{D_1} = \frac{\rho_S b_1 |g_{D_1}|^2}{\rho_S b_2 |g_{D_1}|^2 + \eta_1 + 1} \tag{4.3}$$

Where $\rho_s = \frac{E_{BS}}{\sigma^2}$ is the transmission SNR at the BS. The SINR to decode signal m_1 at user D_2 can be given by:

$$\gamma_{D_{12}} = \frac{\rho_S b_1 |g_{D_2}|^2}{\rho_S b_2 |g_{D_2}|^2 + \eta_2 + 1} \tag{4.4}$$

To apply NOMA, by executing SIC, it determined to detect signal m_2 at D_2 the SINR as [54]:

$$\gamma_{D_2} = \frac{\rho_s b_2 |g_{D_2}|^2}{1 + \eta_2} \tag{4.5}$$

After receiving the signal D_j ,j=1,2 will send the message $s_j = \widetilde{m_j}$ with power E_R to D_j,j=3,4 where $\widetilde{m_j}$ denote the decoded version of m_j. If D_j correctly decodes m_j, we achieve $\widetilde{m_j} = m_j$. If not, we achieve $\widetilde{m_j} \neq m_j$.

In the second time slot, the received signals at destination D_j,j=3,4 is expressed by:

$$y_{D_j} = g_{D_j}\sqrt{E_R}s_j + I_j + n_j \tag{4.6}$$

After D_j competently decodes s_j, the SINR at D_j,j=3,4, to get its own data, i.e.,s_j is shown by [69] [74] :

$$\gamma_{D_j} = \frac{\rho_R \left|g_{D_j}\right|^2}{\eta_j + 1} \tag{4.7}$$

Where $\rho_R = \frac{E_R}{{\sigma_R}^2}$.

4.3.1.1 OP under Perfect SIC and CSI

In this section, we investigate the outage probability of the underlying CR-NOMA-based D2D system. The probability that the achievable SNR is less than the predefined SNR is the meaning of the message's OP. It is computed using the probability density function (PDF) and cumulative distribution function (CDF) of the channel g_{D_k}, can be written as follows:

$$f_{\left|g_{D_j}\right|^2}(y) = \frac{1}{\lambda_{D_j}} e^{-\frac{y}{\lambda_{D_j}}} \tag{4.8}$$

$$f_{\left|g_{D_j}\right|^2}(y) = 1 - e^{-\frac{y}{\lambda_{D_j}}} \tag{4.9}$$

Where Pr$(\cdot)$: the probability function, the channel gain expressed as $\lambda_{D_j} = d_{D_j}^{-\alpha}$, α : is the path-loss exponent and it should be noted that the correct operation of D_4 occurs on based on the SIC. Using equations (8) and (9), we can compute the OP at D_4 as follows [69], [54]:

$$OP_{D_4} = 1 - \Pr\left\{\gamma_{D_{12}} \geq \gamma_{D_{4,th}}, \gamma_{D_4} \geq \gamma_{D_{4,th}}, \gamma_{D_2} \geq \gamma_{D_{2,th}}\right\} \tag{4.10}$$

The expression (8) can be rewritten as follows.

$$OP_{D_4} = 1 - \begin{bmatrix} \Pr\left\{\left|g_{D_2}\right|^2 \geq \frac{\theta}{\rho_S}, \left|g_{D_4}\right|^2 \geq \frac{\zeta_4 \gamma D_{4,th}}{\rho_R}, \left|g_{sc}\right|^2 < \frac{\rho_I}{\rho_S}\right\} + \\ \Pr\left|g_{D_2}\right|^2 < \frac{\theta\left|g_{sc}\right|^2}{\rho_I}, \left|g_{D_4}\right|^2 < \frac{\zeta_4 \gamma D_{4,th}\left|g_{sc}\right|^2}{\rho_I}, \left|g_{sc}\right|^2 > \frac{\rho_I}{\rho_S} \end{bmatrix} \tag{4.11}$$

The outage probability of D_4 can be shown by [73] :

$$\begin{aligned} OP_{D4} = 1 - \Bigg[& \int_0^{\frac{\rho_I}{\rho_S}} f_{|g_{sc}|^2}(x) \int_{\frac{o}{\rho_S}}^{\infty} f_{|g_{D_2}|^2}(y) \int_{\frac{\zeta_4 \gamma_{4,th}}{\rho_R}}^{\infty} f_{|g_{D_4}|^2}(z)\, dz\, dy\, dx \\ & + \int_{\frac{\rho_I}{\rho_S}}^{\infty} f_{|g_{sc}|^2}(x) \int_{\frac{o\,x}{\rho_I}}^{\infty} f_{|g_{D_2}|^2}(y) \int_{\frac{x\,\zeta_4\,\gamma_{4,th}}{\rho_I}}^{\infty} f_{|g_{D_4}|^2}(z)\, dz\, dy\, dx \Bigg] \end{aligned} \tag{4.12}$$

We denote $\gamma_{D_{j,th}}, j \in 1,2,3,4:$ as the target SINRs to decode D_j's message, $\theta = \max\left(\frac{\zeta_2\gamma_{D_4,th}}{(b_1-b_2\gamma_{D,\gamma_{th}})}, \frac{\zeta_2\gamma_{D_2,th}}{b_2}\right)$ and $\zeta_j = (1+\eta_j)$. Thus, after some manipulations we can rewrite it to the following form:

$$OP_{D4} = 1 - \left(\left(1 - e^{-\frac{\rho_I}{\rho_S\lambda_{sc}}}\right) \times e^{-\frac{\theta}{\rho_S\lambda_{D2}}} \times e^{-\frac{\zeta_4\gamma_{4,th}}{\rho_R\lambda_{D4}}}\right) + l_1 e^{-\frac{\zeta_4\gamma_{4,th}\lambda_{sc}\lambda_{D2}+\lambda_{D4}\theta\lambda_{sc}+\lambda_{D4}\rho_I\lambda_{D2}}{\lambda_{D4}\lambda_{sc}\lambda_{D2}\rho_S}} \quad (4.13)$$

Where $l_1 = \frac{\lambda_{D4}\rho_1\lambda_{D2}}{\zeta_4\gamma_{4,th}\lambda_{sc}\lambda_{D2}+\lambda_{D4}o\lambda_{sc}+\lambda_{D4}\rho_1\lambda_{D2}}$

The outage probability at D3 can be expressed by [69], [54]:

$$OP_{D_4} = 1 - Pr\{\gamma_{D_{12}} \geq \gamma_{D_{4,th}}, \gamma_{D_4} \geq \gamma_{D_{4,th}}, \gamma_{D_2} \geq \gamma_{D_{2,th}}\} \quad (4.14)$$

The expression (14) can be rewritten as follows:

$$OP_{D_3} = 1 - \left[\begin{array}{c} \Pr\left\{|g_{D_1}|^2 \geq \frac{\zeta_1\delta}{\rho_S}, |g_{D_3}|^2 \geq \frac{\zeta_3\gamma D_{3,th}}{\rho_R}, |g_{sc}|^2 < \frac{\rho_I}{\rho_S}\right\} \\ + \Pr|g_{D_1}|^2 < \frac{\zeta_1\delta|g_{sc}|^2}{\rho_I}, |g_{D_3}|^2 < \frac{\zeta_3\gamma D_{3,th}|g_{sc}|^2}{\rho_I}, |g_{sc}|^2 > \frac{\rho_I}{\rho_S} \end{array}\right] \quad (4.15)$$

The same as solving expressions from equations (10), the OP at D_3 as

$$OP_{D_3} = 1 - \left[\left(1 - e^{-\frac{\rho_I}{\rho_S\lambda_{sc}}}\right) \times e^{-\frac{\zeta_1\delta}{\rho_S\lambda_{D_1}}} \times e^{-\frac{\zeta_3\gamma_{D_3,th}}{\rho_R\lambda_{D_3}}}\right] + l_2 \times e^{-\frac{\zeta_3\gamma_{D_3,th}\lambda_{sc}\lambda_{D_1}+\lambda_{D_3}\zeta_1\delta\lambda_{sc}+\lambda_{D_3}\rho_I\lambda_{D_1}}{\lambda_{D_3}\lambda_{sc}\lambda_{D_1}\rho_S}} \quad (4.16)$$

Where $l_2 = \frac{\lambda_{D3}\rho_1\lambda_{D1}}{\zeta_3\gamma_{D3,th}\lambda_{sc}\lambda_{D1}+\lambda_{D3}\zeta_1\delta\lambda_{sc}+\lambda_{D3}\rho_1\lambda_{D1}}, \delta = \frac{\gamma_{D1,th}}{b_1-b_2\gamma_{D1,th}}$

4.3.2 Imperfect SIC

In this scenario, it is assumed that user D_2 has not complete knowledge of the user D1 signal. Therefore, it is assumed that D_2 cannot completely remove the interference from D_1, which offers a more actual scenario than the perfect SIC scenario [75]. The received signal at the user D_2 becomes [70] ,[76]:

$$y_{D_2}^{SIC} = \sqrt{E_{BS}}\sqrt{b_2}m_2g_2 + \sqrt{\epsilon b_1}m_1\sqrt{E_{BS}}g_2 + I_2 + n_{D_2} \quad (4.17)$$

Where the variable 0< ε <1 , ε is the level of residual interference. The SNR at D_2 becomes:

$$\gamma_{D_2}^{SIC} = \frac{\rho_S b_2|g_{D_2}|^2}{\varepsilon\rho_S b_1|g_{D_2}|^2 + 1 + \eta_2} \quad (4.18)$$

4.3.2.1 OP under Imperfect SIC

In this section, we investigate the outage probability under imperfect SIC. The outage event at D_4 can be written by:

$$OP_{D_4}^{SIC} = 1 - Pr\{\gamma_{D_{12}} \geq \gamma_{D_{4,th}}, \gamma_{D_4} \geq \gamma_{D_{4,th}}, \gamma_{D_2}^{SIC} \geq \gamma_{D_{2,th}}\} \tag{4.19}$$

The expression (19) can be rewritten as follows:

$$\begin{aligned} OP_{D4}^{SIC} = 1 - &\left[\Pr\left\{ |g_{D_2}|^2 \geq \frac{\theta^{SIC}}{\rho_S}, |g_{D_4}|^2 \geq \frac{\gamma_{D_{4,th}}\zeta_4}{\rho_R}, |g_{sc}|^2 < \frac{\rho_I}{\rho_S} \right\} \right. \\ &\left. + \Pr\left\{ |g_{D_2}|^2 < \frac{\theta^{SIC}|g_{sc}|^2}{\rho_I}, |g_{D_4}|^2 < \frac{\gamma_{D_{4,th}}\zeta_4|g_{sc}|^2}{\rho_I}, |g_{sc}|^2 > \frac{\rho_I}{\rho_S} \right\} \right] \end{aligned} \tag{4.20}$$

Thus, after some manipulations we can rewrite it to the following form as in (21)

$$OP_{D4}^{SIC} = 1 - \left(\left(1 - e^{-\frac{\rho_I}{\rho_S \lambda_{sc}}} \right) \times e^{-\frac{\theta^{SIC}}{\rho_S \lambda_{D2}}} \times e^{-\frac{\zeta_4 \gamma_{4,th}}{\rho_R \lambda_{D4}}} \right) + l_1^{SIC} e^{-\frac{\zeta_4 \gamma_{4,th} \lambda_{sc} \lambda_{D2} + \lambda_{D4} \theta^{SIC} \lambda_{sc} + \lambda_{D4} \rho_I \lambda_{D2}}{\lambda_{D4} \lambda_{sc} \lambda_{D2} \rho_S}} \tag{4.21}$$

Where $l_1^{SIC} = \frac{\lambda_{D4}\rho_I\lambda_{D2}}{\zeta_4\gamma_{4,th}\lambda_{sc}\lambda_{D2}+\lambda_{D4}\theta^{SIC}\lambda_{sc}+\lambda_{D4}\rho_I\lambda_{D2}}$, $\theta^{SIC} = \max\left(\frac{\zeta_2\gamma_{D_{4,th}}}{(b_1 - b_2\gamma_{D_{4,th}})}, \frac{\zeta_2\gamma_{D_{2,th}}}{(b_2 - \varepsilon b_1\gamma_{D_{2,th}})} \right)$

4.3.3 Imperfect CSI

In this scenario, we consider that the imperfect CSI at users is available. The channel coefficients that are modeled using the minimum mean square error channel estimation error as shown in [72], [77],[78] as well as written as : $g_{D_k} = h_k + e_k, \quad \forall_k \in \{1, 2, 3, 4\}$ where h_k represents the estimated channel coefficient with $CN(0, \sigma_{h_k}^2)$. While e_k is the error term, which is typically modeled as a complex Gaussian distributed random variable with $CN(0, \sigma_{e_k}^2)$.

In this section, we assume that $\sigma_{e_k}^2$ is constant. The received signal at the user D_j is expressed as:

$$y_{D_j}^{CSI} = S(h_j + e_j) + I_j + n_{D_j} \tag{4.22}$$

The SINR after detecting m_1 of user D_1 can be calculated as:

$$\gamma_{D_1}^{CSI} = \frac{\rho_S b_1 |h_{D_1}|^2}{\rho_S b_2 |h_{D_1}|^2 + |e_1|^2 \rho_S + \eta_1 + 1} \tag{4.23}$$

The SINR to decode signal $m_1$at user D_2 can be written by:

$$\gamma_{D_12}^{CSI} = \frac{\rho_S b_1 |h_{D_2}|^2}{\rho_S b_2 |h_{D_2}|^2 + |e_2|^2 \rho_S + \eta_2 + 1} \tag{4.24}$$

To apply NOMA, by executing SIC, it determined to detect signal m_2 at D_2 the SINR as [54]:

$$\gamma_{D_2}^{CSI} = \frac{\rho_S b_2 |h_{D_2}|^2}{|e_2|^2 \rho_S + 1 + \eta_2} \tag{4.25}$$

The received signal at destination is expressed by:

$$y_{D_i}^{CSI} = h_{D_i}\sqrt{P_R} s_i + e_{D_i}\sqrt{P_R} s_i + I_i + n_i \tag{4.26}$$

After D_j competently decodess$_i$, the SINR at D_i,respectively, to get its own data, i.e., s_i is shown by:

$$\gamma_{D_i}^{CSI} = \frac{\rho_R |h_{D_i}|^2}{|e_i|^2 \rho_R + \eta_+ 1} \tag{4.27}$$

4.3.3.1 OP under Imperfect CSI

The outage probability under imperfect CSI [72], [54],[79],[76] can be written as:

$$OP_{D_4}^{CSI} = Pr\{\gamma_{D_{12}} \geq \gamma_{D_{4,th}}, \gamma_{D_4} \geq \gamma_{D_{4,th}}, \gamma_{D_2} \geq \gamma_{D_{2,th}}\} \tag{4.28}$$

Where $\emptyset_4 = \gamma_{D_{4,th}} |e_4|^2, \emptyset_2 = \theta^{csi} |e_2|^2, \theta^{CSI} = \max\left(\frac{\gamma_{D_{4,th}}}{(b_1 - b_2 \gamma_{D_{4,th}})}, \frac{\gamma_{D_{2,th}}}{b_2}\right)$

Thus, after some manipulations we can rewrite it to the following form as in (16)

$$\begin{aligned} OP_{D_4}^{CSI} &= \left(1 - e^{-\frac{\rho_I}{\rho_S \lambda_{sc}}}\right) \times e^{-\frac{\zeta_2 \theta^{CSI}}{\rho_S \lambda_{D_2}} + \emptyset_2} \times e^{-\frac{\zeta_4 \gamma_{4,th}}{\rho_R \lambda_{D_4}} + \emptyset_4} \\ &+ e^{-\psi_2} \times e^{-\psi_4} \times l_2^{CSI} \times e^{-\frac{1}{\rho_S}\left(\frac{\zeta_4 \gamma_{4,th} \lambda_{sc} \lambda_{D_2} + \lambda_{D_4} \zeta_2 \theta^{CSI} \lambda_{sc} + \lambda_{D_4} \rho_I \lambda_{D_2}}{\lambda_{D_4} \lambda_{sc} \lambda_{D_2}}\right)} \end{aligned} \tag{4.29}$$

Where $l_2^{CSI} = \frac{\lambda_{D4} \rho_I \lambda_{D2}}{\zeta_4 \gamma_{4,th} \lambda_{sc} \lambda_{D2} + \lambda_{D4} \theta^{CSI} \zeta_2 \lambda_{sc} + \lambda_{D4} \rho_I \lambda_{D2}}$

The outage probability at D3 is calculated as [69], [54]:

$$OP_{D_3}^{CSI} = 1 - Pr\{\gamma_{D_1} \geq \gamma_{D_{1,th}}, \gamma_{D_3} \geq \gamma_{D_{3,th}}\} \tag{4.30}$$

The outage probability of D3 is given as in (31)

$$\begin{aligned} OP_{D_3}^{CSI} = 1 - &\left[\left(1 - e^{-\frac{\rho_I}{\rho_S \lambda_{sc}}}\right) \times e^{-\left(\frac{\zeta_1 \delta^{CSI}}{\rho_S \lambda_{D_1}} + \psi_1\right)} \times e^{-\left(\frac{\zeta_3 \gamma_{D_{3,th}}}{\rho_R \lambda_{D_3}} + \psi_3\right)}\right] \\ &+ e^{-\psi_1} \times e^{-\psi_3} \times l_1^{CSI} \times e^{-\frac{\zeta_3 \gamma_{D_{3,th}} \lambda_{sc} \lambda_{D_1} + \lambda_{D_3} \zeta_1 \delta^{CSI} \lambda_{sc} + \lambda_{D_3} \rho_I \lambda_{D_1}}{\lambda_{D_3} \lambda_{sc} \lambda_{D_1} \rho_S}} \end{aligned} \tag{4.31}$$

Where $\delta^{CSI} = \frac{\gamma_{D_{1,th}}}{b_1 - b_2 \gamma_{D_{1,th}}}, \emptyset_3 = \gamma_{D_{3,th}} |e_3|^2, \emptyset_1 = \delta^{CSI} |e_1|^2, \psi_1 = \frac{\emptyset_1}{\lambda_{D1}}, \psi_3 = \frac{\emptyset_3}{\lambda_{D3}}$, $l_1^{CSI} = \frac{\lambda_{D3} \rho_I \lambda_{D1}}{\zeta_3 \gamma_{D3,th} \lambda_{sc} \lambda_{D1} + \lambda_{D3} \zeta_1 \delta^{CSI} \lambda_{sc} + \lambda_{D3} \rho_I \lambda_{D1}}$

4.3.4 Throughput

The throughput can be calculated by interpreting each user's outage behavior:

$$T_4 = R_4(1 - OP_{D_4}) \tag{4.32}$$

$$T_3 = R_3(1 - OP_{D_3}) \tag{4.33}$$

4.4 Results and Discussion

In this section, we use Monte Carlo simulations to verify the analytical OP expressions from the previous section. In all figures, the markers denote the analytical curves, and the lines depict the simulation's results. We set the following simulation parameters : d_2=d_4=d_{sp}=1, α=3,b_1=0.85,I_{ITC}=30dB and R_3=0.5 BPCU, R_4=1 BPCU, η_1=η_2= η_3= η_4 The terms "Sim" and "Th." refer to simulation and analytical results and curves, respectively.

Fig. 4.2 illustrates the outage probability performance comparison between CR-OMA and CR-NOMA of users (D3, D4) versus SNR, respectively. For CR-NOMA, the outage of D4 performs better than that of D3 for all SNR values, the performance gap between two users exists because each user's power allocation factors have always been different. At high SNR, the OP curves for CR-NOMA users begin to saturate. The simulations also confirmed the OP_{D3} and OP_{D4} analytical results. It can be seen clearly that the performance of CR-NOMA is higher than that of CR-OMA.

Fig. 4.3 depicts the outage performance CR-NOMA of users (D_3, D_4) versus the transmit SNR in both perfect and imperfect SIC modes. The exact analytical results agree well with the numerical simulations and the outage probabilities decrease with the increase of transmit SNR, until the outage performance reaches saturation at high SNR. The impact of residual interference level on the outage probability of user (D4) can be seen. It is shown that the outage probability of D4 decreases when the level of residual interference increases.

Fig. 4.4 indicates the Outage performance CR-NOMA of users (D3, D4) versus the transmit SNR with perfect and imperfect CSI. The exact analytical results agree well with the numerical simulations and the outage probabilities decrease with the increase of transmit SNR, until the outage performance reaches saturation at high SNR. In aspects of imperfect CSI, it should be noted that imperfect CSI reduces the OP of the signal of users D3 and D4.

Fig. 4.5 presents the throughput performance comparison between CR-NOMA and CR-OMA of users (D3, D4) versus SNR, respectively. The performance of CR-NOMA is higher than that of CR-OMA and the throughput of D4 performs better than that of D3. The impact of residual interference signal on throughput of user D4 can be seen in Fig. 4.6. It is shown that the throughput of D4 decreases when the level of residual interference increases. The effect of perfect and imperfect CSI is evaluated for the throughput performance and presented in Fig. 4.7, it should be noted that imperfect CSI reduces the throughput performance of the signal of users (D_3,D_4). Fig. 4.8 depicts various trends in the outage probability of users (D_3,D_4) as the power allocation factor b_1 increases. Higher I_{ITC} results in decreased outage performance because more power is used for signal processing in transmission. It should be noted that b_1 must be greater than 0.5 due to weak users demand for a higher power allocation factor. As a result, OP occurs if $b_1 < 0.5$ for users D_3 and D_4 in both scenarios of transmission I_{ITC}. The main reason is that b_1 affects SINR variation, which significantly impacts outage performance.

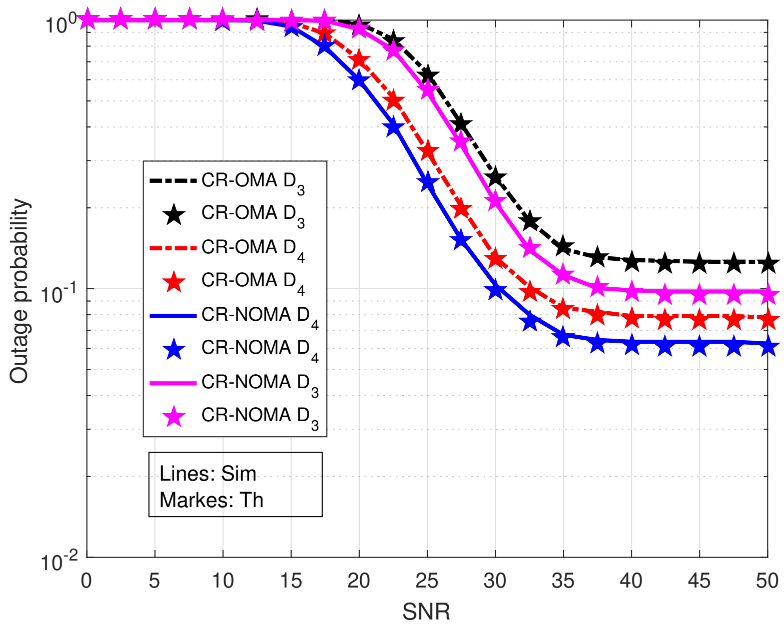

Figure 4.2: Outage performance comparison between CR-OMA and CR-NOMA of users (]D_3, D_4) versus SNR.

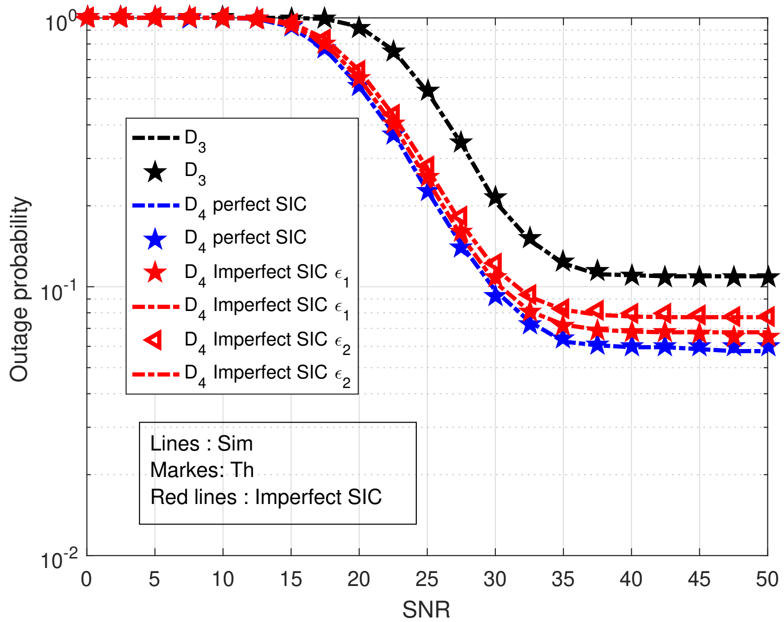

Figure 4.3: Outage performance CR-NOMA of users (D_3, D_4) versus the transmit SNR in both perfect and imperfect SIC modes.

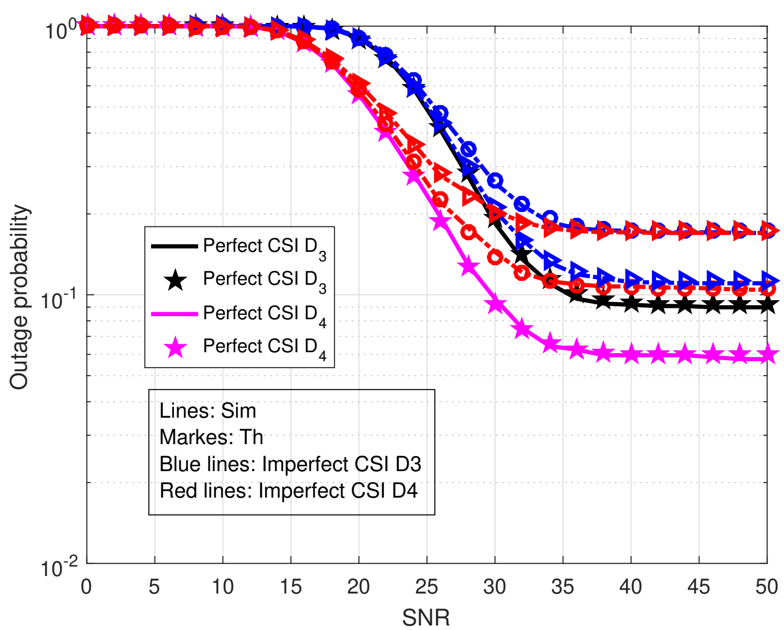

Figure 4.4: Outage performance CR-NOMA of users (D_3, D_4) versus the transmit SNR with perfect and imperfect CSI.

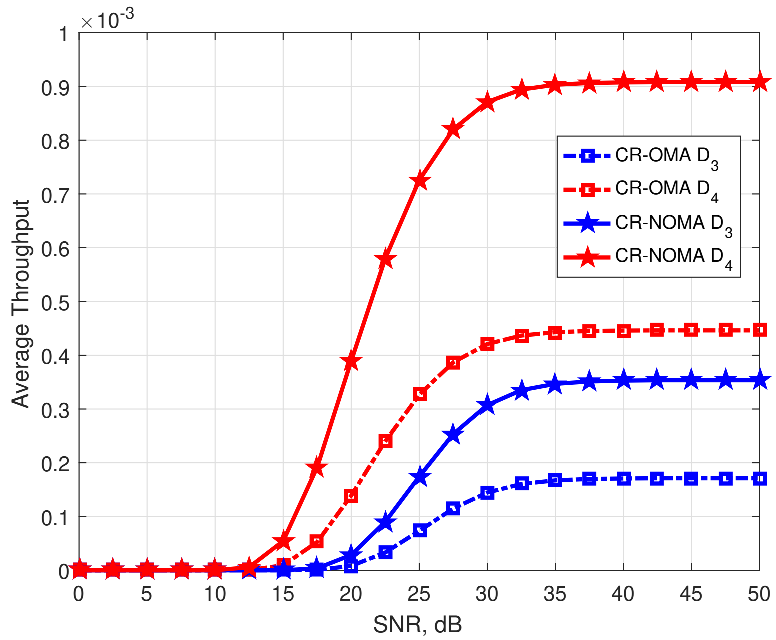

Figure 4.5: Throughput comparison between CR-NOMA and CR-OMA of users (D_3, D_4) versus SNR.

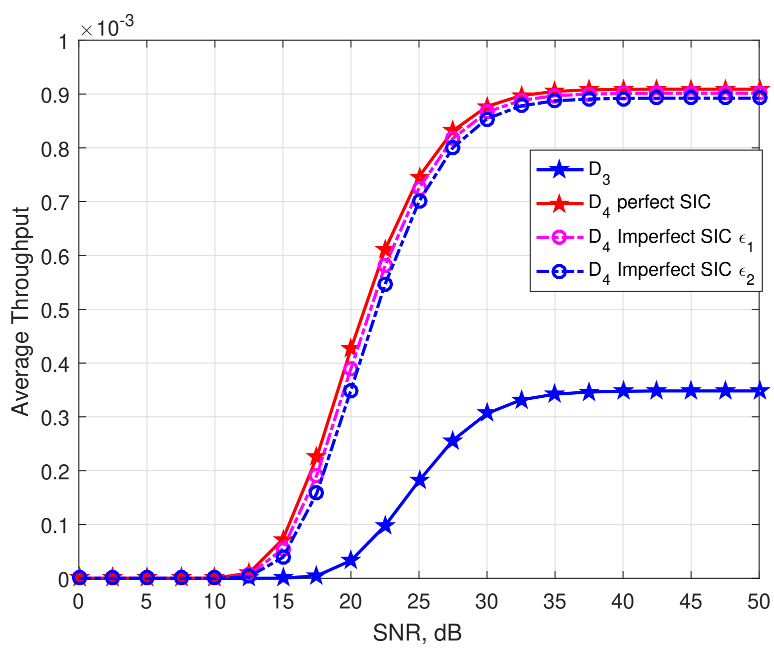

Figure 4.6: Throughput CR-NOMA of users (D_3, D_4) versus the transmit SNR in both perfect and imperfect SIC modes.

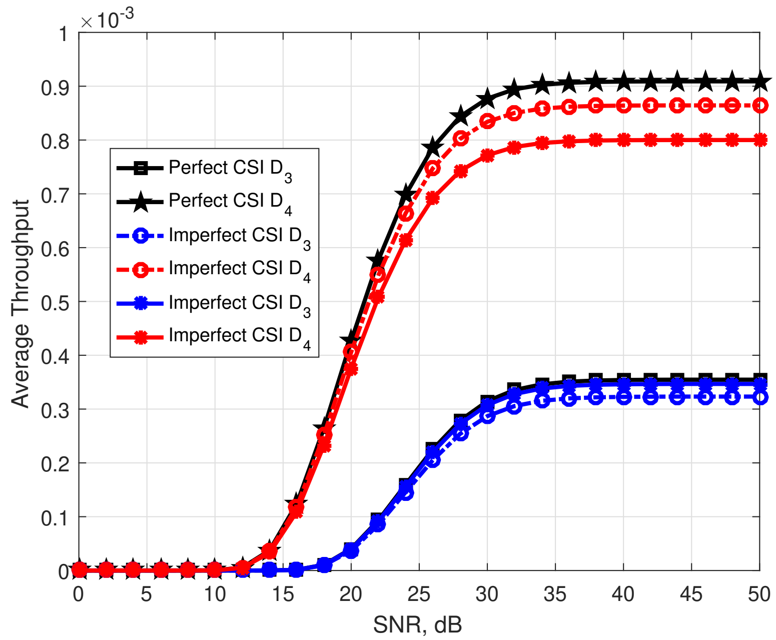

Figure 4.7: Throughput CR-NOMA of users (D_3,D_4) versus the transmit SNR, with perfect and imperfect CSI.

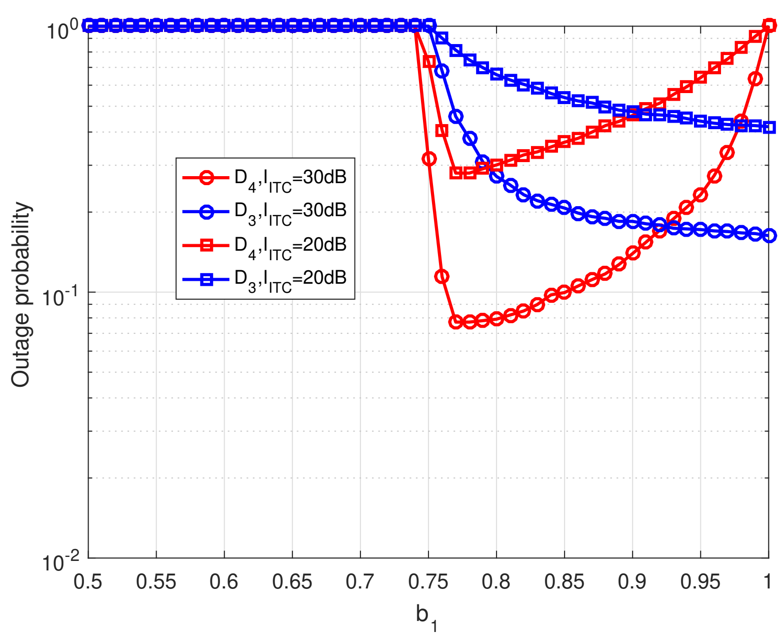

Figure 4.8: Outage performance CR-NOMA of users (D_3, D_4) versus power division as varying I_{ITC}.

4.5 Conclusion

In this chapter, the OP performance of underlay CR-NOMA based D2D communications in a downlink system was investigated over-generalized Rayleigh fading environment. The presence of imperfect CSI and SIC is taken into consideration while analyzing the users. The outage probability and throughput are derived from the end users cooperating with the near and far users. The results confirm that the system has demonstrated that D_4 outperforms D_3. The analysis results are validated with the help of simulations. The derived expressions of the downlink scenario are plotted numerically, as well as results are compared with the traditional cooperative CR-OMA system. The presence of imperfect CSI and imperfect SIC degrades the performance of the system. Moreover, we investigated the optimum value of power allocation.

Chapter 5

BER Analysis of Underlay Cooperative CR-NOMA System.

5.1 Introduction

The exponential growth of the 5G network allows companies and researchers to focus on the next-generation network. Many IoT devices need more than 5G to relay real-time data. Besides 5G, various research institutions are working on 6G, which is projected to generate high-QoS, energy and spectrum-efficient networks. Future application requirements will demand significant architectural changes in mobile networks. Security is one of the most significant challenges facing future generations [80]. 6G networks are larger, faster, and have lower latency than 5G [81]. Researchers in worldwide are suggesting advanced technologies like AI/ML, quantum communication/quantum machine learning (QML), blockchain, THz and mmWaves communication, tactile Internet,NOMA, CRNs, Cooperative Communications (CC) etc., as key technologies for the creation of 6G communications [82]. NOMA allows users to share the same resource elements in the time, frequency, space, or code domains. In NOMA, every user operates across the same frequency spectrum and simultaneously, with their power levels serving as a different factor. NOMA utilizes SC at the transmitter to enable the SIC receiver to separate between users in both the uplink and downlink channels [73]. Integrating NOMA with CC and CR presents great potential for 6G networks. Within the CC-NOMA system, a relay node with a robust channel decodes messages intended for users with weaker channels and utilizes this information to enhance the weaker user's performance. CR-NOMA allows unlicensed users to send signals over spectrum bands licensed to licensed users in an opportunistic and non-intrusive way. Recently, there has been a notable interest in combining cooperative and CR-NOMA concepts, known as CCR-NOMA, to enhance the spectral efficiency of dense wireless networks [83], [84].

5.1.1 Related Works

The authors analyzed the performance of a downlink NOMA system with SIC errors over the Rayleigh fading channels. They calculated the exact mathematical formulas for the BER at the near-user and far-user. A study of the achievable rate of the NOMA system, showing that its possible rate surpasses that of traditional OMA systems is presented in [85] with the calculation of the optimum power allocation coefficient for the NOMA systems. The authors of [86] derived an exact closed-form BER expression under SIC error for downlink NOMA over the Rayleigh fading channel and they develop exact equations for BER in the form of a one-degree integral and closed-form approximations for uplink NOMA. In [73], the authors examined the integration of NOMA in MANET for sustainable future radio access. They have evaluated the performance of the NOMA-based system using Nakagami-m fading channels in the downlink scenario. In [87] , the authors examined a downlink C-NOMA-WDC, where a nearby user acts as a helper user in DF mode to assist a distant user. The BER calculation is studied in a closed form for the nearby and far users under the Rayleigh fading channel. The authors of [88], investigated the BER performance of pre-paired cooperative Relaying full duplex NOMA (CR-FD-NOMA) users in downlink and uplink situations under the Nakagami-m fading distribution. Quadrature Phase Shift Keying (QPSK) is utilized for near-user information, while Binary Phase Shift Keying (BPSK) is employed for far-user information. An approximated closed-form BER expression for each user in downlink and uplink systems is developed by taking advantage of self-interference and the characteristics of Gaussian Q-functions at a high SNR regime. In [89] the authors investigated how relay-assisted NOMA performs in an underlay cognitive radio system with selective relays. K relays facilitate communication between secondary NOMA users and a secondary base station (SBS). The relay with the strongest connection to the SBS is chosen to amplify-and-forward (AF) received signals to the secondary receivers. The authors analyzed the pairwise error probability (PEP) for secondary users using imperfect SIC. The PEP formula is then used to derive a union bound. The authors in [90] discussed employing NOMA in the cognitive butterfly network, where a secondary relay aids a primary transmitter-receiver pair without a direct link, enabling spectrum sharing with a secondary pair. The network integrates uplink and downlink NOMA principles, leveraging nearby transmitters' side information to enhance SIC at the receivers. In [67], the authors highlighted the advantageous impact of

NOMA-CR on vehicle-to-everything (V2X) communication, showing its superior spectrum efficiency. This research examines two scenarios: one with the support of CR scheme and one without. Two system metrics in the suggested system examined to assess the performance of vehicles requiring greater QoS. The OP is initially calculated exactly, and then followed by the determination of the BER.

5.1.2 Motivation and Contributions

Motivated by the above references and the existing literature, most studies concentrate on obtaining the OP by assuming a perfect CSI scenario. However, these idealized conditions do not reflect practical realities. To the best of our knowledge, the exact closed-form expressions of the BER performance of underlay CCR-NOMA under imperfect CSI have not been extensively investigated. In [68], we examined the derivation of the OP. In this chapter, we derive the exact mathematical formulas for BER of distant users under both perfect and imperfect CSI conditions. The contributions of this study are summarized as follows:

- The derivation of the exact closed-form expression that characterizes the BER observed by distant users in the underlay CCR-NOMA system under Rayleigh fading conditions.
- Performance analysis of the considered system under both perfect and imperfect CSI conditions.
- Examination of the impact of varying the interference temperature constraint (I_{ITC}).
- Comparison of the proposed system with the conventional CCR-OMA protocol.

The remainder of the chapter is organized as follows: Section 2 explains the system model, Section 3 presents the results, Section 4 offers a discussion, and the conclusion is provided in Section 5.

5.2 System Model

This section investigates the BER performance of an underlay CCR-NOMA system in a downlink scenario over a Rayleigh fading channel. Fig. 5.1 depicts the system model, which includes a SN and a PN.

The PN comprises a user (PU) and a base station (BS). The SN includes four users and a base station(SBS). In the power domain, user (PU) coexists with two NOMA users: the near user (D_2) and the far user (D_1), who cooperate with two weak users (D_4 and D_3)

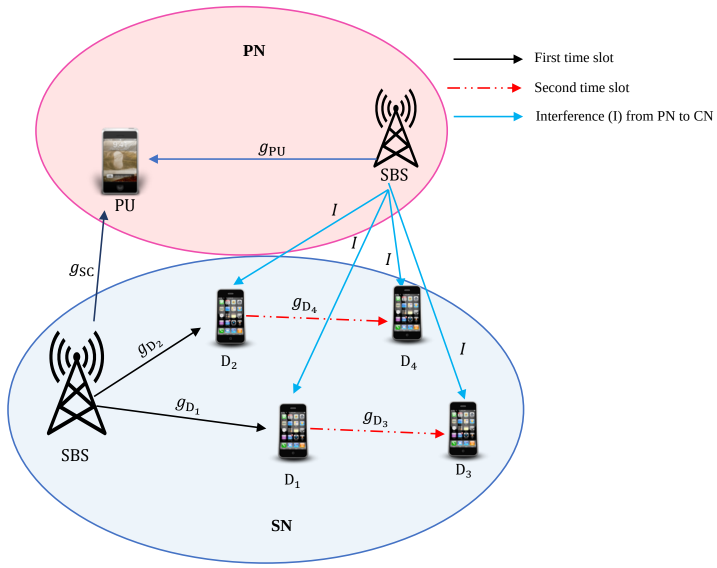

Figure 5.1: System model of underlay CCR with NOMA.

located at the cell edge. The power levels of the four individual users are influenced by the user PU. The base station(BS) also affects user PU, with g_{SC} link from BS to user PU. The interference channels from the PN affecting users in the CN are denoted as I $\sim CN(0, \eta N_0)$. The Rayleigh fading channel coefficients, denoted as g_{CU_q}, where q=j for 11,22 and q=i for 1,2: are used for the links BS-D_2, BS-D_1,D_2-D_4 and D_1-D_3, respectively. The base station (BS) transmits a SC signal consisting of the D_1 message m_1 and the D_2 message m_2. The SC signal can be given by:

$$S = \sqrt{E_{BS}}\left(\sqrt{b_1}m_1 + \sqrt{b_2}m_2\right) \tag{5.1}$$

Transmit power constraints restrict the SN transmission in the following ways:

$$E_{BS} \leq \min\left(\frac{I_{ITC}}{|g_{SC}|^2}, \bar{E}_{BS}\right) \tag{5.2}$$

Where I_{ITC} and $\bar{E}_{BS}$ represent the ITC at cognitive users (D_2,D_1,D_3,D_4) and the maximum average transmit power at BS, respectively. Users D_2 and D_1 have different PA coefficients, denoted as b_1 and b_2. n_{D_j} denoted the Additive White Gaussian Noise (AWGN) with mean 0 and variance $\sigma^2_{D_j}$ at D_j

5.3 Performance Evaluation

5.3.1 BER under Perfect CSI

This section focuses on calculating the BER for D_1 and D_2 users and the end-to-end BER users under the assumption of perfect CSI. The signal received by users D_j ,j=1,2 in the first time slot can be expressed as:

$$y_{D_j} = Sg_j + I + n_j \tag{5.3}$$

5.3.1.1 BER of the User D_1

The maximum likelihood detection (MLD) technique is employed by D_2 user to identify the symbol of the D_1 user. The BER in this case is determined based on whether the received signal is below or above zero [9],[10] and [15]. The BER of m_1 at D_1 user can be represented by

$$BER_{D_1} = \frac{1}{2}\left[P\left(I + n_{D_1} \geq \sqrt{E_{BS}b_1}g_{D_1} - \sqrt{E_{BS}b_2}g_{D_2}\right) + P\left(I + n_{D_1} > \sqrt{E_{BS}b_1}g_{D_1} + \sqrt{E_{BS}b_2}g_{D_1}\right)\right] \tag{5.4}$$

The Q function and the alternative form of Q(.) function are denoted respectively as in [87]:

$$Q(z) = \frac{1}{\sqrt{2\pi}}\int_z^\infty e^{-\frac{t^2}{2}}dt \tag{5.5}$$

$$Q(z) = \frac{1}{\pi}\int_0^{\frac{\pi}{2}} e^{-\frac{z^2}{2\sin^2(\vartheta)}}d\vartheta, z \geq 0 \tag{5.6}$$

The probability density function (PDF) and the moment generating function (MGF) are expressed respectively as in [87], [91] :

$$P(x) = \frac{1}{\sqrt{2\pi\sigma^2}}e^{-\frac{(x-\mu)^2}{2\sigma^2}}, x \sim (\mu, \sigma^2) \tag{5.7}$$

$$M_\rho(s) = \int_0^\infty e^{s\rho}\frac{1}{\rho}e^{-\frac{\rho}{\bar{\rho}}}d\rho = \frac{1}{1-s\bar{\rho}} \tag{5.8}$$

Where $\mu \in R, \sigma > 0, x \sim (\mu, \sigma^2)$,X is the random variable, μ is mean and σ is the variance. By utilizing equations (7) and (5), we may represent equation (4) as:

$$BER_{D_1} = \frac{1}{2}\left[Q\left(\sqrt{\rho_{D_2}}\right) + Q\left(\sqrt{\rho_{D_1}}\right)\right] \tag{5.9}$$

Where $\rho_{D_1} = \frac{2(\sqrt{E_{BS}b_1}-\sqrt{E_{BS}b_2})^2|g_{D_1}|^2}{\sigma_I^2+\sigma_{D_1}^2}, \rho_{D_2} = \frac{2(\sqrt{E_{BS}b_1}+\sqrt{E_{BS}b_2})^2|g_{D_1}|^2}{\sigma_I^2+\sigma_{D_2}^2}$

By utilizing equations (6) and (8), followed by several mathematical manipulations, the average bit error rate (ABER) of (9) is given as:

$$ABER_{D_1} = \frac{1}{4}\left[\left(1-\sqrt{\frac{\bar{\rho}_{D_1}}{2+\bar{\rho}_{D_1}}}\right) + \left(1-\sqrt{\frac{\bar{\rho}_{D_2}}{2+\bar{\rho}_{D_2}}}\right)\right] \tag{5.10}$$

Where $\bar{\rho}_{D_2} = \frac{2(\sqrt{E_{BS}b_1}-\sqrt{E_{BS}b_2})^2}{\sigma_I^2+\sigma_{D_2}^2}E[|g_{D_1}|^2], \bar{\rho}_{D_1} = \frac{2(\sqrt{E_{BS}b_2}+\sqrt{E_{BS}b_1})^2}{\sigma_I^2+\sigma_{D_2}^2}E[|g_{D_1}|^2]$

5.3.1.2 BER of the User D_2

The BER for D_2 is calculated through the applying of SIC, considering two scenarios: when D_1 user symbols are detected correctly and incorrectly [85], [92] and [93]. The BER for the user D_2 can be expressed as:

$$BER_{D_2} = BER_{D_{2e}} + BER_{D_{2c}} \tag{5.11}$$

Where $BER_{D_{2e}}$ and $BER_{D_{2e}}$ are the probabilities when detected D_1 user symbols erroneously and correctly, respectively.

The BER for these two scenarios is expressed as follows:

$$BER_{D_{2c}} = \frac{1}{2}\left[P\left(\sqrt{E_{BS}b_2}g_{D_2} < n_{D_4} + I\right) + P\left(\sqrt{E_{BS}b_2}g_{D_2} < n_{D_2} + I < \left(\sqrt{E_{BS}b_1} + \sqrt{E_{BS}b_2}\right)g_{D_2}\right)\right] \tag{5.12}$$

$$\begin{aligned} BER_{D_{2,e}} = \frac{1}{2}\Big[&P\left(\left(2\sqrt{E_{BS}\,b_1} + \sqrt{E_{BS}\,b_2}\right)g_{D_2} < n_{D_2} + I\right) \\ &+ P\left(\left(\sqrt{E_{BS}\,b_1} - \sqrt{E_{BS}\,b_2}\right)g_{D_2} < n_{D_2} + I < \left(2\sqrt{E_{BS}\,b_1} - \sqrt{E_{BS}\,b_2}\right)g_{D_2}\right)\Big] \end{aligned} \tag{5.13}$$

Through substituting equations (14) and (13) with equation (10) and utilizing equations (5) and (7), we can represent equation (11) as in (14):

$$BER_{D_2} = \frac{1}{2}\left[2Q\left(\frac{\sqrt{E_{BS}b_2}g_{D_2}}{\sigma_{D_2}+\sigma_I}\right) - Q\left(\frac{(\sqrt{E_{BS}b_1}+\sqrt{E_{BS}b_2})g_{D_2}}{\sigma_{D_2}+\sigma_I}\right) + Q\left(\frac{(2\sqrt{E_{BS}b_1}+\sqrt{E_{BS}b_2})g_{D_2}}{\sigma_{D_2}+\sigma_I}\right) + Q\left(\frac{(\sqrt{E_{BS}b_1}-\sqrt{E_{BS}b_2})g_{D_2}}{\sigma_{D_2}+\sigma_I}\right) - Q\left(\frac{(2\sqrt{E_{BS}b_1}-\sqrt{E_{BS}b_2})g_{D_2}}{\sigma_{D_2}+\sigma_I}\right)\right] \tag{5.14}$$

Therefore, we represent equation (14) by utilizing (6) and (8) as (15):

$$ABER_{D_2} = \frac{1}{4}\left[2\left(1-\sqrt{\frac{\bar{\rho_1}}{2+\bar{\rho_1}}}\right) - \left(1-\sqrt{\frac{\bar{\rho_2}}{2+\bar{\rho_2}}}\right) + \left(1-\sqrt{\frac{\bar{\rho_3}}{2+\bar{\rho_3}}}\right) + \left(1-\sqrt{\frac{\bar{\rho_4}}{2+\bar{\rho_4}}}\right) - \left(1-\sqrt{\frac{\bar{\rho_5}}{2+\bar{\rho_5}}}\right)\right] \tag{5.15}$$

Where $\bar{\rho_1} = \sqrt{P_S b_2}\frac{E[|g_{D_2}|^2]}{\sigma_I^2+\sigma_{D_2}^2}$, $\bar{\rho_2} = \frac{(\sqrt{P_S b_1}+\sqrt{P_S b_2})^2 E[|g_{D_2}|^2]}{\sigma_I^2+\sigma_{D_2}^2}$, $\bar{\rho_3} = \frac{(2\sqrt{P_S b_1}+\sqrt{P_S b_2})^2 E[|g_{D_2}|^2]}{\sigma_I^2+\sigma_{D_2}^2}$, $\bar{\rho_4} = \frac{(\sqrt{P_S b_1}-\sqrt{P_S b_2})^2 E[|g_{D_2}|^2]}{\sigma_I^2+\sigma_{D_2}^2}$, $\bar{\rho_5} = \frac{(2\sqrt{P_S b_1}-\sqrt{P_S b_2})^2 E[|g_{D_2}|^2]}{\sigma_I^2+\sigma_{D_2}^2}$

5.3.1.3 The End-to-End (E2E) BER of Users

In the second time slot, the CCR-NOMA D_1 and D_2 users support vulnerable users by receiving and decoding the signal.The signal from D_j ,j={3,4} received is described as:

$$y_{CU_j} = g_{D_j}\sqrt{E_R}s_{D_j} + I + n_j \tag{5.16}$$

Where E_R is the D_j transmit power, we assume the message of user $D_j : s_{D_j} = x_j$,j={3,4}.

The BER of D_j can be represented as in [87]:

$$BER_{D_j} = P\left(\sqrt{E_R}g_{D_j} < n_j + I\right) \tag{5.17}$$

Through employing (5) and (7) can be written as :

$$BER_{D_j} = Q\left(\sqrt{\rho_{D_j}}\right) \tag{5.18}$$

The ABER is determined by utilizing equations (6) and (8) as:

$$ABER_{D_j} = \frac{1}{2}\left(1-\sqrt{\frac{\bar{\rho_j}}{2+\bar{\rho_j}}}\right) \tag{5.19}$$

Where $\bar{\rho_{D_j}} = \frac{E_R E[|g_{D_j}|^2]}{\sigma_I^2+\sigma_{D_j}^2}$. For the considered dual hop system, the equivalent end-to-end BER at users D_j ,j$\in \{3,4\}$ it is given as:

$$ABER_{E2E,D_j} = 1 - [(1 - ABER_{D_j})(1 - ABER_{D_j})] \tag{5.20}$$

Where $ABER_{D_j}$ and $ABER_{D_j}$ are ABER of D_j,j $\in \{3,4\}$ in the second phase and the ABER of D_j message at D_j, j $\in \{11,22\}$. The user signals are modulated using BPSK [73].

5.3.2 BER under Imperfect CSI

In this case, we assume that imperfect CSI is provided at users. The channel coefficients are represented by the equation:

$$g_{D_j} = h_{D_j} + e_{D_j}, \quad \forall q \in \{1,2,3,4\} \tag{5.21}$$

Where h_{D_j} is the estimated channel coefficient with a complex normal distribution $\mathcal{CN}(0, \sigma^2_{h_{D_j}})$

The error term $e_{D_j}$is usually represented as a complex Gaussian distributed random variable with $\mathcal{CN}(0, \sigma_{e^2_{D_j}})$

The signal received by user D_j under the assumption of imperfect CSI is represented as [68],[94] and [5]:

$$y_{D_j}^{CSI} = S(h_{D_j} + e_{D_j}) + I + n_j \tag{5.22}$$

5.3.2.1 BER of User D_1

The MLD technique is employed by D_2 user to identify the symbol of the D_1 user. The BER in this case is determined based on whether the received signal is below or above zero. The BER of m_1 at D_1 user under the assumption of imperfect CSI can be represented by:

$$\begin{aligned}\mathrm{BER}_{D_1} = \frac{1}{2}\Bigg[& P\left(I + n_{D_1} + \sqrt{E_{BS}\left(\sqrt{b_1} - \sqrt{b_2}\right) e_{D_1}} \geq (\sqrt{b_1} - \sqrt{b_2})\sqrt{E_{BS} h_{D_1}}\right) \\ & + P\left(I + n_{D_1} + \sqrt{E_{BS}\left(\sqrt{b_1} + \sqrt{b_2}\right) e_{D_1}} > (\sqrt{b_1} + \sqrt{b_2})\sqrt{E_{BS} h_{D_1}}\right)\Bigg]\end{aligned} \tag{5.23}$$

Further, followed by the same steps in previous section for obtain formula (10), the closed-form expression of ABER is given as:

$$ABER_{D_1} = \frac{1}{4}\left[\left(1-\sqrt{\frac{\bar{\rho}_{D_1}}{2+\bar{\rho}_{D_1}}}\right)+\left(1-\sqrt{\frac{\bar{\rho}_{D_1}}{2+\bar{\rho}_{D_1}}}\right)\right] \tag{5.24}$$

Where $\bar{\rho}_{D_2} = \frac{E_{BS}(\sqrt{b_1}-\sqrt{b_2})^2}{\sqrt{E_{BS}(\sqrt{b_1}-\sqrt{b_2})\sigma^2_{e_{D_2}}+\sigma^2_I+\sigma^2_{D_2}}}E[|h_{D_2}|^2], \bar{\rho}_{D_1} = \frac{E_{BS}(\sqrt{b_1}+\sqrt{b_2})^2}{\sqrt{E_{BS}(\sqrt{b_1}+\sqrt{b_2})\sigma^2_{e_{D_1}}+\sigma^2_I+\sigma^2_{D_2}}}E[|h_{D_1}|^2]$

5.3.2.2 BER of User D_2

Followed by the same steps in previous section for obtain formula (15), the ABER of D_2 user under the assumption of imperfect CSI can be written by:

$$\begin{aligned} ABER_{D_2} = \frac{1}{4}\Bigg[&2\left(1-\sqrt{\frac{\bar{\rho}_1}{2+\bar{\rho}_1}}\right)-\left(1-\sqrt{\frac{\bar{\rho}_2}{2+\bar{\rho}_2}}\right)+\left(1-\sqrt{\frac{\bar{\rho}_3}{2+\bar{\rho}_3}}\right) \\ &+\left(1-\sqrt{\frac{\bar{\rho}_4}{2+\bar{\rho}_4}}\right)-\left(1-\sqrt{\frac{\bar{\rho}_5}{2+\bar{\rho}_5}}\right)\Bigg] \end{aligned} \tag{5.25}$$

Where $\bar{\rho}_1 = \frac{\sqrt{E_{BS}b_2}E[|h_{D_2}|^2]}{\sqrt{E_{BS}(\sqrt{b_1}-\sqrt{b_2})\sigma^2_{e_{D_2}}+\sigma^2_I+\sigma^2_{D_2}}}, \bar{\rho}_2 = \frac{E_{BS}(\sqrt{b_1}+\sqrt{b_2})^2E[|h_{D_2}|^2]}{\sqrt{E_{BS}(\sqrt{b_1}+\sqrt{b_2})\sigma^2_{e_{D_2}}+\sigma^2_I+\sigma^2_{D_2}}},$
$\bar{\rho}_3 = \frac{E_{BS}(2\sqrt{b_1}+\sqrt{b_2})^2E[|h_{D_2}|^2]}{\sqrt{E_{BS}(\sqrt{b_1}+\sqrt{b_2})\sigma^2_{e_{D_2}}+\sigma^2_I+\sigma^2_{D_2}}}, \bar{\rho}_4 = \frac{E_{BS}(\sqrt{b_1}-\sqrt{b_2})^2E[|h_{D_2}|^2]}{\sqrt{E_{BS}(\sqrt{b_1}-\sqrt{b_2})\sigma^2_{e_{D_2}}+\sigma^2_I+\sigma^2_{D_2}}}, \bar{\rho}_5 = \frac{E_{BS}(2\sqrt{b_1}-\sqrt{b_2})^2E[|h_{D_2}|^2]}{\sqrt{E_{BS}(\sqrt{b_1}-\sqrt{b_2})\sigma^2_{e_{D_2}}+\sigma^2_I+\sigma^2_{D_2}}}$

5.3.2.3 The E2E BER of Users

In the second time slot, the signal from D_j , j={3,4} received under imperfect CSI is described as:

$$y_{D_j} = (h_{D_j}+e_{D_j})\sqrt{E_R}s_{D_j}+I+n_j \tag{5.26}$$

The BER at D_j can be represented by:

$$BER_{D_j} = P\left(\sqrt{E_R}h_{D_j} < n_j + I + \sqrt{E_R}e_{D_j}\right) \tag{5.27}$$

The ABER is defined after employing the (6) and (8) as

$$ABER_{D_j} = \frac{1}{2}\left(1-\sqrt{\frac{\bar{\rho}_j}{2+\bar{\rho}_j}}\right) \tag{5.28}$$

Where $\bar{\rho}_j = \frac{E_R E[|h_{D_j}|^2]}{E_R\sigma^2_{e_{D_j}}+\sigma^2_I+\sigma^2_{D_j}}$.The equivalent end-to-end ABER equation at users D_j, calculated by the same formula (20).

5.4 Results and Discussion

In this section, we utilize Monte Carlo simulations to validate the analytical BER equations elucidated in the preceding sections, ensuring the robustness and accuracy of our theoretical framework. Throughout all figures, markers depict the analytical curves, while lines depict the simulation results, providing a comprehensive comparison between theoretical predictions and empirical observations. The simulation parameters are meticulously defined as in table Table. 5.1.

Parameter	**Value**
The distance between BS-D_4	1 m
The distance between BS-D_3	2 m
PA coefficient of D_4	0.85
PA coefficient of D_3	0.15
The interference temperature constraint	35 dB
The scaling coefficient of the interference from the PN affecting users in the CN	0.8
The user relay transmit power	$0.5 \times E_S$
The pathloss exponent	4

Table 5.1: Simulation Parameters

We will discuss our results obtained using Monte Carlo simulations of BER of our considered system CCR NOMA. Fig. 5.2 illustrates the ABER versus SNR for two users (D_4 and D_3) under CCR-OMA and CCR-NOMA schemes. Simulation results are shown as lines, and analytical results are indicated by markers. It is evident that as SNR increases, ABER decreases for all scenarios, signifying improved performance. D_4 consistently outperforms D_3 in both OMA and NOMA schemes. Notably, CCR-OMA demonstrates superior performance compared to CCR-NOMA, particularly at higher SNR values, where D_4 under CCR-OMA achieves the lowest ABER. Additionally, the close alignment between the simulation lines and analytical markers validates the accuracy of the theoretical models. Both users and schemes exhibit an error floor at high SNR, indicating that further increases in SNR do not significantly reduce ABER due to system limitations. This comparison underscores CCR-OMA's better error performance over CCR-NOMA while confirming the reliability of the analytical predictions.

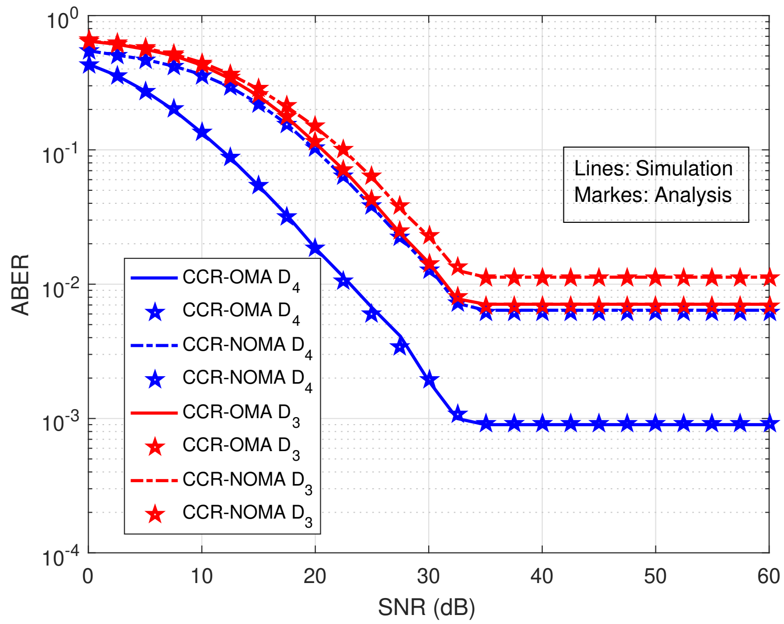

Figure 5.2: ABER performance evaluation of end users for CCR-NOMA compared to CCR-OMA.

Fig. 5.3 displays the ABER versus SNR for two users (D_4 and D_3) under conditions of perfect and imperfect CSI. The results are distinguished by lines for simulation data and markers for analytical data. It is observed that as SNR increases, ABER decreases for both perfect and imperfect CSI scenarios, indicating improved performance with higher SNR. Perfect CSI consistently results in lower ABER compared to imperfect CSI for both users, highlighting the impact of accurate channel information on system performance. D_4 exhibits better performance than D_3 across all conditions due to the use of SIC technology at D_2. This technology mitigates interference at user D_2, which cooperated with user D_4. The disparity between perfect and imperfect CSI becomes more pronounced at higher SNR levels, where the error floor for imperfect CSI is notably higher. This emphasizes the importance of precise CSI in minimizing errors. The close alignment between simulation lines and analytical markers confirms the validity of the theoretical models used. Generally, this figure demonstrates that while high SNR improves ABER for both users, perfect CSI significantly enhances performance, reducing ABER more effectively than imperfect CSI. In practical scenarios, it is challenging to obtain perfect CSI. Therefore, in our system model analyses, we consider these imperfections to better reflect real-world conditions. Imperfect CSI arises due to real-life phenomena. It presents the changes in the environment, such as moving obstacles, weather conditions, and signal reflections, which unpredictably alter the channel characteristics.

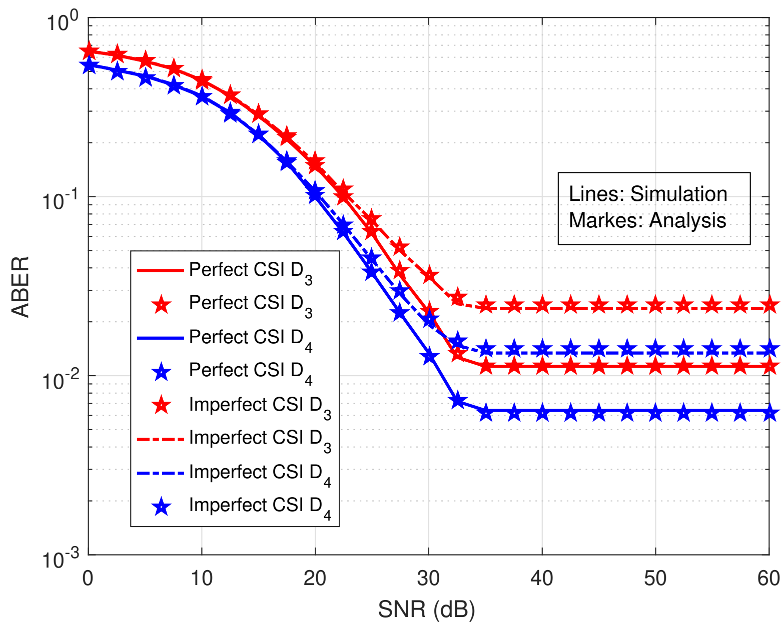

Figure 5.3: ABER performance evaluation of end users for CCR-NOMA under perfect and imperfect CSI.

Fig. 5.4 provides a comprehensive view of the ABER performance for users D_4 and D_3 within the CCR-NOMA framework, showcasing the impact of SNR variations across different (I_{ITC}) values (15 dB, 25 dB, and 35 dB). The results unequivocally demonstrate a positive correlation between the increase in the interference temperature constraint (I_{ITC}) and the enhancement of ABER performance for both users. Notably, the figure reveals that the optimal ABER performance is attained at an I_{ITC} value of 35 dB, indicating the pivotal role of effectively managing interference levels in achieving reliable communication. This insight underscores the significance of fine-tuning system parameters, such as I_{ITC} values, to strike a balance between interference mitigation and signal reliability in CCR-NOMA deployments, thereby offering valuable guidance for optimizing system performance in real-world cognitive radio networks.

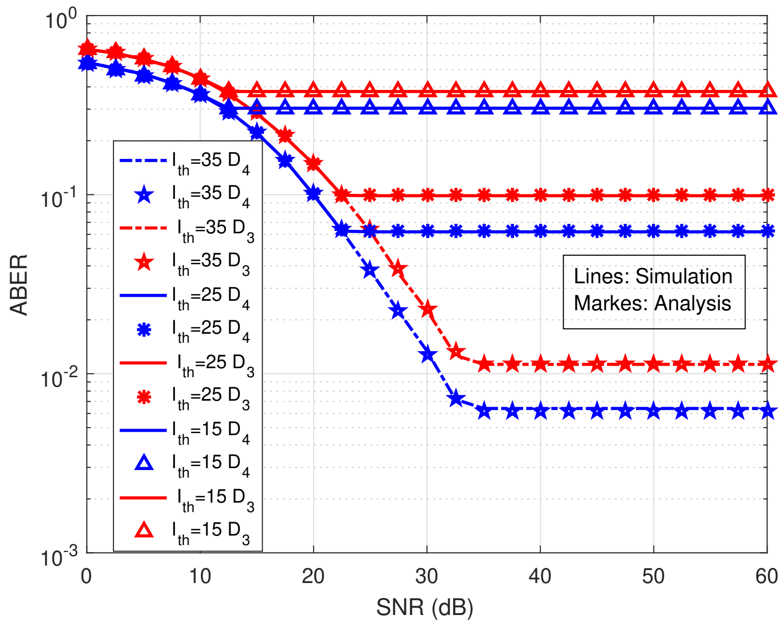

Figure 5.4: ABER performance evaluation of end users for CCR-NOMA with various I_{ITC} values .

5.5 Conclusion

This chapter investigates the BER performance of underlay CCR-NOMA in a downlink system under generalized Rayleigh fading conditions. The end users' cooperation with both near and distant users is used to derive the BER. The analysis of the users considers the existence of imperfect CSI. The analytical results are confirmed through simulations. The findings validate that D_4 performs better than D_3 within the system. The derived formulas for the downlink scenario are graphed numerically and compared to results from the traditional cooperative CR-OMA system. The system's performance deteriorates due to the existence of imperfect CSI. The impact of ITC is the main factor affecting to system performance.

General conclusion

As the field progresses towards 6G, there is an increasing demand for ultra-high data rates, low latency, enhanced reliability, and massive connectivity to support emerging applications such as holographic communications and the Internet of Everything. To meet these challenging requirements, the integration of CR with NOMA presents a promising and innovative approach. The combination of CR and NOMA not only offers an efficient and scalable solution but also effectively addresses the stringent requirements of 6G, ensuring optimal spectrum utilization and significantly improved network performance. This thesis aims to provide an analysis of the effectiveness of the CR-NOMA system in alleviating spectrum scarcity and enhancing system performance. It investigates the challenges impacting the performance of CR-NOMA systems, with a particular emphasis on imperfections in CSI and SIC. The analysis evaluates key performance metrics, including BER, OP, achievable data rate, and throughput across various conditions. Furthermore, it offers valuable insights into the resilience and practical viability of CR-NOMA systems in real-world applications. The contributions of this thesis are outlined in the following chapters:

- **Chapter 1** provides the primary notions related to 6G networks, beginning with their development from 1G to 5G. It emphasizes the Peak Data Rate as an essential performance metric alongside other KPIs. The suggested 6G architecture has been discussed, illustrating the important function of AI in developing new infrastructure. The new metric QoPE, has been introduced to handle the increasing focus on human-centric services. The chapter additionally discusses the role of standardization and patents in improving mobile networks, classifying essential technologies into novel categories: spectrum, air interface, networking, and paradigm. Lastly, it reviews key use cases which involve communication, navigation, sensing, and services.

- **Chapter 2** covered key aspects related to CR, including its definition, network components, CR transceiver functionality, various spectrum sharing methods, and a comparative analysis of these methods. Cognitive Radio offers an optimal solution to the issue of limited availability of radio frequencies. To improve the effectiveness of cognitive radio technology, some research projects have suggested combining it with NOMA technology. In addition, we provide a comprehensive explanation of the NOMA methodology, including its description and important techniques such as SIC and SC.

- **Chapter 3** presents and examines the performance of a simple underlay CR-NOMA system. We obtained the analytical formulas for the outage probability, achievable data rates, and throughput of this system. The results validate that the system has demonstrated superior performance with D_2 in comparison to D_1. The performance of the CR-NOMA system is primarily influenced by the I_{TC} determined by the primary network. The system achieved its best performance when the I_{TC} was set to 35dB. The CR-NOMA system showed superior performance compared to CR-OMA for both users.

- **Chapter 4** discusses the performance of the CR-NOMA. An investigation has been performed on D2D communications in a downlink system in a generalized Rayleigh fading environment. When assessing the users, the analysts evaluate the presence of perfect and imperfect CSI and SIC. The outage probability and throughput are determined by the cooperation between the end users and the nearby and distant users. The results validate that the system has proven that D_4 surpasses D_3. The analysis results are verified using simulations and compared to those of the conventional cooperative CR-OMA system. The system's performance is degraded by the existence of imperfect CSI and imperfect SIC. Furthermore, we completed an investigation to determine the optimal value of power allocation.

- **Chapter 5** investigates the BER performance of underlay CCR-NOMA in a downlink system, specifically under generalized Rayleigh fading conditions. The cooperation between end users and both nearby and distant users is utilized for calculating the BER. The study of the users considers the presence of imperfect CSI. The analysis results are validated using simulations. The results confirm that D_4 outperforms D_3 in the system and distinguished with results from the conventional cooperative CR-OMA system. The system's performance degrades because of the presence of imperfect CSI.

Although this thesis has investigated several aspects of CR-NOMA, numerous opportunities for future research continue to exist. Moreover, the integration of technologies such as Massive MIMO has the potential to significantly enhance spectral efficiency by enabling simultaneous transmissions to multiple users, thereby maximizing the utilization of the available spectrum. Additionally, RIS can further improve signal quality and coverage, ultimately leading to a more effective spectrum management approach. Furthermore, the incorporation of AI into CR-NOMA systems can profoundly augment their performance and adaptability. By optimizing key functions, AI facilitates the analysis of complex environments and user behavior, enabling informed decisions for dynamic resource optimization.

Bibliography

[1] Naveed Ali Khan and Stefan Schmid. Ai-ran in 6g networks state-of-the-art and challenges. *IEEE Open Journal of the Communications Society*, 2023.

[2] Sree Krishna Das, Benoit Champagne, Ioannis Psaromiligkos, and Yunlong Cai. A survey on federated learning for reconfigurable intelligent metasurfaces-aided wireless networks. *IEEE Open Journal of the Communications Society*, 2024.

[3] Syed Agha Hassnain Mohsan and Yanlong Li. A survey of noma: State of the art, key techniques, open challenges, security issues and future trends. *arXiv preprint arXiv:2306.06664*, 2023.

[4] A. Meriem and K. Abdellatif. Ber analysis of underlay cooperative cognitive radio-based noma system. *SWCC*, 2024.

[5] A. Meriem and K. Abdellatif. Outage performance of underlay cr-noma-based d2d communications under imperfect csi and sic. *SWCC*, 14, January 2024.

[6] Haythem Bany Salameh, Sharief Abdel-Razeq, and Haitham Al-Obiedollah. Integration of cognitive radio technology in noma-based b5g networks: State of the art, challenges, and enabling technologies. *IEEE Access*, 11:12949–12962, 2023.

[7] Lavan Perera, Pasika Ranaweera, Sachitha Kusaladharma, Shen Wang, and Madhusanka Liyanage. A survey on blockchain for dynamic spectrum sharing. *IEEE Open Journal of the Communications Society*, 2024.

[8] Sultangali Arzykulov. *Enhanced Cognitive radio with energy harvesting and non-orthogonal multiple access.* PhD thesis, Nazarbayev University, 2019.

[9] R. Prasad, A. R. Prasad, A. Mihovska, and Nidhi. *6G Enabling Technologies: New Dimensions to Wireless Communication.* River Publishers, New York, 1st edition, 2022.

[10] Xianzhong Xie, Bo Rong, and Michel Kadoch. *6G wireless communications and mobile networking*. Bentham Science Publishers, 2021.

[11] X. Lin, J. Zhang, Y. Liu, and J. Kim, editors. *Fundamentals of 6G Communications and Networking*. Signals and Communication Technology. Springer International Publishing, Cham, 2024.

[12] R. Dangi, G. Choudhary, N. Dragoni, P. Lalwani, U. Khare, and S. Kundu. 6g mobile networks: Key technologies, directions, and advances. *Telecom*, 4(4):836–876, Dec. 2023.

[13] Y. Wu et al., editors. *6G Mobile Wireless Networks*. Computer Communications and Networks. Springer International Publishing, Cham, 2021.

[14] P. Ahokangas and A. Aagaard, editors. *The Changing World of Mobile Communications: 5G, 6G and the Future of Digital Services*. Springer International Publishing, Cham, 2024.

[15] Pawani Porambage and Madhusanka Liyanage. *Security and Privacy Vision in 6G: A Comprehensive Guide*. John Wiley & Sons, 2023.

[16] Wei Jiang and Fa-Long Luo. *6G Key Technologies: A Comprehensive Guide*. John Wiley & Sons, 2022.

[17] R. Chataut and R. Akl. Massive mimo systems for 5g and beyond networks—overview, recent trends, challenges, and future research direction. *Sensors*, 20(10):2753, May 2020.

[18] H.-H. Lu et al. 5g wavelength-division-multiplexing-based bidirectional optical wireless communication system with signal remodulation employing cascaded reflective semiconductor optical amplifiers. *Commun Eng*, 3(1):85, Jun. 2024.

[19] Martin Maier. Toward 6g: A new era of convergence. In *Optical fiber communication conference*, pages F4H–1. Optica Publishing Group, 2021.

[20] Qingqing Wu, Shuowen Zhang, Beixiong Zheng, Changsheng You, and Rui Zhang. Intelligent reflecting surface-aided wireless communications: A tutorial. *IEEE transactions on communications*, 69(5):3313–3351, 2021.

[21] Emil Björnson, Henk Wymeersch, Bho Matthiesen, Petar Popovski, Luca Sanguinetti, and Elisabeth De Carvalho. Reconfigurable intelligent surfaces: A signal processing perspective with wireless applications. *IEEE Signal Processing Magazine*, 39(2):135–158, 2022.

[22] Sai Lv, Hui Li, Jiangxing Wu, He Bai, Xi Chen, Yufei Shen, Jun Zheng, Rui Ding, Huajun Ma, and Wenjun Li. Routing strategy of integrated satellite-terrestrial network based on hyperbolic geometry. *IEEE Access*, 8:113003–113010, 2020.

[23] Paulo Sergio Rufino Henrique and Ramjee Prasad. *6G: the road to the future wireless technologies 2030*. River Publishers, 2022.

[24] J. O. Neel. *Analysis and Design of Cognitive Radio Networks and Distributed Radio Resource Management Algorithms*. 2008.

[25] S. Haykin. Cognitive radio: brain-empowered wireless communications. *IEEE Journal on Selected Areas in Communications*, 23(2):201–220, February 2005.

[26] Linda Doyle. *Essentials of cognitive radio*. Cambridge university press, 2009.

[27] I. F. Akyildiz, W.-Y. Lee, M. C. Vuran, and S. Mohanty. A survey on spectrum management in cognitive radio networks. *IEEE Communications Magazine*, page 9, 2008.

[28] A. Nafkha, C. Moy, P. Leray, R. Seguier, and J. Palicot. Software defined radio platform for cognitive radio: Design and hierarchical management. In J.-C. Lin, editor, *Recent Advances in Wireless Communications and Networks*. InTech, 2011.

[29] B. A. Fette, editor. *Cognitive Radio Technology*. Academic Press/Elsevier, Amsterdam; Boston, 2nd edition, 2009.

[30] Z. Wang and W. Zhang. *Opportunistic Spectrum Sharing in Cognitive Radio Networks*. SpringerBriefs in Electrical and Computer Engineering. Springer International Publishing, Cham, 2015.

[31] M. Ibnkahla. *Cooperative Cognitive Radio Networks: The Complete Spectrum Cycle*. 2008.

[32] R. Biswas. *Basics of Cognitive Radio Networks: An Appraisal*, page 7. 2008.

[33] M. H. Rehmani and R. Dhaou, editors. *Cognitive Radio, Mobile Communications and Wireless Networks*. EAI/Springer Innovations in Communication and Computing. Springer International Publishing, Cham, 2019.

[34] S. Pandit and G. Singh. *Spectrum Sharing in Cognitive Radio Networks*. Springer International Publishing, Cham, 2017.

[35] A. Goldsmith, S. A. Jafar, I. Maric, and S. Srinivasa. Breaking spectrum gridlock with cognitive radios: An information theoretic perspective. *Proceedings of the IEEE*, 97(5):894–914, May 2009.

[36] H. Arslan, editor. *Cognitive Radio, Software Defined Radio, and Adaptive Wireless Systems*. Springer Netherlands, Dordrecht, 2007.

[37] M. Vaezi, Z. Ding, and H. V. Poor. *Multiple Access Techniques for 5G Wireless Networks and Beyond*. Springer International Publishing, Cham, 2019.

[38] L. Dai, B. Wang, Z. Ding, Z. Wang, S. Chen, and L. Hanzo. A survey of non-orthogonal multiple access for 5g. *IEEE Communications Surveys and Tutorials*, 20(3):2294–2323, 2018.

[39] Recent advances in information, communications and signal processing. Accessed: Jan. 07, 2024.

[40] R. C. Kizilirmak. Non-orthogonal multiple access (noma) for 5g networks. In H. K. Bizaki, editor, *Towards 5G Wireless Networks - A Physical Layer Perspective*. InTech, 2016.

[41] L. Wen. Non-orthogonal multiple access schemes for future cellular systems, 2024.

[42] I. Bukar. Spectrally efficient non-orthogonal multiple access (noma) techniques for future generation mobile systems, 2024.

[43] Z. Wei. Performance analysis and design of non-orthogonal multiple access for wireless communications, 2019. arXiv:1910.00946 [cs, eess, math], Accessed: Sep. 02, 2020.

[44] Y. Liu, Z. Qin, M. Elkashlan, Z. Ding, A. Nallanathan, and L. Hanzo. Nonorthogonal multiple access for 5g and beyond. *Proceedings of the IEEE*, 105(12):2347–2381, December 2017.

[45] Mayur Katwe, Keshav Singh, Chih-Peng Li, and Zhiguo Ding. Spectral-efficient downlink systems under imperfect sic and csi: Mc-noma or partial noma? *IEEE Wireless Communications Letters*, 2023.

[46] Shiyu Jiao. *Resource allocation for non-orthogonal multiple access networks*. PhD thesis, University of Manchester, 2023.

[47] Y. Liu, Z. Ding, and H. V. Poor. Evolution of noma toward next generation multiple access (ngma) for 6g. *IEEE Journal on Selected Areas in Communications*, 40(4):1037–1071, April 2022.

[48] Mojtaba Vaezi, Robert Schober, Zhiguo Ding, and H Vincent Poor. Non-orthogonal multiple access: Common myths and critical questions. *IEEE Wireless Communications*, 26(5):174–180, 2019.

[49] T.-H. Vu, T.-V. Nguyen, and S. Kim. Wireless powered cognitive noma-based iot relay networks: Performance analysis and deep learning evaluation. *IEEE Internet of Things Journal*, 9(5):3913–3929, March 2022.

[50] A. Kumar and K. Kumar. Multiple access schemes for cognitive radio networks: A survey. *Physical Communication*, 38:100953, February 2020.

[51] S. Arzykulov, T. A. Tsiftsis, G. Nauryzbayev, M. Abdallah, and G. Yang. Outage performance of underlay cr-noma networks with detect-and-forward relaying. In *2018 IEEE Global Communications Conference (GLOBECOM)*, pages 1–6, Abu Dhabi, United Arab Emirates, December 2018. IEEE.

[52] Z. Ding, P. Fan, and H. V. Poor. Impact of user pairing on 5g nonorthogonal multiple-access downlink transmissions. *IEEE Transactions on Vehicular Technology*, 65(8):6010–6023, August 2016.

[53] Y. Liu, Z. Ding, M. Elkashlan, and J. Yuan. Non-orthogonal multiple access in large-scale underlay cognitive radio networks. *IEEE Transactions on Vehicular Technology*, 65(12):10152–10157, December 2016.

[54] D.-T. Do, A.-T. Le, C.-B. Le, and B. M. Lee. On exact outage and throughput performance of cognitive radio based non-orthogonal multiple access networks with and without d2d link. *Sensors*, 19(15):3314, July 2019.

[55] H. T. Madan and P. I. Basarkod. Throughput and outage probability analysis for cognitive radio-non-orthogonal multiple access in uplink and downlink scenarios. *Mathematical Methods in the Applied Sciences*, 7(4):659–666, December 2020.

[56] T.-A. Hoang, C.-B. Le, and D.-T. Do. Security performance analysis for power domain noma employing in cognitive radio networks. *Bulletin of Electrical Engineering and Informatics*, 9(3):1046–1054, June 2020.

[57] M. Aldababsa, M. Toka, S. Gökçeli, G. K. Kurt, and O. Kucur. A tutorial on nonorthogonal multiple access for 5g and beyond. *Wireless Communications and Mobile Computing*, 2018:1–24, June 2018.

[58] D.-T. Do, A.-T. Le, and B. M. Lee. Noma in cooperative underlay cognitive radio networks under imperfect sic. *IEEE Access*, 8:86180–86195, 2020.

[59] D.-T. Do, A.-T. Le, and B. M. Lee. On performance analysis of underlay cognitive radio-aware hybrid oma/noma networks with imperfect csi. *Electronics*, 8(7):819, July 2019.

[60] A. Kumar, S. Perveen, S. Singh, S. Majhi, and S. K. Das. 6th generation: Communication, signal processing, advanced infrastructure, emerging technologies and challenges. In *26th International Conference on Computing, Communication and Security (ICCS)*, pages 1–16, 2021.

[61] R. Elouafadi and M. Benjillali. Cooperative noma-based d2d communications: A survey in the 5g/iot context. In *19th IEEE Mediterranean Electrotechnical Conference (MELECON)*, pages 132–137, 2018.

[62] M. Hassan, M. Singh, and K. Hamid. Survey on noma and spectrum sharing techniques in 5g. In *IEEE International Conference on Smart Information Systems and Technologies (SIST)*, pages 1–4, 2021.

[63] Galymzhan Nauryzbayev, Orken Omarov, Sultangali Arzykulov, Khaled M Rabie, Xingwang Li, and Ahmed M Eltawil. Performance limits of wireless powered cooperative noma over generalized fading. *Transactions on Emerging Telecommunications Technologies*, 33(4):e4415, 2022.

[64] S. M. R. Islam, N. Avazov, O. A. Dobre, and K. Kwak. Power-domain non-orthogonal multiple access (noma) in 5g systems: Potentials and challenges. *IEEE Communications Surveys and Tutorials*, 19(2):721–742, 2017.

[65] L. Lv, J. Chen, Q. Ni, Z. Ding, and H. Jiang. Cognitive non-orthogonal multiple access with cooperative relaying: A new wireless frontier for 5g spectrum sharing. 2018.

[66] S. Gupta, R. Patel, R. Gupta, S. Tanwar, and N. Patel. A survey on resource allocation schemes in device-to-device communication. In *12th International Conference on Cloud Computing, Data Science and Engineering (Confluence)*, pages 140–145, 2022.

[67] M. Jain, N. Sharma, A. Gupta, D. Rawal, and P. Garg. Performance analysis of noma assisted mobile ad hoc networks for sustainable future radio access. *IEEE Transactions on Sustainable Computing*, 6(2):347–357, Apr 2021.

[68] F. Khennoufa and A. Khelil. Exact bit error rate of cooperative noma without diversity combining. In *International Conference on Artificial Intelligence for Cyber Security Systems and Privacy (AI-CSP)*, pages 1–5, 2021.

[69] H.-P. Dang, M.-S. V. Nguyen, and D.-T. Do. Comparison on af/df for device-to-device noma networks. *International Journal of Applied Engineering Research*, 13(10):6, 2018.

[70] Md. F. Kader, M. B. Shahab, and S. Y. Shin. Exploiting non-orthogonal multiple access in cooperative relay sharing. *IEEE Communications Letters*, 21(5):1159–1162, 2017.

[71] X. Liang, Y. Wu, D. W. K. Ng, S. Jin, Y. Yao, and T. Hong. Outage probability of cooperative noma networks under imperfect csi with user selection. *IEEE Access*, 8:117921–117931, 2020.

[72] S. Arzykulov, T. A. Tsiftsis, G. Nauryzbayev, and M. Abdallah. Outage performance of cooperative underlay cr-noma with imperfect csi. *IEEE Communications Letters*, 23(1):176–179, 2019.

[73] M. Ad and A. Khelil. Performance investigation of cr-noma based underlay paradigm. In *Fifth International Conference on Electrical Engineering And Control Applications (ICEECA)*, 2022.

[74] T.-N. Tran, D.-T. Do, and M. Voznak. On outage probability and throughput performance of cognitive radio inspired noma relay system. *Advances in Electrical and Electronic Engineering*, 16(4):501–512, 2018.

[75] S. Menaa and A. Khelil. On the performance of siso, simo and miso-noma systems under perfect and imperfect sic. In *19th International Multi-Conference on Systems, Signals and Devices (SSD)*, pages 458–463, 2022.

[76] S. Bisen, P. Shaik, and V. Bhatia. On performance of energy harvested cooperative noma under imperfect csi and imperfect sic. *IEEE Transactions on Vehicular Technology*, 70(9):8993–9005, 2021.

[77] F. Khennoufa and K. Abdellatif. Ber performance of cooperative relay noma assisted ps protocol with imperfect sic and csi. *International Journal of Sensors, Wireless Communications and Control*, 2022.

[78] S. Beddiaf, A. Khelil, F. Khennoufa, and K. Rabie. On the impact of iqi on cooperative noma with direct links in the presence of imperfect csi. *Physical Communication*, 56:101952, 2023.

[79] J. Zhao, X. Yue, S. Kang, and W. Tang. Joint effects of imperfect csi and sic on noma based satellite-terrestrial systems. *IEEE Access*, 9:12545–12554, 2021.

[80] A. Bazzi and M. Chafii. Secure full duplex integrated sensing and communications. *IEEE Transactions on Information Forensics and Security*, 19:2082–2097, 2024.

[81] A. Bazzi and M. Chafii. On outage-based beamforming design for dual-functional radar-communication 6g systems. *IEEE Transactions on Wireless Communications*, 22(8):5598–5612, Aug 2023.

[82] D. Wang, A. Bazzi, and M. Chafii. Ris-enabled integrated sensing and communication for 6g systems. In *IEEE Wireless Communications and Networking Conference (WCNC)*, 2024.

[83] R. Dangi, G. Choudhary, N. Dragoni, P. Lalwani, U. Khare, and S. Kundu. 6g mobile networks: Key technologies, directions, and advances. *Telecom*, 4(4):836–876, Dec 2023.

[84] S. Naoumi, A. Bazzi, R. Bomfin, and M. Chafii. Complex neural network based joint aoa and aod estimation for bistatic isac. *IEEE Journal of Selected Topics in Signal Processing*, Mar 2024.

[85] S. Naoumi, A. Bazzi, R. Bomfin, and M. Chafii. Deep learning-enabled angle estimation in bistatic isac systems. In *2023 IEEE Globecom Workshops (GC Wkshps)*, pages 854–859, Dec 2023.

[86] M. W. Akhtar, S. A. Hassan, R. Ghaffar, H. Jung, S. Garg, and M. S. Hossain. The shift to 6g communications: vision and requirements. *Human-Centric Computing and Information Sciences*, 10(1):53, Dec 2020.

[87] S. Arzykulov, A. Celik, G. Nauryzbayev, and A. M. Eltawil. Uav-assisted cooperative and cognitive noma: Deployment, clustering, and resource allocation. *IEEE Transactions on Cognitive Communications and Networking*, 8(1):263–281, Mar 2022.

[88] H. B. Salameh, S. Abdel-Razeq, and H. Al-Obiedollah. Integration of cognitive radio technology in noma-based b5g networks: State of the art, challenges, and enabling technologies. *no page numbers*, 11, 2023.

[89] M. Jain, S. Soni, N. Sharma, and D. Rawal. Performance analysis at far and near user in noma based system in presence of sic error. *AEU - International Journal of Electronics and Communications*, 114:152993, Feb 2020.

[90] F. Kara and H. Kaya. Ber performances of downlink and uplink noma in the presence of sic errors over fading channels. *IET Communications*, 12(15):1834–1844, Sep 2018.

[91] L. Bariah, S. Muhaidat, and A. Al-Dweik. Error performance of noma-based cognitive radio networks with partial relay selection and interference power constraints. *IEEE Transactions on Communications*, 68(2):765–777, Feb 2020.

[92] M. Sashiganth, S. J. Thiruvengadam, and D. Sriram Kumar. Ber analysis of full duplex noma downlink and uplink co-operative user relaying systems over nakagami-m fading environment. *Physical Communication*, 38:100963, Feb 2020.

[93] S. Üstünbaş and Ü. Aygölü. Ber analysis of non-orthogonal multiple access-based cognitive butterfly network. *Electronics Letters*, 56(7):357–360, Mar 2020.

[94] Chi-Bao Le, Dinh-Thuan Do, Zaharias D Zaharis, Constandinos X Mavromoustakis, George Mastorakis, and Evangelos K Markakis. System performance analysis in cognitive radio-aided noma network: An application to vehicle-to-everything communications. *Wireless Personal Communications*, pages 1–26, 2021.

[95] V. Loscri, L. Chiaraviglio, and A. M. Vegni, editors. *The Road towards 6G: Opportunities, Challenges, and Applications: A Comprehensive View of the Enabling Technologies*. Springer Nature Switzerland, Cham, 2024.

[96] X. Liu, Z. Chen, Y. Wang, F. Zhou, Y. Luo, and R. Q. Hu. Ber analysis of noma-enabled visible light communication systems with different modulations. *IEEE Transactions on Vehicular Technology*, 68(11):10807–10821, November 2019.

[97] A. Goldsmith. *Wireless Communications*. Cambridge University Press, 2005.

[98] F. Wei, T. Zhou, T. Xu, and H. Hu. Ber analysis for uplink noma in asymmetric channels. *IEEE Communications Letters*, pages 1–1, 2020.

[99] S. Arzykulov, T. A. Tsiftsis, G. Nauryzbayev, and M. Abdallah. Outage performance of cooperative underlay cr-noma with imperfect csi. *IEEE Communications Letters*, 23(1):176–179, January 2019.

[100] T.-A. Hoang, C.-B. Le, and D.-T. Do. Security performance analysis for power domain noma employing in cognitive radio networks. *Bulletin of Electrical Engineering and Informatics*, 9(3):1046–1054, June 2020.

[101] Mehdi Haghshenas, Parisa Ramezani, Maurizio Magarini, and Emil Björnson. Parametric channel estimation with short pilots in ris-assisted near-and far-field communications. *IEEE Transactions on Wireless Communications*, 2024.

[102] Muhammad Usman, Sarah Basharat, Syed Ali Hassan, Haris Pervaiz, Zhiguo Ding, and Haejoon Jung. Performance analysis of noma-enabled ris-assisted backscatter communication. *IEEE Transactions on Vehicular Technology*, 2024.